MARIA BIANNEY BERMÚDEZ CARDONA

MICROSCOPIC, BIOCHEMICAL AND PHYSIOLOGICAL ASPECTS OF THE MAIZE-*Stenocarpella macrospora* INTERACTION

Tese apresentada à Universidade Federal de Viçosa, como parte das exigências do Programa de Pós-Graduação em Fitopatologia, para obtenção do título de *Doctor Scientiae*.

VIÇOSA
MINAS GERAIS – BRASIL
2014

Ficha catalográfica preparada pela Biblioteca Central da Universidade Federal de Viçosa - Câmpus Viçosa

T
B516m
2014

Bermúdez Cardona, Maria Bianney, 1973-
Microscopic, biochemical and physiological aspects of the maize - S*tenocarpella macrospora* interaction / Maria Bianney Bermúdez Cardona. – Viçosa, MG, 2014.
xiii, 115f. : il. (algumas color.) ; 29 cm.

Orientador: Fabrício de Ávila Rodrigues.
Tese (doutorado) - Universidade Federal de Viçosa.
Inclui bibliografia.

1. Fitopatologia. 2. Milho. 3. *Stenocarpella macrospora. 4.* Doença. I. Universidade Federal de Viçosa. Departamento de Fitopatologia. Programa de Pós-graduação em Fitopatologia. II. Título.

CDD 22. ed. 571.92

MARIA BIANNEY BERMÚDEZ CARDONA

MICROSCOPIC, BIOCHEMICAL AND PHYSIOLOGICAL ASPECTS OF THE MAIZE-*Stenocarpella macrospora* INTERACTION

Tese apresentada à Universidade Federal de Viçosa, como parte das exigências do Programa de Pós-Graduação em Fitopatologia, para obtenção do título de *Doctor Scientiae*.

Aprovada: 23 de maio de 2014

_____	_____
Dr. João Américo Wordell Filho	Prof. Luis Antonio Maffia
_____	_____
Prof. Paulo Cesar Cavatte	Dra. Renata Sousa Resende

_____

Prof. Fabrício Ávila Rodrigues
Orientador

Aos meus pais, Alba Lucía e Ricaurte, aos meus irmãos Martha Lucía, Angela María e Oswaldo e a minha amada filha, Laura

OFEREÇO e DEDICO

AGRADECIMENTOS

À Deus, por cada bênção.

Aos meus pais Alba Lucía e Ricaurte por seu amor e exemplo, aos meus irmãos Martha Lucía, Angela Maria e Oswaldo e aos meus sobrinhos pelo imenso apoio e amor em todas as horas. A todos eles por terem sido grandes motivadores em minha caminhada.

À Laura, "meu milagre de abril" por ser o amor e a luz em minha vida, que embora na distância nunca deixou de estar presente em cada segundo.

Ao meu orientador professor Fabrício de Ávila Rodrigues pela orientação, paciência, ensinamentos e exemplos.

À Universidade Federal de Viçosa e ao Departamento de Fitopatologia pela oportunidade oferecida.

À Universidad del Tolima-Ibagué-Colombia pela concessão da bolsa de estudo e por todo o apoio oferecido.

Ao Programa de Estudantes-Convênio de Pós-Graduação (PEC-PG) da CAPES pela concessão da bolsa de estudo.

Ao Dr. João Américo Wordell da EPAGRI-SC pelo apoio e porque gentilmente tem fornecido as sementes das cultivares de milho e os isolados de *S. macrospora* utilizados neste estudo

Aos amigos do laboratório de Interação Planta - Patógeno Jonas, Isaias, Leonardo, Daniel, Wiler, Karla e Alessandro pela amizade, pela forca e pela boa vontade e disponibilidade em ajudar sempre que precisei. Aos demais colegas do laboratório estagiários e bolsistas Danielle, Leandro, Andre, Joyce, Vinicius, Cristiane e Ernesto pelo apoio e em especial para Renata, Patrícia, Wilka, Carlos e Maria Fernanda que além da amizade contribuíram na realização deste trabalho.

Aos os professores do Departamento de Fitopatologia da UFV por contribuir com minha formação acadêmica.

Ao Núcleo de Microscopia e Microanálise da Universidade Federal de Viçosa pelo uso dos equipamentos

Aos funcionários do Departamento de Fitopatologia, principalmente ao Bruno, Camilo, Sara e Elenice, e aos queridos amigos Sueli e Macabeu pela imensa força e conselhos.

Aos grandes amigos Vanessa, Gloria, André, Renata, Wilka, Patricia e Gustavo pela amizade e por tornarem meus anos no Brasil mais alegres e inesquecíveis.

A todos meus amigos e amigas que não mencionei, porém, que estão sempre presentes em meu coração e que me apoiaram e incentivaram ao longo do caminho.

SUMÁRIO

RESUMO

BERMÚDEZ-CARDONA, Maria Bianney, D. Sc., Universidade Federal de Viçosa, Maio de 2014. **Microscopic, biochemical and physiological aspects of the maize-*Stenocarpella macrospora* interaction.** Orientador: Fabrício Ávila Rodrigues. Coorientador: Gleiber Quintão Furtado.

A mancha de macrospora, causada por *Stenocarpella macrospora*, é uma importante doença do milho. O objetivo geral do presente trabalho foi investigar alguns aspectos da interação milho - *S. macrospora* ao nível microscópico, fisiológico e bioquímico. No primeiro estudo foram determinados os eventos do processo infeccioso de *S. macrospora* em folhas de plantas de milho do cultivar HIB 32R48H, o qual é altamente susceptível a *S. macrospora*. Conídios germinados não apresentaram tropismo positivo em direção aos estômatos. Após 24 hai, o crescimento dos tubos germinativos foi seguido pela formação do apressório, sendo que a penetração dos tubos germinativos através da cutícula da folha foi principalmente direta. Após a penetração, as hifas do fungo colonizaram primeiro as células epidérmicas adjacentes. Aos 20 dai, foi observado o crescimento proeminente do fungo no floema, nas células do parênquima, nos vasos do xilema e nas células da bainha vascular, bem como nos elementos de vaso. Aos 20 dai, nos tecidos foliares necróticos foram observadas hifas fúngicas saindo através dos estômatos e picnídios em diferentes estádios de desenvolvimento. No segundo estudo, em folhas de plantas de duas cultivares de milho (ECVSCS155 e HIB 32R48H) suscetíveis e altamente suscetíveis a *S. macrospora*, foi investigado o efeito da doença no desempenho fotossintético através dos parâmetros de trocas gasosas e análises dos parâmetros da fluorescência da clorofila *a*. A severidade da mancha de macrospora foi significativamente menor nas folhas das plantas da cultivar ECVSCS155 em relação às folhas das plantas da cultivar HIB 32R48H. Em ambas as cultivares, A, g_s and E

diminuiram significativamente, enquanto que C_i/C_a aumentou nas plantas inoculadas em relação às plantas não-inoculadas. F_0 e NPQ aumentaram significativamente nas plantas inoculadas das cultivares ECVSCS155 e HIB 32R48H, respectivamente, em relação às plantas não-inoculadas. O F_m, F_v/F_m, q_P e ETR diminuiram significativamente nas plantas inoculadas em relação às plantas não-inoculadas. Para ambas as cultivares, as concentrações de clorofila total (Chl) (a + b) e carotenóides e da relação Chl a/b diminuiram significativamente nas plantas inoculadas em relação às plantas não inoculadas. No terceiro estudo, foram investigadas as alterações bioquímicas e fisiológicas induzidas por *S. macrospora* através da análise das imagens dos parâmetros da fluorescência da clorofila *a*, avaliação da atividade de algumas enzimas do estresse oxidativo e concentração de ROS. Independentemente da cultivar de milho, as primeiras mudanças em todos os parâmetros da fluorescência da clorofila *a* foram observadas as 48 hai, as quais aumentaram com o progresso da doença. Diminuição na F_m, F_v/F_m, Y(II) e Y(NPQ) juntamente com o aumento na F_0 e Y(NO) foram diretamente relacionados com a perda progressiva da atividade fotossintética. Em ambas as cultivares os mecanismos enzimáticos e não-enzimáticos do sistema antioxidativo foram alterados drasticamente nas folhas das plantas infectadas. A atividade da SOD, CAT, POX, APX, GR, GPX e GST, bem como a concentração de AsA e GSH + GSSG foram maiores nos estágios iniciais da doença, porém houveram quedas acentuadas com o progresso da doença, sugerindo uma resposta inicial por parte do hospedeiro. Nos estágios mais avançados da doença a atividade dessas enzimas e a concentração de metabólitos antioxidantes diminuíram. Concomitantemente, a concentração de H_2O_2 e MDA aumentaram, contribuindo por tanto para o aumento da peroxidação de lipídeos das membranas celulares.

ABSTRACT

BERMÚDEZ-CARDONA, Maria Bianney, D. Sc., Universidade Federal de Viçosa, Maio de 2014. **Microscopic, biochemical and physiological aspects of the maize-*Stenocarpella macrospora* interaction.** Orientador: Fabrício Ávila Rodrigues. Coorientador: Gleiber Quintão Furtado.

Macrospora leaf spot (MSL), caused by *Stenocarpella macrospora*, is an important disease of maize. The general objective of this work was investigated some aspects of maize-*S. macrospora* interaction at microscopic, physiological and biochemical level. In this first study were determined the events of the infection process of *S. macrospora* in leaves of plants from cultivar HIB 32R48H highly susceptible to *S. macrospora*. Germinated conidia did not showed positive tropism to stomata. After 24 hai, the germ tubes growth was followed by appressoria formation and the penetration of the germ tubes through the leaf cuticle was mainly direct. After penetration, fungal hyphae first colonized adjacent epidermal cells. At 20 dai, prominent fungal growth was observed in phloem vessels, in the parenchyma cells, in the xylem vessels and bundle sheath cells as well as in the vessel elements. Fungal hyphae emerged through the stomata and pycnidia in different developmental stages were observed in the necrotic leaf tissues at 20 dai. In this second study was investigated the effect of MLS on the photosynthetic performance through the photosynthetic gas exchange parameters and chlorophyll *a* fluorescence parameter in leaves of plants from two maize cultivars (ECVSCS155 and HIB 32R48H) susceptible and highly susceptible, respectively, to *S. macrospora*. MLS severity was significantly lower in the leaves of plants from cultivar ECVSCS155 relative to the leaves of plants from cultivar HIB 32R48H. In both cultivars, A, g_s and E significantly decreased, while C_i/C_a increased in inoculated plants relative to non-inoculated plants. F_0 and NPQ significantly increased in inoculated plants of the

ECVSCS155 and HIB 32R48H cultivars, respectively, relative to non-inoculated plants. The F_m, F_v/F_m, q_P and ETR significantly decreased in inoculated plants relative to non-inoculated plants. For both cultivars, concentrations of total chlorophyll (Chl) (*a* + *b*) and carotenoids and the Chl *a*/*b* ratio significantly decreased in inoculated plants relative to non-inoculated plants. In this third study were investigated the biochemical and physiological alterations induced by infection process through the chlorophyll *a* fluorescence imaging and the activities of some antioxidative enzymes and the concentration of ROS in leaves of plants from two maize cultivars (ECVSCS155 and HIB 32R48H) susceptible and highly susceptible, respectively, to *S. macrospora*. Regardless of maize cultivar, the first changes were observed at 48 hai for all parameters of chlorophyll *a* fluorescence which prominently increased as the MLS progressed. Decreases in F_m, F_v/F_m, Y(II) and Y(NPQ) coupled with increases in F_0 and Y(NO were directly related to the progressive loss of photosynthetic activity. In both cultivars the enzymatic and non-enzymatic components of the antioxidative system were both dramatically altered on infected leaves. The SOD, CAT, POX, APX, GR, GPX and GST activities as well as the concentrations of AsA and GSH+GSSG were quite higher at the early stages of fungal infection, but suffered accentuated decreases as the MLS progressed suggesting the occurrence of an initial mechanism defense from the host's side. As the symptoms of MLS on maize leaves become more drastic, the activities of these enzymes, and the concentration of metabolites buffers decreased. Although, H_2O_2 and MDA concentration increased contributing, therefore, for the intensification of lipid peroxidation upon damage to cell membranes.

GENERAL INTRODUCTION

Macrospora leaf spot (MLS), caused by the necrotrophic fungus *Stenocarpella macrospora* (Earle) Sutton (syn. *Diplodia macrospora* Earle) (Latterell and Rossi, 1983; Casa, et al., 1998; White, 1999), is one de major fungal disease of maize (*Zea mays* L.), especially in warm and humid conditions in tropical and subtropical regions worldwilde (Anderson and White, 1987, Dai, et al., 1987).

On leaves, the symptoms the MLS appear as small, water-soaked lesions (Dai, et al., 1987; Casa, et al., 2006). Under warm and humid conditions, lesions quickly expand on leaf blades, become elliptical or irregular brown lesions with yellow or orange edges, which may have dark concentric rings and contain black structures called pycnidia (Anderson and White, 1987). *S. macrospora* can overwinter on maize debris and on seeds in form of the mycelia and pycnidia (Reis and Mario, 2003). Whenever warm and moist conditions are favorable, conidia are extruded from pycnidia in long cirri and are disseminated by wind and rain (Anderson and White, 1987; Casa, et al 1998; 2003; 2004). Give of limited efficiency of the fungicides and the unavailability of resistance cultivars (Olatinwo, et al., 1999; Bampi, et al., 2012), maize residue management, crop rotation and use of healthy seed are the most important strategies to control MSL (Casa, et al., 2006).

The fungi causing diseases on several crops have developed a large set of the strategies and mechanisms to break the cuticle and epidermal cell wall to colonize the plant tissues (Dean, 1997; van Kan, 2006). The pathogenesis by necrotrophic plant pathogenic fungi generally starts with conidia adhesion on the leaf blade, which is followed by germination and penetration, with the sporulation being the last step in the infection process (Nicholson et al., 1988; Laluk and Mengiste, 2010).

Necrotrophic pathogens besides penetrate their hosts through natural opening and wounds, have developed the ability to penetrate directly through the surface by means of the secretion of non-host selective toxins and lytic enzymes causing dissolution of cell walls and disintegration of tissue (Kolattukudy, 1985; Have et al., 2001; Cabanne and Donéche, 2002).

Several studies have shown that the infection by pathogens can directly and indirectly affect several physiological processes in their host (Owera, et al., 1981). Fungal infection may reduce the photosynthetic efficiency which is frequently associated with direct damage to the photosynthetic apparatus (Bastiaans, 1991; Berger, et al., 2007). A decrease in the photosynthesis rates, frequently, is correlated with stomatal and mesophyll limitations as well as biochemical alterations induced by pathogen infection (Berger, et al., 2007; Barón, et al., 2012). Damages to the photosynthetic apparatus induced by pathogen infection can result in the unbalance between light energy absorption and light energy utilization via the Calvin-Benson cycle (Logan et al., 2006; Rolfe and Scholes, 2010). The energy that is not adequately dissipated can lead to the production of reactive oxygen species (ROS) (Bowler et al., 1992; Arora et al., 2002; Wilhelm and Selmar), which can lead to the oxidative processes such as membrane lipid peroxidation, protein oxidation, enzyme inhibition and DNA and RNA damage (Imlay, 2003; Heller and Tudzynskui, 2011; Sharma et al., 2012). Additionally, in plants under pathogen attack, oxidative burst is often identified as the rapid host defense reaction (Bolwell and Wojtaszek, 1997; Shetty et a*l*., 2008). Plants are provided of the antioxidative systems, that is of complex arrays of enzymatic and nonenzymatic systems that detoxify the ROS (Plazek and Zur, 2004; Asada, 2006).

The physiological state of plants infected by pathogens can be investigated in a noninvasive way by the simultaneous measurement of leaf gas exchange and chlorophyll *a* fluorescence parameter (Berger, et al., 2007). Thus, chlorophyll *a* fluorescence imaging is a useful tool to estimate the operating quantum efficiency of photosystem II (PSII), which can be used to reveal heterogeneous patterns of photosynthetic performance occurring within of leaf tissue infected with pathogens (Baker et al., 2001, 2008; Berger et al., 2004; Scholes and Rolfe, 2009). Rapid alteration in the intensity of chlorophyll *a* fluorescence in the chloroplast is correlated with any photooxidative impairment of the photosynthetic apparatus (Baker et al., 2001). Considering the limited information on the maize-*S. macrospora* interaction at the microscopic, biochemical and physiological levels, this study aimed to fill out this gap by studying the events of the infection process of *S. macrospora* on maize leaves by using both light and scanning electron microscopy and by investigating the spatial-temporal alterations, photosynthetic performance and antioxidative systems on leaves of maize plants during the fungal infection process through the chlorophyll *a* fluorescence imaging, the activities of some antioxidative enzymes and the concentration of ROS.

REFERENCES

Anderson, B., and White, D. G. 1987. Fungi associated with corn stalks in Illinois in 1982 and 1983. Plant Dis. 71:135-137.

Arora, A., Sairam, R. K, and Srivastava, G. C. 2002. Oxidative stress and antioxidative system in plants. Curr. Sci. India 82:1227-1238.

Asada, K. 2006. Production and scavenging of reactive oxygen species in chloroplasts and their functions. Plant Physiol. 141:391-396.

Baker, N. R., Oxborough, K., Lawson, T., and Morison, J. I. L. 2001. High resolution imaging of photosynthetic activities of tissues, cells and chloroplast in leaves. J. Exp. Bot. 52:615-621.

Bampi, D., Casa, R. T., Bogo, A., Sangoi, L., Sachs, C., Bolzan, J. M., and Piletti, G. 2012. Fungicide performance on the control of macrospora leaf spot in corn. Summa Phytopathol. 38:319-322.

Barón, M., Flexas, J., and Delucia, E. H. 2012. Photosynthetic responses to biotic stress. Pages 331-351. in: Terrestrial photosynthesis in a changing environment a molecular, physiological and ecological approach. J. Flexas, F. Loreto, and H. Medrano, eds. Cambridge University Press.

Berger, S., Papadopoulos, M., Schreiber, U., Kaiser, W., and Roitsch, T. 2004. Complex regulation of genes expression, photosynthesis and sugar levels by pathogen infection in tomato. Physiol. Plantarum 122:419-428.

Berger, S., Sinha, A. K., and Roitsch, T. 2007. Plant physiology meets phytopathology: plant primary metabolism and plant-pathogen interactions. J. Exp. Bot. 58:4019-4026.

Bolwell, G. P., and Wojtaszek, P. 1997. Mechanisms for the generation of reactive oxygen species in plant defence-a broad perspective. Physiol. Mol. Plant Pathol. 51:347-366.

Bowler, C., Van Montagu, M., and Inzé, D. 1992. Superoxide dismutase and stress tolerance. Annu. Rev. Plant Physiol. Plant Mol. Biol. 43:83-116.

Casa, R. T., Zambolim, L., and Reis, E. M. 1998. Transmissão e controle de *Diplodia* em sementes de milho. Fitopatol. Bras. 23:436-441.

Casa, R. T., Reis, E. M., and Zambolim, L. 2003. Decomposição dos restos culturais do milho e sobrevivência saprofítica de *Stenocarpella macrospora* e *Stenocarpella maydis*. Fitopatol. Bras. 28:355-361.

Casa, R. T., Reis, E. M., and Zambolim, L. 2004. Dispersão vertical e horizontal de conídios de *Stenocarpella macrospora* e *Stenocarpella maydis*. Fitopatol. Bras. 29:141-147.

Casa, R. T., Reis, E. M., and Zambolim, L. 2006. Doenças do milho causadas por fungos do gênero *Stenocarpella*. Fitopatol. Bras. 31:427-439.

Cabanne, C., and Donéche, B. 2002. Polygalacturonase isoenzymes produced during infection of the grape berry by *Botrytis cinerea*. Vitis 41:129-132.

Dai, K., Nagai, M., Sasaki, H., Nakamura, H., Tachechi, K., and Warabi, M. 1987. Detection of *Diplodia maydis* (Berkeley) Saccardo from imported corn seed. Res. Bull. Plant Protect. Serv. 23:1-6.

Dean, R. A. 1997. Signal pathways and appressorium morphogenesis. Annu. Rev. Phytopathol. 35:211-234.

Have, A. T., Breuli, W. O., Wubben, J. P., Visser, J., and van Kan, J. A. L. 2001. *Botrytis cinerea* endopolygalacturonase genes are differentially expressed in various plant tissues. Fungal Genet. Biol. 33:97-105.

Heller, J., Tudzynski, P. 2011. Reactive oxygen species in phytopathogenic fungi: signaling, development, and disease. Annu. Rev. Phytopathol. 49:369-390.

Imlay, J. A. 2003. Pathways of oxidative damage. Annu. Rev. Microbiol. 57:395-418.

Kolattukudy, P. E. 1985. Enzymatic penetration of the cuticle by fungal pathogens. Annu. Rev. Phytopathol. 23:223-250.

Laluk, K., and Mengiste, T. 2010. Necrotroph attacks on plants: wanton destruction or covert extortion? The Arabidopsis Book. 12:1-34.

Latterell, F. M., and Rossi, A. E. 1983. *Stenocarpella macrospora* (=*Diplodia macrospora*) and *S. maydis* (=*D. maydis*) compared as pathogens of corn. Plant Dis. 67:725-729.

Logan, B. A., Koryeyev, D., Hardison, J., and Holaday, S. 2006. The role of antioxidant enzymes in photoprotection. Photosynth. Res. 88:119-132.

Nicholson, R. L., Yoshioka, H., Yamaoka, N., and Kunoh, H. 1988. Preparation of the infection court by *Erysiphe gramnis*. II release of esterase enzyme from conidia in response to a contact stimulus. Exp. Mycol. 12:336-349.

141 Olatinwo, R., Cardwell, K., Menkin, A., Deadman, M., and Julian, A. 1999.
142 Inheritance of resistance to *Stenocarpella macrospora* (Earle) ear rot of maize in the
143 mid-altitude zone of Nigeria. Eur. J. Plant Pathol. 105:535-543.
144 Owera, S. A. P., Farrar, J. F., and Whitbread, R. 1981. Growth and photosynthesis in
145 barley infected with brown rust. Physiol. Plant Pathol. 18:79-90.
146 Plazek, A., Rapacz, M., and Hura, K. 2004. Relationship between quantum
147 efficiency of PSII and cold-induced plant resistance to fungal pathogens. Acta
148 Physiol. Plant. 26:141-148.
149 Reis, E. M., and Mario, J. L. 2003. Quantification of *Diplodia macrospora* and *D.*
150 *maydis* inoculum in crop residues, in the air, and its relationship with infection of
151 corn kernels. Fitopatol. Bras. 28:143-147.
152 Rolfe, S. A., and Scholes, J. D. 2010. Chlorophyll fluorescence imaging of plant-
153 pathogen interaction. Protoplasma 247:163-175.
154 Sharma, P., Jha, A. B., Dubey, R. S., and Pessarakli, M. 2012. Reactive oxygen
155 species, oxidative damage, and antioxidative defense mechanism in plants under
156 stressful conditions. J. Bot. 2012:1-26.
157 Shetty, N. P., Jorgensen, H. J. L., Jensen, J. D., Collinge, D. B., and Shetty, H. S.
158 2008. Roles of reactive oxygen species in interactions between plants and pathogens.
159 Eur. J. Plant Pathol. 121:267-280.
160 Sholes, J. D., and Rolfe, S. A. 2009. Chlorophyll fluorescence imaging as tool for
161 understanding the impact of fungal diseases on plant performance: a phenomics
162 perspective. Funct. Plant Biol. 36:880-892.
163 van Kan, J. A. L. 2006. Licensed to kill: the lifestyle of a necrotrophic plant
164 pathogen. Trends Plant Sci. 11:248-253.
165 White, D. G. 1999. Compendium of corn diseases. 3rd Ed. St. Paul, MN, USA: The
166 American Phytopythological Society.
167 Wilhelm, C., and Selmar, D. 2011. Energy dissipation is an essential mechanism to
168 sustain the viability of plants: the physiological limits of improved photosynthesis. J.
169 Plant Physiol. 168:79-87.
170
171
172
173

CHAPTER 1

Infection process of *Stenocarpella macrospora* on maize leaves

Maria Bianney Bermúdez Cardona*, Maria Fernanda Antunes Cruz and Fabrício Ávila Rodrigues

ABSTRACT

Bermúdez-Cardona, M., Antunes, M. F. C., and Rodrigues, F. A. 2014. Infection process of *Stenocaperlla macrospora* on maize leaves.

Macrospora leaf spot, caused *by Stenocarpella macrospora*, is an important disease of maize. Adaxial leaf surface was inoculated with a conidial suspension of S. macrospora. Samples were collected from 24 to 96 h after inoculation and then again 20 days. Germinated conidia did not showed positive tropism to stomata. After 24 hai, the germ tubes growth was followed by appressoria formation and the penetration of the germ tubes through the leaf cuticle was mainly direct. After penetration, fungal hyphae first colonized adjacent epidermal cells as well as the underlying mesophyll cells. At 20 dai, prominent fungal growth was observed in phloem vessels, in the parenchyma cells, in the xylem vessels and bundle sheath cells as well as in the vessel elements. Fungal hyphae emerged through the stomata and pycnidia in different developmental stages were observed in the necrotic leaf tissues at 20 dai. Results from this study provide new insights into the infection process of S. macrospora on maize leaf.

INTRODUCTION

Maize (*Zea mays* L.) is one of the most important cereal crops in the world and is widely cultivated in both tropical and subtropical regions (Lobell et al., 2009; CIMMYT, 2012). Among the diseases affecting maize production, macrospora leaf spot (MLS), caused by the fungus *Stenocarpella macrospora* (Earle) Sutton (syn. *Diplodia macrospora* Earle), is one of the greatest economic importance especially in humid subtropical and tropical regions (Latterell and Rossi, 1983; Dai et al., 1987).

The symptoms of MLS first appears as small brown spots with chlorotic halo and with water soaked appearance on maize leaf blades (Dai et al., 1987). As the infection progresses, the lesions expand and become irregular or elliptical, in color brown with concentric rings and reddish or yellow halo (Dai et al., 1987; Casa et al., 2006, Bradley et al., 2010). Inside the necrotic leaf tissues, subepidermal, globose or elongated pycnidia in color dark brown are produced (Bradley et al., 2010). *S. macrospora* survives saprophytically in maize debris in form of mycelia and pycnidia which constitute the main source of primary inoculum (Casa et al., 2003). Conidia are often released from pycnidia in cirri and easily spread by wind and rain (Flett et al., 1992; Casa et al., 1998; Casa et al., 2004). Once little information is available about chemical control and resistant cultivars, the main measures to control of MLS are based on the reduction of primary inoculum, crop rotation and the use of healthy seed (Casa et al., 2006; Bampi et al., 2012).

The fungi causing diseases on several crops have developed a large set of strategies and mechanisms to break the cuticle and epidermal cell wall to colonize the plant tissues (Dean, 1997; van Kan, 2006). The infection process by necrotrophic plant pathogenic fungi generally starts with with conidia adhesion on the leaf surface

following by germination and penetration and the sporulation being the last step in the pathogenesis (Nicholson et al., 1988; Prins et al., 2000; Laluk and Mengiste, 2010). Necrotrophic pathogens may penetrate their hosts through wounds, natural opening and directly through the surface through the secretion of lytic enzymes or non-host selective toxins causing dissolution of cell walls and disintegration of tissue (Kolattukudy, 1985; Have et al., 2001; Cabanne and Donéche, 2002; van Kan, 2006). Oxidases, cutinases and lipases are secreted by the fungi to modify the plant cutin and wax layer (Movahedi and Heale, 1990; Laluk and Mengiste, 2010). Once the cuticle has been weakened, proteases, pectinases and specifically polygalacturonases play a pivotal role for the success of fungal infection as reported by Have et al, (2001) in tomato leaves infected with *Botrytis cinerea*.

Considering the importance of MLS in decreasing maize yield and that little information is available regarding the infection process of *S. macrospora* on maize leaves, this study aimed to determine the events of the infection process of *S. macrospora* on maize leaves by using both light and scanning electron microscopy.

MATERIALS AND METHODS

Plant cultivation. Maize seeds from cultivar HIB 32R48H highly susceptible to *S. macrospora* was sown in plastic pots containing 2 kg of Tropstrato® (Vida Verde, Mogi Mirim, São Paulo, Brazil) substrate composed of a 1:1:1 mixture of pine bark, peat and expanded vermiculite. A total of 1.63 g of calcium phosphate monobasic was added to each plastic pot. A total of five seeds were sown per pot and each pot was thinned to three seedlings five days after seedling emergence. Plants were kept in a greenhouse during the experiments (temperature 28 ± 2°C during the day and 12 ± 4°C at night, relative humidity 70 ± 5%) and were fertilized weekly with 50 mL of a nutrient solution composed of 2.6 mM KCl, 0.6 mM K2SO4, 1.2 mM MgSO4, 1.0 mM CH4N2O, 1.2 mM NH4NO3, 0.0002 mM (NH4)6Mo7O24, 0.03 mM H3BO4, 0.04 mM ZnSO4, 0.01 mM CuSO4 and 0.03 mM MnCl2. The nutrient solution was prepared using deionized water. Plants were watered as needed.

Inoculum production and inoculation procedure. Plants were inoculated with a monosporic isolate of *S. macrospora* (UFV-DFP Sm 01). The isolate of S. macrospora was grown in Petri dishes containing oat-agar medium and incubated for 35 days in an incubator (22ºC, photoperiod of 12 h of light and 12 h of darkness). All leaves of each plant were inoculated with a conidial suspension of *S. macrospora* (6 × 10^4 conidia/ml) at 30 days after emergence (growth stage V5) (Bensch et al., 1992) using a VL Airbrush atomizer (Poasche Airbrush Co, Chicago, IL). Gelatin (1% w v-1) was added to the suspension to aid conidial adhesion to the leaf blades. Immediately after inoculation, the plants were transferred to a growth chamber at 25 ± 2ºC, 90 ± 5% relative humidity and a 12 h light: 12 h dark photoperiod for 30 h. After this period, the plants were transferred to a plastic mist growth chamber (MGC) inside a greenhouse for the duration of the experiments. The MGC was made

of wood (2 m wide, 1.5 m high and 5 m long) and covered with 100-µm thick transparent plastic. The temperature inside the MGC ranged from 25 ± 2ºC (day) to 20 ± 2ºC (night). The relative humidity was maintained at 90 ± 5% using a misting system in which nozzles (model NEB-100; KGF Company São Paulo, Brazil) sprayed mist every 30 min above the plant canopies. The relative humidity and temperature were measured with a thermo-hygrograph (TH-508, Impac, São Paulo, Brazil). The maximum natural photon flux density at plant canopy height was approximately 900 µmol m-2 s-1.

Processing of leaf sample for light microscopy. Leaf fragments (≈ 5 mm^2) with symptoms of MLS were collected at 24, 48, 72 and 96 hai and at 20 dai. The fragments were placed in glass vials, fixed with 2.5% glutaraldehyde in 0.1 M sodium cacodylate buffer (pH 7.2) during 48 h, dehydrated in an ethanol series and embedded in methacrylate Historesin (Leica Instruments, Heidelberg, Alemanha). A total of four blocks were made per each treatment and each block contained two leaf fragments. Cross sections of 5 mm² thick obtained with the help of rotary microtome auto-advance model RM 2255 (Leica Microsystems Inc., Deerfield, IL, EUA) were stained with toluidine blue 0.05% (pH 4.7). A total of 25 semi-fine cuts were obtained per each block which were distributed into six glass slides. The semi-fine sections were observed under light microscope model AX70RF with photographic system U‑Photo and digital camera Spot Insightcolour 3.2.0 (Diagnostic Instruments Inc., Merrick, NY, EUA).

Processing of leaf samples for scanning microscopy. Leaf fragments (≈ 5 mm^2) were collected at 24, 48, 72 and 96 hai and at 20 dai. The fragments were placed in glass vials, fixed with 2.5% glutaraldehyde in 0.1 M sodium cacodylate buffer (pH 7.2) and stored at 4°C. The samples were post-fixed for 2 h at room temperature with

299 osmium tetroxide 1% in sodium cacodylate buffer 0.1 M (pH 7.2). The fragments
300 were washed with the same buffer for four times each of 10 min and dehydrated in
301 an ethanol series. After dehydration, the fragments were subjected to a critical point
302 dryer using the unit "Critical Point Dryer" (CPD 020 Model, Bal-Tec, Balzers,
303 Liechtenstein). The fragments were mounted on metal stubs with the aid of an
304 aluminum double-sided tape and coated with colloidal gold in a "Sputter Coater"
305 apparatus coupled with a "Freezing Drying Unit" (FDU010 Model, Bal-Tec, Balzers,
306 Liechtenstein). The fragments were examined by SEM (Leo 1430 VP Model, Zeiss,
307 Cambridge, UK) operated at 10 kV.
308
309
310
311
312
313
314
315
316
317
318
319
320
321

RESULTS

Macrospora leaf spot symptoms on maize leaf blades. The lesions of MLS of water-soaked appearance were noticed on the leaf blades at 48 hai. As the lesions expanded, they became elliptical or irregular of the brown color surrounded by chlorotic or reddish haloes. At 10 dai, the lesions appeared as large brown parches of desiccated tissue with darker concentric rings. Pycnidia of different developmental stages were observed in the necrotic lesions at 20 dai (Fig. 1).

Conidial germination and fungus penetration. At 24 hai, conidia started to germinate on the leaf blades without a specific pattern. The germ tubes were formed from one of the conidial cells and eventually germination tended to be bipolar (Fig. 2A). The germ tubes grew along the leaf blade and apparently without any positive tropism to the stomata. Occasionally, the germ tube grew toward to the stomata direction without any evidence of direct penetration (Fig. 2B). The weakening of the leaf surface in the regions around the conidia and germ tubes were observed (Fig. 2A). The germ tubes growth was followed by appressoria formation after 24 hai suggesting that around 24 hours after the conidia contact with the leaf surface and under appropriate conditions of humidity and temperature, the germ tube differentiated into an apressorium. The penetration of the germ tubes directly through the leaf cuticle was mainly direct.

Fungus colonization and sporulation. Fungal hyphae abundantly colonized inter and intracellularly the leaf tissues at 20 dai causing, therefore, profound destruction of the cells (Figs.. 2, 3 and 4). Fungal hyphae first colonized adjacent epidermal cells as well as the underlying mesophyll cells (Figs. 2C and 3C). Prominent fungal growth was also observed in phloem vessels (Figs. 4C and E), in the parenchyma cells (Fig. 4E-H), in the xylem vessels and bundle sheath cells (Figs. 3G and H; 4D)

as well as in the vessel elements (Fig. 4F-H). Fungal hyphae emerged through the stomata at 20 dai (Figs. 2F; 3A and B). Pycnidia in different developmental stages were observed in the necrotic leaf tissues at 20 dai (Figs. 3C-F and 3I and J).

DISCUSSION

The present study provides, to the best of the author´s knowledgment, the first microscopic details of the infection process of *S. macrospora* on maize leaf blades. There are certain physical and chemical features of host surface that appears to influence conidia germination, germ tubes growth and appressoria formation in some fungi causing diseases on several plant species (Wynn, 1982; Howard and Valent, 1996; Dean, 1997). The bicellular conidia of *S. macrospora* produced one or several germ tubes from each cell. The germ tube penetrated in maize leaves principally by direct penetration of the plant cuticle. Kema et al. (1996) and Palme and Skinner (2002) reported that *Mycosphaerela graminicola* penetrated the wheat leaves directly. Occasionally, the germ tubes passed through the stomata without any evidence of their penetration. For the maize-*Cercospora zeae-maydis* (Beckman and Payne, 1982), wheat-*Mycosphaerella graminicola* (Kema et al., 1996), maize-*S. macrospora* (Brunelli et al., 2004) and cassava-*Cercospora hennigsii* (Babu et al., 2009) interactions, there was no evidence of fungal penetration through the stomata.

The epicuticular wax layer in the surrounding areas of the conidia and germ tubes of *S. macrospora* were dramatically affected. The weakening of the leaf blades at the locations of conidia deposition and adhesion as well as in regions around the germ tubes suggests that the action of lytici enzymes secreted by *S. macrospora* acted on the modification of leaf surface to ensure the attachment of conidia and germ tubes and prepare of the host surface for penetration. Similar observations were reported by Kunoh et al. (1990) and Howard and Valent (1996), respectively, for the barley-*Erysiphe graminis* and rice-*Magnaporthe grisea* interactions. These authors evidenced that the erosion of the host cuticle occurred due to enzymatic modification

396 possibly by hydrolytic enzymes such as cutinases and esterases released by these
397 fungi.

398 After fungal penetration, two patterns of tissue colonization were observed. At
399 early stages of infection, fungal hyphae were less abundant in the epidermal and
400 subepidermal cells with profound alterations in the integrity of the cell walls
401 suggesting the participation of non-host selective toxins in this process. Mesophyll
402 cells of sorghum and wheat were profoundly affected, respectively, by
403 *Colletotrichum sublineolum* and *M. graminicola* infections without the presence of
404 mycelia of these fungi suggesting that cell wall degrading enzymes and non-host
405 selective toxins were greatly important for leaf tissue colonization (Wharton and
406 O'Connell, 2001; Palme and Skinner, 2002).

407 In the present study, the gradual fungal colonization of the leaf tissues, dissolution
408 of cell walls and great extension of cells necroses were noticed. Fungal hyphae were
409 noticed in the epidermis and parenchyma cells, phloem and xylem vessels as well as
410 in the vessels elements and bundle sheath cells. Extensive growth of hyphae of *C.*
411 *graminicola* in maize leaves and of *Rhynchosporium secalis* on barley leaves were
412 reported, respectively, by Mims and Vaillancourt (2002) and Jorgensen et al. (1993).
413 After massive cell collapse, fungal hyphae emerging through the stomata in the
414 necrotic leaf tissues were observed suggesting that this was the initial phase for the
415 pycnidia formation. This finding is in agreement with has been reported for wheat-*M.*
416 *graminicola* (Kema et al., 1996; Palme and Skinner, 2002) and macadamia-
417 *Pseudocercospora macadamiae* (Miles et al., 2009) interactions.

418 Considering the importance of MLS to maize production worldwide and the lack
419 of information in the literature regarding the infectious process of *S. macrospora*, the
420 results from the present study brings novel information for a better understanding of

421 the fungal infection process that may help for evolving more effective disease control
422 strategies.
423
424
425
426
427
428
429
430
431
432
433
434
435
436
437
438
439
440
441
442
443
444

LITERATURE CITED

Babu, A. M., Philip, T., Kariappa, B. K., and Kamble, C. K. 2009. Scanning electron microscopy of the infection process of *Cercospora henningsii* on cassava leaves. J. Phytopathol. 157:57-62.

Bampi, D., Casa, R. T., Bogo, A., Sangoi, L., Sachs, C., Bolzan, J. M., and Piletti, G. 2012. Fungicide performance on the control of macrospora leaf spot in corn. Summa Phytopathol. 38:319-322.

Beckman, P. M., and Payne, G. A. 1982. External growth, penetration, and development of *Cercospora zeae-maydis* in corn leaves. Phytopathology 72:810-815.

Bensch, M. J., Van Staden, J., and Rijkenberg, F. H. J. 1992. Time and site inoculation of maize for optimum infection of ears by *Stenocarpella maydis*. J. Phytopathol. 136:265-269.

Bradley, C. A., Pedersen, D. K., Zhang, G. R., and Pataky, N. R. 2010. Occurrences of diplodia leaf streak caused by *Stenocarpella macrospora* on corn (*Zea mays*) in Illinois. Plant Dis. 94:1262.

Brunelli, K. R., Athayde Sobrinho, C., Cavalcanti, L. S., Ferreira, P. T. O., and Camargo, L. E. A. Germinação e Penetração de *Stenocarpella macrospora* em folhas de milho. Fitopatol. Bras. 30:187-190.

Cabanne, C., and Donéche, B. 2002. Polygalacturonase isoenzymes produced during infection of the grape berry by *Botrytis cinerea*. Vitis 41:129-132.

Casa, R. T., Zambolim, L., and Reis, E. M. 1998. Transmissão e controle de *Diplodia* em sementes de milho. Fitopatol. Bras. 23:436-441.

Casa, R. T., Reis, E. M., and Zambolim, L. 2003. Decomposição dos restos culturais do milho e sobrevivência saprofítica de *Stenocarpella macrospora* e *Stenocarpella maydis*. Fitopatol. Bras. 28:355-361.

471 Casa, R. T., Reis, E. M., and Zambolim, L. 2004. Dispersão vertical e horizontal de
472 conídios de *Stenocarpella macrospora* e *Stenocarpella maydis*. Fitopatol. Bras.
473 29:141-147.
474 Casa, R. T., Reis, E. M., and Zambolim, L. 2006. Doenças do milho causadas por
475 fungos do gênero *Stenocarpella*. Fitopatol. Bras. 31:427-439.
476 CIMMYT, 2012. Maize Annual Report: Research Program on Maize. CGIAR. 28 p.
477 Dai, K., Nagai, M., Sasaki, H., Nakamura, H., Tachechi, K., and Warabi, M. 1987.
478 Detection of *Diplodia maydis* (Berkeley) Saccardo from imported corn seed. Res.
479 Bull. Plant Protect. Serv. 23:1-6.
480 Dean, R. A. 1997. Signal pathways and appressorium morphogenesis. Annu. Rev.
481 Phytopathol. 35:211-234.
482 Flett, B. C., Wehner, F. C., and Smith, M. F. 1992. Relationship between maize
483 stubble placement in soil and survival of *Stenocarpella maydis* (*Diplodia maydis*). J.
484 Phytopathol. 134:33-38.
485 Have, A. T., Breuli, W. O., Wubben, J. P., Visser, J., and van Kan, J. A. L. 2001.
486 *Botrytis cinerea* endopolygalacturonase genes are differentially expressed in various
487 plant tissues. Fungal Genet. Biol. 33:97-105.
488 Howard, R. J., and Valent, B. 1996. Penetration by the fungal rice blast pathogen
489 *Magnaporthe grisea*. Annu. Rev. Microbiol. 50:491-512.
490 Jorgensen, H. J. L., De Neergaard, E., and Smedegaard-Petersen, V. 1993.
491 Histological examination of the interaction between *Rhynchosporium secalis* and
492 susceptible and resistant cultivars of barley. Physiol. Mol. Plant Pathol. 42:345-358.
493 Kema, G. H. J., Yu, DaZhap., Rijkenberg, F. H. J., Shaw, M. W., and Baayen, R. P.
494 1996. Histology of the pathogenesis of *Mycosphaerella graminicola* in wheat.
495 Phytopathology 86:777-786.

496 Kolattukudy, P. E. 1985. Enzymatic penetration of the cuticle by fungal pathogens.
497 Annu. Rev. Phytopathol. 23:223-250.
498 Kunoh, H., Nicholson, R. L., Yosioka, H., Yamaoka, N., and Kobayashi, I. 1990.
499 Preparation of the infection court by *Erysiphe graminis*: degradation of the host
500 cuticle. Physiol. Mol. Plant Pathol. 36:397-407.
501 Laluk, K., and Mengiste, T. 2010. Necrotroph attacks on plants: wanton destruction
502 or covert extortion? The Arabidopsis Book.. 1-34.
503 Latterell, F. M., and Rossi, A. E. 1983. *Stenocarpella macrospora* (=*Diplodia*
504 *macrospora*) and *S. maydis* (=*D. maydis*) compared as pathogens of corn. Plant Dis.
505 67:725-729.
506 Lobell, D. B., Cassman, K. G., and Field, C. B. 2009. Crop yield gaps: their
507 importance, magnitudes and causes. Annu. Rev. Env. Resour. 34:179-204.
508 Miles, A. K., Akinsanmi, O. A., Sutherland, P. W., Aitken, E. A. B., and Drenth, A.
509 2009. Infection, colonization and sporulation by *Pseudocercospora macadamiae* on
510 macadamia fruit. Australas. Plant Path. 38:36-43.
511 Mims, C. W., and Vaillancourt, L. J. 2002. Ultraestructural characterization of
512 infection and colonization of maize leaves by *Colletotrichum graminicola*, and by a
513 *C. graminicola* pathogenicity mutant. Phytopathology 92:803-812.
514 Movahedi, S., and Heale, J. B. 1990. The roles of aspartic proteinase and endo-pectin
515 lyase enzymes in the primary stages of infection and pathogenesis of various host
516 tissues by different isolates of *Botrytis cinerea* Pers ex. Pers. Physiol. Mol. Plant
517 Pathol. 36: 303-324.
518 Nicholson, R. L., Yoshioka, H., Yamaoka, N., and Kunoh, H. 1988. Preparation of
519 the infection court by *Erysiphe gramnis*. II release of esterase enzyme from conidia
520 in response to a contact stimulus. Exp. Mycol. 12:336-349.

521 Prins, T. W., Tudzynski, P., Tiedemann, A. V., Tudzynski, B., Have, A., Hansem, M.
522 E., Tenberge, K., and van Kan, J. A. L. 2000. Infection strategies of *Botrytis cinerea*
523 and related necrotrophic pathogens. Pages 33-64. In Fungal Pathology. J. W.
524 Kronstad, ed. Netherlands, Kluwer Academic Publishers.
525 van Kan, J. A. L. 2006. Licensed to kill: the lifestyle of a necrotrophic plant
526 pathogen. Trends Plant Sci. 11:248-253.
527 Wharton, P. S., Julian, A. M., and O'Connel, R. J. 2001. Ultraestructure of the
528 infection of *Sorghum bicolor* by *Colletotrichum sublineolum*. Phytopathology
529 91:149-158.
530 White, D. G. 1999. Compendium of corn diseases. 3rd Ed. St. Paul, MN, USA: The
531 American Phytopathological Society.
532 Wynn, W. K. 1981. Tropic and taxic response of pathogens to plants. Ann. Rev.
533 Phytopathol. 19:237-255.
534

535 **LIST OF FIGURES**

536

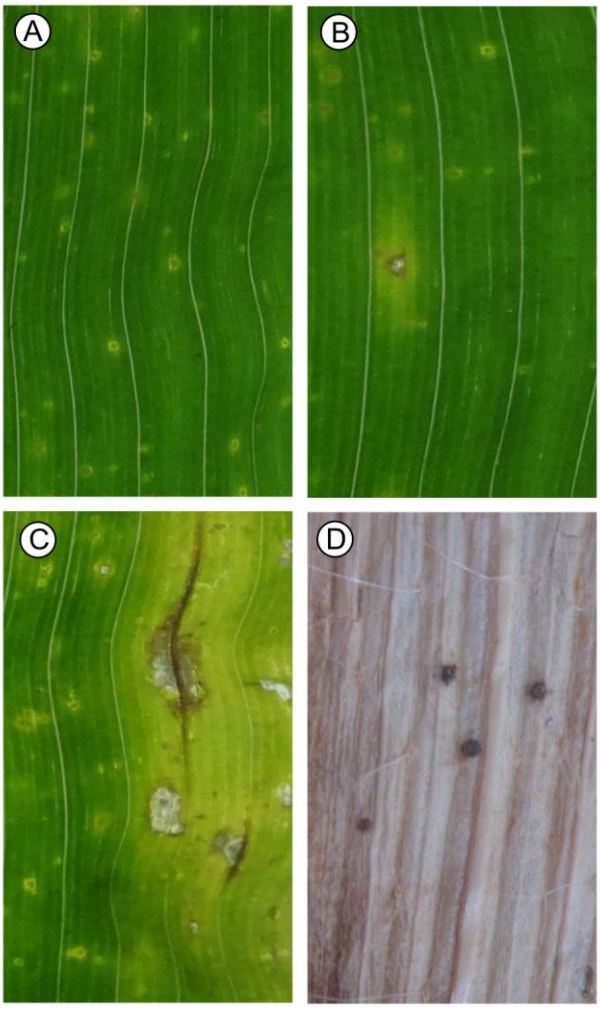

537

538 **Fig. 1.** Symptoms of macrospora leaf spot, caused by *Stenocarpella macrospora*, on
539 maize leaf blades. A. small lesions with water-soaked start to develop at 48 hours
540 after inoculation (hai); B. lesions with brown colour surrounded by yellow halos
541 became apparent at 96 hai; C. lesions expanded causing intense leaf tissue necrosis at
542 10 days after inoculation (dai); D. dark brown sub-epidermal pycnidia on the necrotic
543 leaf tissue at 20 dai.

544

545

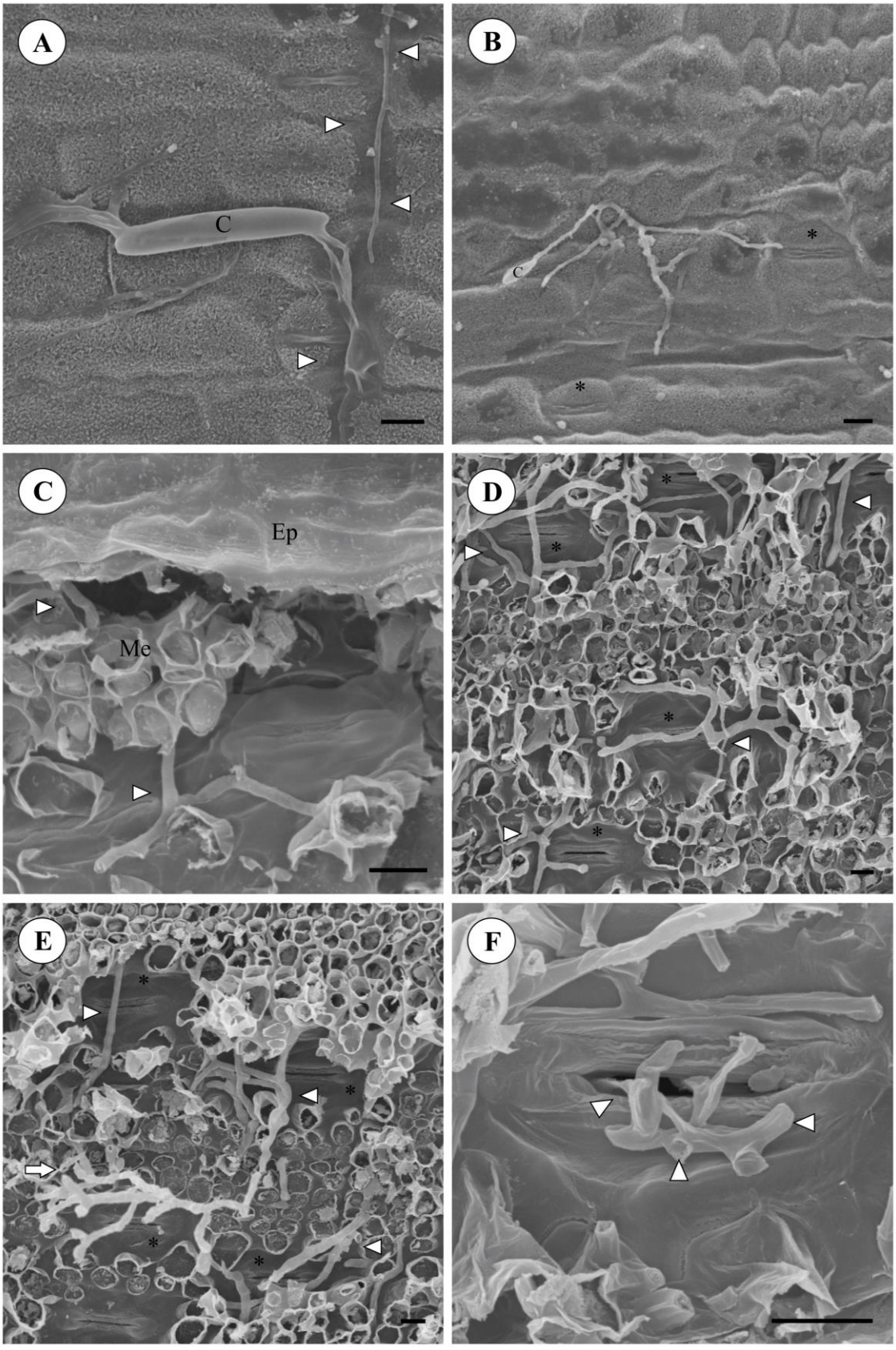

546

547

548 **Fig. 2.** Scanning electron micrographs of the surface of maize leaves at 24 hours
549 after inoculation (A and B) and of fractured leaf samples at 20 days after inoculation
550 with *Stenocarpella macrospora* (C-F). A. bipolar-germinated conidium with germ
551 tubes emerging from each cell. Germ tubes grow through the stomata without any
552 evidence of penetration. Erosion of the host cuticle around the conidia and germ
553 tubes on the adaxial leaf surface; B. conidia producing one germ tube with its tip
554 growing in the direction of the stomata. C-E. profuse hyphal growth in the mesophyll
555 cells; F. hyphae emerging through stomata. C = conidia; Ep = epidermis; Me =
556 mesophyll; * = stomata; arrowhead = hyphae; arrow = branching hyphae. Bars: 10
557 µm.
558
559
560
561
562
563
564
565
566
567
568
569
570
571
572

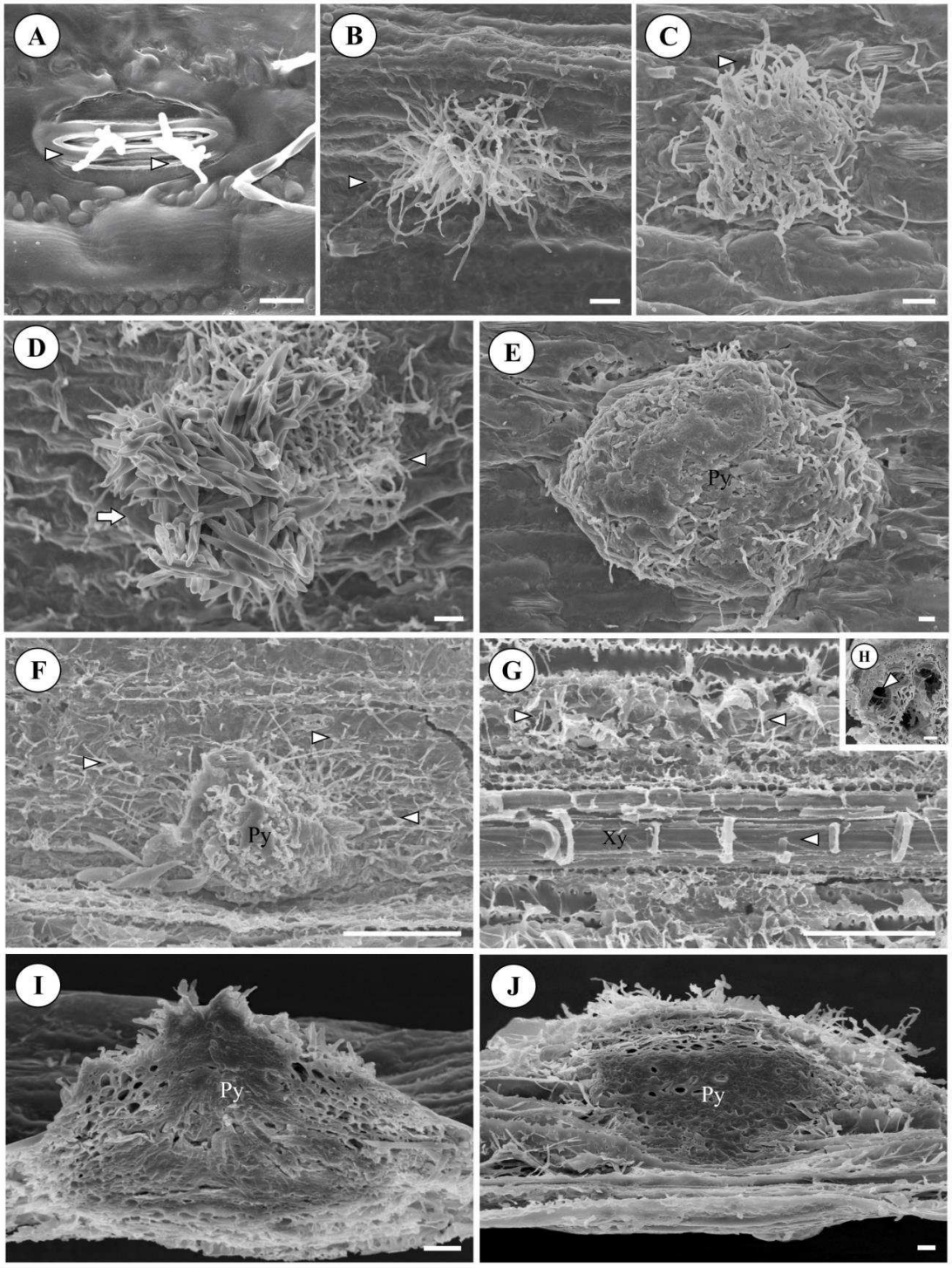

573

574

575

576

577

578 **Fig. 3.** Scanning electron micrographs of the surface of maize leaves at 24 hours
579 after inoculation (A-E) and of fractured leaf samples at 20 days after inoculation with
580 *Stenocarpella macrospora* (F-J). A. fungal hyphae emerging through stomata on the
581 adaxial leaf surface; B-F. pycnidia formation; G and H. profuse fungal hyphae
582 colonizing the xylema vessels; I and J. pycnidia formation. C = conidium. arrowhead
583 – fungal hyphae, arrow = conidia, Py = pycnidia, Xy = xylem vessels. Bars: A, E, J -
584 10 μm, B, C, D, H, I - 20 μm, F, G - 100 μm.
585
586
587
588
589
590
591
592
593
594
595
596
597
598
599
600
601
602

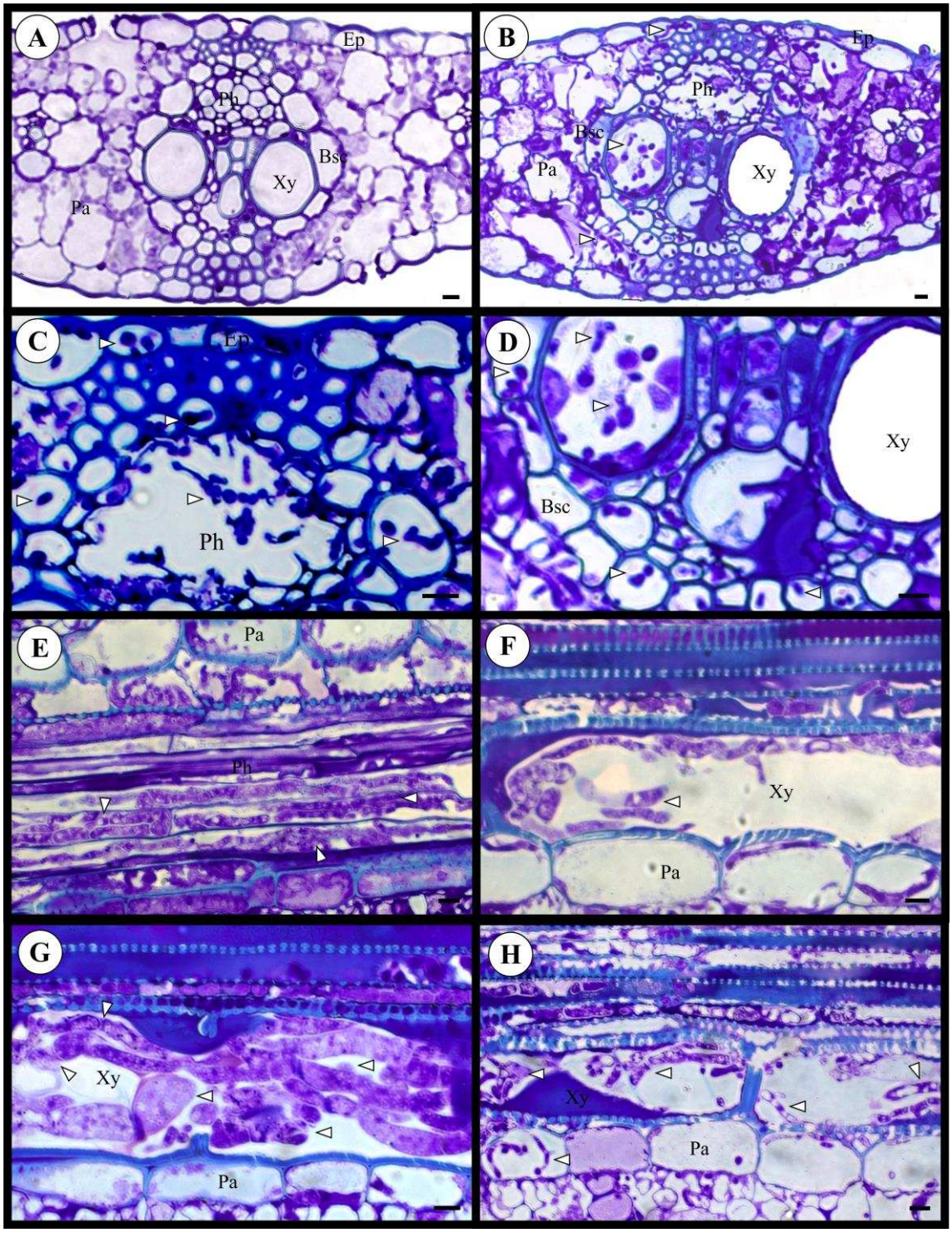

603

604

605

606

607

608 **Fig. 4.** Light micrographs of transverse (A-D) and longitudinal (E-H) maize leaf
609 sections at 20 days after inoculation with *Stenocarpella macrospora*. Sections
610 obtained from non-inoculated (A) and inoculated plants (B-H). C. fungal hyphae
611 colonize the epidermal cells and the phloem vessels; D. fungal hyphae colonizes the
612 xylem vessels and the bundle sheath cells; E. fungal hyphae colonizes the
613 parenchyma cells and the phloem vessels; F-H. fungal hyphae colonize the entire
614 vessels element. Ep = epidermis; Pa = parenchymal; Ph = phloem; Xy = xylem; Bsc
615 = bundle sheath cells; arrowhead = fungal hyphae. Bars: 10 μm.
616
617
618
619
620
621
622
623
624
625
626
627
628
629
630
631

CHAPTER 2

Submitted as original paper to *Phytopathology*

Leaf Gas Exchange and Chlorophyll *a* Fluorescence in Maize Leaves Infected with *Stenocarpella macrospora*

Maria Bianney Bermúdez-Cardona*, João Américo Wordell Filho and Fabrício Ávila Rodrigues

First and third authors: Universidade Federal de Viçosa, Departamento de Fitopatologia, Laboratório da Interação Planta-Patógeno, Viçosa, Minas Gerais State, Zip Code 36.570-900, Brazil; second author: Laboratório de Fitossanidade, EPAGRI/CEPAF, Chapecó, Santa Catarina State, Zip Code 89801-970, Brazil

ABSTRACT

Bermúdez-Cardona, M., Wordell Filho, J. A., and Rodrigues, F. A. 2014. Leaf gas exchange and chlorophyll *a* fluorescence in maize leaves infected with *Stenocarpella macrospora*. Phytopathology 104:xx-xx

This study investigated the effect of macrospora leaf spot (MLS), caused by *Stenocarpella macrospora*, on photosynthetic gas exchange parameters [net CO_2 assimilation rate (A), stomatal conductance to water vapor (g_s), internal CO_2 concentration (C_i) and transpiration rate (E)] and on chlorophyll *a* fluorescence parameters [maximum quantum quenching (F_v/F_m and F_v'/F_m'), photochemical (q_P) and nonphotochemical (NPQ) quenching coefficients and electron transport rate (ETR)] determined in leaves of plants from two maize cultivars (ECVSCS155 and HIB 32R48H) susceptible and highly susceptible, respectively, to *S. macrospora*.

MLS severity was significantly lower in the leaves of plants from cultivar ECVSCS155 relative to the leaves of plants from cultivar HIB 32R48H. In both cultivars, A, g_s and E significantly decreased, while C_i/C_a increased in inoculated plants relative to non-inoculated plants. F_0 and NPQ significantly increased in inoculated plants of the ECVSCS155 and HIB 32R48H cultivars, respectively, relative to non-inoculated plants. The F_m, F_v/F_m, q_P and ETR significantly decreased in inoculated plants relative to non-inoculated plants. For both cultivars, concentrations of total chlorophyll (Chl) (a + b) and carotenoids and the Chl a/b ratio significantly decreased in inoculated plants relative to non-inoculated plants. In conclusion, the results from the present study demonstrate, for the first time, that photosynthesis in the leaves of maize plants is dramatically impacted during the infection process of *S. macrospora*, and impacts are primarily associated with limitations of a diffusive and biochemical nature.

INTRODUCTION

Maize (*Zea mays* L.) is one of the world´s most important and widely grown cereal crops and serves as a staple human food, feed for livestock and raw material for many industrial products (19,33). Macrospora leaf spot (MLS), caused by the necrotrophic fungus *Stenocarpella macrospora* (Earle) Sutton (syn. *Diplodia macrospora* Earle) (15,32,58), is one the major diseases affecting maize yield worldwide (2,18,22,39), mainly when maize is grown under warm and humid conditions in tropical and subtropical regions (24,58). On leaves, MLS symptoms appear as small, water-soaked lesions (18,22). As the elliptical lesions expand, they become brown in color with yellow or reddish edges that may have darker concentric rings and contain black structures called pycnidia (2,18). The mycelia and pycnidia of *S. macrospora* can overwinter on maize debris and on seeds (47). Under warm and moist conditions, conidia are extruded from pycnidia in long cirri and are disseminated by wind, rain and insects, favoring severe MLS epidemics and great yield losses (2,15,16,17). The major strategies to control MLS are maize residue management, use of healthy seed and crop rotation (18). To date, there are no fungicides registered for the control of MLS, and information about the resistance of commercial hybrids is scarce (6,41).

Pathogens can directly and indirectly affect several physiological processes in their hosts (42). The alteration in the rate of physiological processes in asymptomatic leaf tissue may be proportional to, proportionally greater or proportionally smaller than the corresponding infected leaf tissue caused by a certain disease (42,54). The physiological state of plants infected by pathogens can be investigated in a noninvasive way by the simultaneous measurement of leaf gas exchange and chlorophyll *a* fluorescence parameters (12). A decrease in the photosynthetic

efficiency and stomatal and mesophyll conductance limitations as well as biochemical alterations are the primary effects caused by pathogen infection (7,12). Fungal infection may reduce photosynthesis rates through a number of potential mechanisms: impairment of the functional leaf area and reduction in the photosynthetic efficiency of the remaining green leaf area, as reported for interactions between barley and *Rhynchosporium secalis* (36) and bean and *Colletotrichum lindemuthianum* (34); alterations in chloroplasts and a reduction in chlorophyll concentration, as reported in barley leaves infected with *Puccinia hordei* (42); stomatal closure, as reported in potato leaves infected with *Verticillium dahlias* (14); and impairment of the photosynthetic apparatus or disruption in photosynthetic metabolic pathways, as reported in poplar leaves infected with *Marsonia brunnea* f.sp. *brunnea* (23). Measurement of chlorophyll *a* fluorescence is an important tool for assessing the photosynthetic performance of the leaves of plants submitted to many types of abiotic and biotic stresses (4,11,50,53). Analysis of chlorophyll *a* fluorescence is a quantitative measure of both photochemical and non-photochemical energy dissipation processes occurring in leaves (29,49). Changes in the intensity of chlorophyll *a* fluorescence in the chloroplasts reflect its functional state (30) and provide important information related to the composition of the pigment systems, excitation energy transfer, physical changes in pigment-protein complexes, primary photochemistry and kinetics and rates of electron transfer reactions in photosystem II (28). Several studies reported that the infection of plants by pathogens often leads to complex alterations in chlorophyll *a* fluorescence that can be related to changes in the efficiency of photosynthetic processes (50,53). Measurements of chlorophyll *a* fluorescence have shown that the maximum fluorescence (F_m), maximum photochemical efficiency of PSII (F_v/F_m) of dark-adapted leaves and electron

733 transport rate (ETR) are often decreased during the infection process of pathogens, as
734 described for *Phaeoisariopsis griseola* and *Uromyces appendiculatus* in bean (9) and
735 *Bremia lactucae* in lettuce (46). The fraction of absorbed light energy that was
736 thermally dissipated (NPQ) increased in tomato leaves infected with *Odium*
737 *neolycopersici* (45).

738 Due to the importance of MLS in decreasing maize yield, this study was designed
739 to examine how the infection process of *S. macrospora* could affect the
740 photosynthetic performance of plants using a combination of gas exchange and
741 chlorophyll *a* fluorescence measurements along with an analysis of chlorophyll
742 pools.

743
744
745
746
747
748
749
750
751
752
753
754
755

MATERIALS AND METHODS

Plant cultivation. Maize seeds from cultivars ECVSCS155 and HIB 32R48H, susceptible and highly susceptible, respectively, to *S. macrospora,* were sown in plastic pots containing 2 kg of Tropstrato® (Vida Verde, Mogi Mirim, São Paulo, Brazil) substrate composed of a 1:1:1 mixture of pine bark, peat and expanded vermiculite. A total of 1.63 g of calcium phosphate monobasic was added to each plastic pot. A total of five seeds were sown per pot, and each pot was thinned to three seedlings five days after seedling emergence. Plants were kept in a greenhouse during the experiments (temperature 28 ± 2°C during the day and 12 ± 4°C at night, relative humidity 70 ± 5%) and were fertilized weekly with 50 mL of a nutrient solution composed of 2.6 mM KCl, 0.6 mM K_2SO_4, 1.2 mM $MgSO_4$, 1.0 mM CH_4N_2O, 1.2 mM NH_4NO_3, 0.0002 mM $(NH_4)_6Mo_7O_{24}$, 0.03 mM H_3BO_4, 0.04 mM $ZnSO_4$, 0.01 mM $CuSO_4$ and 0.03 mM $MnCl_2$. The nutrient solution was prepared using deionized water. Plants were watered as needed.

Inoculum production and inoculation procedure. Plants were inoculated with a monosporic isolate of *S. macrospora* (UFV-DFP *Sm* 01). The isolate of *S. macrospora* was grown in Petri dishes containing oat-agar medium and incubated for 35 days in an incubator (22ºC, photoperiod of 12 h of light and 12 h of darkness). All of the leaves on each plant were inoculated with a conidial suspension of *S. macrospora* (6×10^4 conidia/ml) at 30 days after emergence (growth stage V5) (10) using a VL Airbrush atomizer (Poasche Airbrush Co, Chicago, IL). Gelatin (1% w v^{-1}) was added to the suspension to aid conidial adhesion to the leaf blades. Immediately after inoculation, the plants were transferred to a growth chamber at 25 ± 2ºC, 90 ± 5% relative humidity and a 12 h light: 12 h dark photoperiod for 30 h. After this period, the plants were transferred to a plastic mist growth chamber

781 (MGC) inside a greenhouse for the duration of the experiments. The MGC was made
782 of wood (2 m wide, 1.5 m high and 5 m long) and covered with 100-µm thick
783 transparent plastic. The temperature inside the MGC ranged from 25 ± 2ºC (day) to
784 20 ± 2ºC (night). The relative humidity was maintained at 90 ± 5% using a misting
785 system in which nozzles (model NEB-100; KGF Company São Paulo, Brazil)
786 sprayed mist every 30 min above the plant canopies. The relative humidity and
787 temperature were measured with a thermo-hygrograph (TH-508, Impac, São Paulo,
788 Brazil). The maximum natural photon flux density at plant canopy height was
789 approximately 900 µmol m^{-2} s^{-1}.

790 **Assessment of MLS severity.** The fourth leaves (counted from the base to the
791 top) of each plant per replication of each treatment were marked and collected to
792 evaluate MLS severity at 48, 72, 96, 120 and 168 hours after inoculation (hai). The
793 collected leaves were scanned at 300 dpi resolution and the obtained images were
794 processed using QUANT software (55) to obtain severity (chlorosis and necrosis
795 symptoms) values. The area under disease progress curve (AUDPC) for each leaf in
796 each plant was computed using trapezoidal integration of the MLS progress curves
797 over time using the formula proposed by Shaner and Finney (52).

798 **Photosynthetic measurements.** The leaf gas exchange parameters were
799 simultaneously determined by conducting the measurements of chlorophyll *a*
800 fluorescence using a portable open-flow gas exchange system (LI-6400XT, LI-COR,
801 Lincoln, NE, USA) equipped with an integrated fluorescence chamber head (LI-
802 6400-40, LI-COR Inc.). The net carbon assimilation rate (*A*), stomatal conductance
803 to water vapor (g_s), transpiration rate (*E*) and internal to ambient CO_2 concentration
804 ratio (C_i/C_a) were measured for the fourth leaf of each plant per replication of each
805 treatment at 48, 72, 96, 120 and 168 hai from 10:00 to 13:00 hours (solar time),

which is when *A* was at its maximum under artificial PAR (*i.e.*, 1,200 µmol photons m^{-2} s^{-1} at leaf level and 400 µmol atmospheric CO_2 mol^{-1}). All of the measurements were performed at 25°C and the vapor pressure deficit was maintained at approximately 1.0 kPa, while the amount of blue light was set to 10% of the photosynthetic photon flux density to optimize the stomatal aperture. Previously dark-adapted leaves (30 min) were illuminated with weak modulated measuring beams (0.03 µmol m^{-2} s^{-1}) to obtain the initial fluorescence (F_0). Saturating white light pulses of 8,000 µmol photons m^{-2} s^{-1} were applied for 0.8 s to ensure maximum fluorescence emissions (F_m), from which the variable to maximum chlorophyll fluorescence ratio, $F_v/F_m = [(F_m - F_0)/F_m)]$, was calculated. In light-adapted leaves, the steady state fluorescence yield (F_s) was measured following a saturating white light pulse (8.000 µmol m^{-2} s^{-1}, 0.8 s) that was applied to achieve the light-adapted maximum fluorescence (F_m'). The actinic light was then turned off and far-red illumination was applied (2 µmol m^{-2} s^{-1}) to measure the light-adapted initial fluorescence (F_0'). Using these parameters, the capture efficiency of the excitation energy by the open PSII reaction centers (F_v'/F_m') was estimated as $F_v'/F_m' = (F_m' - F_0')/F_m'$. The coefficient for photochemical quenching (q_P) was calculated as $q_P = (F_m' - F_s)/(F_m' - F_0')$, while that for non-photochemical quenching (NPQ) was calculated as $NPQ = (F_m/F_m') - 1$. The actual quantum yield of PSII electron transport (Φ_{PSII}) was computed as $\Phi_{PSII} = (F_m' - F_s)/F_m'$, from which the electron transport rate (ETR) was calculated as $ETR = \Phi_{PSII} * PPFD * f * \alpha$, where *f* is a factor that accounts for the partitioning of energy between PSII and PSI and is assumed to be 0.5, which indicates that the excitation energy is distributed equally between the two photosystems, and α is the absorbance by the leaf photosynthetic tissues and is assumed to be 0.84 (37).

Determination of the concentration of photosynthetic pigments. The concentrations of chlorophylls (Chl) *a* and *b* and carotenoids were determined using dimethyl sulfoxide (DMSO) as an extractor (51). Five leaf disks (10-mm in diameter) were punched from the fourth leaves at 48, 72, 96, 120 and 168 hai. The collected disks were immersed in glass tubes containing 5 ml of saturated DMSO solution and calcium carbonate ($CaCO_3$) (5 g L^{-1}) (57) and kept in the dark at room temperature for 24 h. The absorbances of the extracts were read at 480, 649.1 and 665.1 nm using a saturated solution of DMSO and $CaCO_3$ as a blank.

Experimental design and data analysis. A 2 × 2 factorial experiment, consisting of two maize cultivars (ECVSCS155 and HIB 32R48H) and non-inoculated or inoculated plants, was arranged in a completely randomized design with six replications. The experiment was repeated three times. Each experimental unit corresponded to a plastic pot containing three plants. A total of 120 plants were used in each experiment (24 plants per treatment at each evaluation time). All variables were subjected to an analysis of variance (ANOVA) and the treatment means were compared by Tukey´s test ($P \leq 0.05$) using SAS software (SAS Institute Inc., Cary, NC). For MLS severity, the ANOVA was considered to be a 2 × 5 factorial experiment, consisting of two maize cultivars and five evaluation times. For the photosynthetic measurements, the concentration of total Chl ($a + b$), concentration of carotenoids and the Chl a/b ratio, ANOVA was considered to be a 2 × 2 × 5 factorial experiment, consisting of two maize cultivars, non-inoculated or inoculated plants and five evaluation times. For each cultivar, the Pearson correlation was used to determine relationships among the photosynthetic measurements and MLS severity, as well as among the concentration of total Chl ($a + b$), concentration of carotenoids and the Chl a/b ratio and MLS severity.

RESULTS

MLS severity and AUDPC. The factors cultivar and evaluation time as well as their interaction had significant effects ($P \leq 0.05$) on MLS severity (Table 1). Cultivar was the only significant factor ($P \leq 0.05$) for AUDPC (Table 1). MLS severity was significantly lower on the leaves of plants from cultivar ECVSCS155 relative to the leaves of plants from cultivar HIB 32R48H (Fig. 1A). From 48 to 168 hai, MLS severity increased from 0.5 to 5.1% on the leaves of plants from cultivar ECVSCS155 and from 1.4 to 8.0% on the leaves of plants from cultivar HIB 32R48H. For plants of cultivar ECVSCS155, AUDPC was significantly reduced by 34.5% compared to plants from cultivar HIB 32R48H (Fig. 1B).

Photosynthetic parameters. At least one of the evaluated factors (cultivar, plant inoculation and evaluation time) as well as some of their interactions were significant ($P \leq 0.05$) for A, g_s, E and C_i/C_a. Plant inoculation was the most important factor due to its higher F values, and it explained the variation in all variables evaluated. The interaction cultivar × plant inoculation × evaluation time was significant only for A, g_s and E (Table 1).

For both cultivars, A, g_s and E significantly decreased from 48 to 168 hai for inoculated plants relative to their non-inoculated counterparts (Fig. 2A-F). Relative to plants of cultivar ECVSCS155, reductions in the values of the above parameters were greater at 168 hai for plants of cultivar HIB 32R48H, with decreases of 56 and 52% for A, 49 and 41% for g_s and 46 and 41% for E in the inoculated plants relative to the non-inoculated ones, respectively. For C_i/C_a, the highest values occurred in the inoculated plants, with significant differences between non-inoculated and inoculated plants of cultivar ECVSCS155 occurring at 96 and 168 hai. For plants of cultivar HIB 32R48H, significant differences occurred only at 168 hai (Fig. 2G and H). The

881 C_i/C_a increased by 33 and 30% at 168 hai for the inoculated plants of cultivars
882 ECVSCS155 and HIB 32R48H, respectively, compared to the non-inoculated plants.
883 There were significant differences between non-inoculated plants of cultivars
884 ECVSCS155 and HIB 32R48H in *A*, g_s, *E* and C_i/C_a. *A* was 7 and 6% higher for
885 plants of cultivar HIB 32R48H than for plants of cultivar ECVSCS155 at 48 and 120
886 hai, respectively (Fig. 2A and B). g_s was significantly higher for plants of cultivar
887 HIB 32R48H than for plants of cultivar ECVSCS155 at 48 (18%), 72 (11%), 96
888 (20%) and 120 (16%) hai (Fig. 2C and D). *E* was significantly higher in plants of
889 cultivar HIB 32R48H than for plants of cultivar ECVSCS155 by 9, 30 and 10% at
890 48, 96 and 120 hai, respectively (Fig. 2E and F). C_i/C_a was higher at 48 (27%) and 72
891 hai (33%) for plants of cultivar HIB 32R48H than for plants of cultivar ECVSCS155
892 (Fig. 2G and H). g_s and C_i/C_a were significantly higher by 21 and 27%, respectively,
893 at 48 hai (Fig. 2C, D, G and H) for the inoculated plants of cultivar HIB 32R48H
894 compared to the inoculated plants of cultivar ECVSCS155.
895 At least one of the evaluated factors (cultivar, plant inoculation and evaluation
896 time) as well as some of their interactions were significant ($P \leq 0.05$) for F_0, F_m,
897 F_v/F_m, F_v'/F_m', q_P, NPQ and ETR (Table 1). The interaction cultivar × plant
898 inoculation × evaluation time was significant only for F_0 and F_v/F_m (Table 1). At 48
899 hai, F_0 significantly increased by 18 and 27% for inoculated plants of cultivars
900 ECVSCS155 and HIB 32R48H, respectively, in comparison to their non-inoculated
901 counterparts (Fig. 3A and B). F_m, F_v/F_m, q_P and ETR significantly decreased in the
902 inoculated plants in comparison to their non-inoculated counterparts (Fig. 3C-F, 4C,
903 D, G and H). However, the reductions in those parameters were larger at 168 hai for
904 plants of cultivar HIB 32R48H than for plants of cultivar ECVSCS155, with
905 decreases of 21 and 19% for F_m (Fig. 3C and D), 22 and 19% for q_P (Fig. 4C and D)

and 31 and 22% for ETR (Fig. 4G and H). The reductions in F_v/F_m were greater at 96, 120 and 168 hai for plants of cultivar HIB 32R48H than for plants of cultivar ECVSCS155, with decreases of 4 and 2%, 5 and 3% and 11 and 6%, respectively (Fig. 3E and F). NPQ increased for inoculated plants of both cultivars in comparison to their non-inoculated counterparts (Fig. 4E and F). In plants of cultivar HIB 32R48H only, NPQ significantly increased at 120 and 168 hai by 11 and 17%, respectively. In the non-inoculated plants, significant differences in F_v/F_m occurred between cultivars at 48 hai (Fig. 3E and F). For the inoculated plants, significant differences between cultivars occurred at 168 hai in F_v/F_m (Fig. 3E and F) and at 120 hai in F_v'/F_m' (Fig. 4A and B).

Concentrations of leaf pigments. At least one of the factors examined (cultivar, plant inoculation and evaluation time) as well as some of their interactions were significant ($P \leq 0.05$) for the concentrations of total Chl ($a + b$) and carotenoids and for the Chl a/b ratio (Table 1). For both cultivars, concentrations of total Chl ($a + b$) and carotenoids significantly decreased for the inoculated plants relative to the non-inoculated ones. The reduction in total Chl ($a + b$) concentration was higher for plants of cultivar ECVSCS155 than for plants of cultivar HIB 32R48H, with decreases of 58 and 49%, respectively. The reduction in the concentration of carotenoids was higher for plants of cultivar HIB 32R48H than for plants of cultivar ECVSCS155, with decreases of 40 and 17% at 168 hai, respectively. The Chl a/b ratio significantly increased in inoculated plants in comparison to non-inoculated plants of both cultivars.

Pearson correlations. For both cultivars, A was positively correlated with g_s and E, and g_s was positively correlated with E, but A, g_s and E were negatively correlated with MLS severity (Table 2). In plants of cultivar HIB 32R48H, C_i/C_a was positively

931 correlated with g_s, while in plants of cultivar ECVSCS155, C_i/C_a was positively
932 correlated with MLS severity (Table 2). For both cultivars, there were significant
933 positive correlations between F_v/F_m and NPQ, total chlorophyll and carotenoids,
934 between q_P and ETR, and between concentrations of total Chl (a + b) and
935 carotenoids. For both cultivars, significant negative correlations occurred between
936 F_v/F_m and Chl a/b ratio, F_v'/F_m' and NPQ, between total Chl (a + b) and Chl a/b ratio
937 and between Chl a/b ratio and concentration of carotenoids. In both cultivars, F_m,
938 F_v/F_m and total Chl (a + b) concentration were negatively correlated with MLS
939 severity (Table 3).
940
941
942
943
944
945
946
947
948
949
950
951
952
953
954

DISCUSSION

This study provides, to the best of the authors´ knowledge, the first physiological evidence associated with the infection process of *S. macrospora* on maize leaves. A decrease in photosynthesis caused by pathogen infection has been reported to occur in several plant species (1,8,9,48,54). In the present study, there was a progressive decline in A, g_s and E in leaves of inoculated plants compared to leaves of non-inoculated plants of both cultivars tested, which was supported by the negative correlation between MLS severity and these parameters. Moreover, the reduction in A at the early stages of fungal infection was proportionally greater than the MLS severity; severity values ranging from 5 to 8% reduced A by 52 and 56% at 168 hai for plants of cultivars ECVSCS155 and HIB 32R48H, respectively. This finding is in agreement with what was reported for interactions between maize and *Phaeosphaeria maydis* (27), bean and *Colletotrichum lindemuthianum* (38) and *Eucalyptus globules and Micosphaerella* spp (43). The reduction in A was proportionally greater than was expected from the apparent reduction in green leaf tissue as a result of the pathogen infection, and therefore evidenced that asymptomatic tissue was also affected by fungal infection. Concomitantly, as reported for other necrotrophic pathogens, the decrease in A in maize leaf tissue asymptomatic for MLS may be explained by the secretion of lytic enzymes or non-selective toxins by *S. macrospora* that easily diffuse into uncolonized leaf tissue, causing maceration and compromising translocation of water and photoassimilates throughout the leaf tissue (31,35,54).

The concomitant decrease in both g_s and E during the infection process of *S. macrospora* in the leaf blades of plants of both cultivars may be associated with stomatal closure and is in accordance with reports on interactions between wheat and

Puccinia recondita f.sp. *tritici* (35) and tomato and *Oidium neolicopersici* (45). Additionally, in the present study, desiccation of the leaf blades was observed as the MLS progressed, suggesting that the stomata of the infected leaves were closed to prevent excessive water loss and therefore contributed to the observed decrease in *E* values. Resende et al. (48) reported that *E* dramatically decreased in sorghum leaves infected by *Colletotrichum sublineolum* as a method of keeping the stomata closed and maintaining a favorable water status within the leaf blades.

Reductions in g_s are usually associated with decreases in C_i and in C_i/C_a (21,25,26). By contrast, data from the present study showed that despite a concomitant decrease in *A* and g_s, there was a progressive increase in C_i/C_a, which may suggest that the decrease in *A* cannot be explained solely by reduction in g_s, but may also be due to a decrease in mesophyll conductance and impairment of the biochemical capacity of the leaves to adequately assimilate CO_2. Reductions in *A* and g_s related to an increase in C_i/C_a have been reported to occur during interactions between *Eucalyptus urophylla and Puccinia psidii* (1), bean and *Uromyces appendiculatus* (34) and barley and *Rhynchosporium secalis* (36). According to these authors, the reduction in *A* was unlikely to have been solely associated with less CO_2 entry into leaves, but rather with some biochemical limitation to CO_2 fixation at the chloroplast level. Frequently, alterations in leaf photochemistry and carbon metabolism are related to reduced activity of ribulose bisphosphate carboxylase and changes in the capacity for ribulose bisphosphate regeneration (38,40).

Regardless of the maize cultivar, both F_0 and NPQ tended to be higher in the leaves of inoculated plants than in the leaves of non-inoculated plants, suggesting that the PSII reaction centers were somehow damaged or that the transfer of excitation energy from the antenna to the reaction center was impaired (5,13,37).

1006 According to Plazek et al. (44), an increase in the F_0 values on barley leaves infected
1007 with *Bipolaris sorokimiana* was an indicator of antenna damage.

1008 Despite the observed increases in NPQ values, the non-photochemical dissipation
1009 was insufficient to avoid photoinhibitory damage, which was evidenced in decreases
1010 in F_m and F_v/F_m values in the leaves of inoculated plants from both cultivars and was
1011 also supported by the negative correlations of F_m and F_v/F_m with MLS severity. ETR
1012 and q_P decreased in the leaves of inoculated plants of both cultivars, as indicated by
1013 the negative correlations of ETR and q_P with MLS severity. The observed decreases
1014 in q_P could be related to increases in the fraction of reduced Q_A (Q_A^{-}) in PSII, which
1015 indicates an increased possibility for photoinhibition to be affected (5) and, therefore,
1016 the electron transport chain to PSI via the cytochrome b_6/f complex and plastocyanin
1017 (13). Additionally, the decreases in F_v/F_m were accompanied by decreases in F_v'/F_m',
1018 suggesting that the ability of the *S. macrospora* infected leaves to capture and to
1019 transfer collected energy was dramatically compromised.

1020 The concentration of pigments was negatively impacted in the leaves of
1021 inoculated plants from both cultivars as the MLS progressed. The concentration of
1022 total Chl (*a* + *b*) decreased with the progress of MLS, which may have led to an
1023 increase in the Chl *a*/*b* ratio. The reduction in chlorophyll concentration could be
1024 associated with the action of lytic enzymes and non-selective toxins released in the
1025 infected tissues by *S. macrospora,* in accordance with reports on maize leaves
1026 infected with *Exserohilum turcicum* (20). Additionally, the decrease in total Chl (*a* +
1027 *b*) concentration would lead to a reduction in the ability and the efficiency of the
1028 leaves to capture the energy required for the photochemical reactions in
1029 photosynthesis (20).

In conclusion, the results from the present study demonstrate, for the first time, that photosynthesis in the leaves of maize plants is dramatically impacted during the infection process of *S. macrospora*, and impacts are primarily associated with limitations of a diffusive and biochemical nature.

ACKNOWLEDGMENTS

Prof. F. A. Rodrigues thanks the National Council for Technological and Scientific Development (CNPq) for his fellowship. Mrs. M. B. Bermúdez-Cardona was supported by the "Programa de Estudante-Convênio de Pós-Graduação" (PEC-PG) from CAPES and also by the Scholarship Program of the Tolima University, Colômbia. The authors thank Mrs. D. Rezende and Mr. C. E. Aucique Perez for their technical assistance. This study was supported by grants from CAPES, CNPq and the Fundação de Amparo a Pesquisa do Estado de Minas Gerais (FAPEMIG) to Prof. F. A. Rodrigues.

LITERATURE CITED

1. Alves, A. A., Guimarães, L. M. S., Chaves, A. R. M., DaMatta, F. M., and Alfenas, A. C. 2011. Leaf gas exchange and chlorophyll *a* fluorescence of *Eucalyptus urophylla* in response to *Puccinia psidii* infection. Acta Physiol. Plant. 33:1831-1839.

2. Anderson, B., and White, D. G. 1987. Fungi associated with corn stalks in Illinois in 1982 and 1983. Plant Dis. 71:135-137.

3. Anderson, B., and White, D. G. 1994. Evaluation of methods for identification of corn genotypes with stalk rot and lodging resistance. Plant Dis. 78:590-593.

4. Baker, N. R., Oxborough, K., Lawson, T., and Morison, J. I. L. 2001. High resolution imaging of photosynthetic activities of tissues, cells and chloroplast in leaves. J. Exp. Bot. 52:615-621.

5. Baker, N. R. 2008. Chlorophyll fluorescence: a probe of photosynthesis In Vivo. Annu. Rev. Plant Biol. 59:89-113.

6. Bampi, D., Casa, R. T., Bogo, A., Sangoi, L., Sachs, C., Bolzan, J. M., and Piletti, G. 2012. Fungicide performance on the control of macrospora leaf spot in corn. Summa Phytopathol. 38:319-322.

7. Barón, M., Flexas, J., and Delucia, E. H. 2012. Photosynthetic responses to biotic stress. Pages 331-351. in: Terrestrial photosynthesis in a changing environment a molecular, physiological and ecological approach. J. Flexas, F. Loreto, and H. Medrano, eds. Cambridge University Press.

8. Bassanezi, R. B., Amorim, L., and Bergamin Filho, A. 2000. Análise das trocas gasosas em feijoeiro com ferrugem, mancha angular e antracnose. Fitopatol. Bras. 25:643-650.

9. Bassanezi, R. B., Amorim, L., Bergamin Filho, A., and Berger, R. D. 2002. Gas exchange and emission of chlorophyll fluorescence during the monocycle of rust, angular leaf spot and anthracnose on bean leaves as a function of their trophic characteristics. J. Phytopathol. 150:37-47.

10. Bensch, M. J., Van Staden, J., and Rijkenberg, F. H. J. 1992. Time and site inoculation of maize for optimum infection of ears by *Stenocarpella maydis*. J. Phytopathol. 136:265-269.

11. Berger, S., Papadopoulos, M., Schreiber, U., Kaiser, W., and Roitsch, T. 2004. Complex regulation of genes expression, photosynthesis and sugar levels by pathogen infection in tomato. Physiol. Plantarum 122:419-428.

12. Berger, S., Sinha, A. K., and Roitsch, T. 2007. Plant physiology meets phytopathology: plant primary metabolism and plant-pathogen interactions. J. Exp. Bot. 58:4019-4026.

13. Bolhàr-Nordenkampf, H. R., Long, S. P., Baker, N. R., Oquist, G., Schreibers, U., and Lechner, E. G. 1989. Chlorophyll fluorescence as a probe of the photosynthetic competence of leaves in the field: a review of current instrumentation. Funct. Ecol. 3:497-515.

14. Bowden, R. L., Rouse, D. L., and Sharkey, T. D. 1990. Mechanism of photosynthesis decrease by *Verticillium dahliae* in potato. Plant Physiol. 94:1048-1055.

15. Casa, R. T., Zambolim, L., and Reis, E. M. 1998. Transmissão e controle de *Diplodia* em sementes de milho. Fitopatol. Bras. 23:436-441.

16. Casa, R. T., Reis, E. M., and Zambolim, L. 2003. Decomposição dos restos culturais do milho e sobrevivência saprofítica de *Stenocarpella macrospora* e *Stenocarpella maydis*. Fitopatol. Bras. 28:355-361.

1105 17. Casa, R. T., Reis, E. M., and Zambolim, L. 2004. Dispersão vertical e
1106 horizontal de conídios de *Stenocarpella macrospora* e *Stenocarpella maydis*.
1107 Fitopatol. Bras. 29:141-147.
1108 18. Casa, R. T., Reis, E. M., and Zambolim, L. 2006. Doenças do milho causadas
1109 por fungos do gênero *Stenocarpella*. Fitopatol. Bras. 31:427-439.
1110 19. CIMMYT, 2012. Maize Annual Report: Research Program on Maize.
1111 CGIAR. 28 p.
1112 20. Chauhan, R. S., Singh, B. M., and Develash, R. K. 1997. Effect of toxic
1113 compounds of *Exserohilum turcicum* on chlorophyll content, callus growth and cell
1114 viability of susceptible and resistant inbred lines of maize. J. Phytopathol. 145:435-
1115 440.
1116 21. Chaves, M. M., Flexas, J., and Pinheiro, C. 2009. Photosynthesis under
1117 drought and salt stress: regulation mechanisms from whole plant to cell. Ann. Bot.
1118 103:551-560.
1119 22. Dai, K., Nagai, M., Sasaki, H., Nakamura, H., Tachechi, K., and Warabi, M.
1120 1987. Detection of *Diplodia maydis* (Berkeley) Saccardo from imported corn seed.
1121 Res. Bull. Plant Protect. Serv. 23:1-6.
1122 23. Erickson, J. E., Stanosz, G. R., and Kruger, E. L. 2003. Photosynthetic
1123 consequences of marssonina leaf spot differ between two poplar hybrids. New
1124 Phytol. 161:577-583.
1125 24. Flett, B. C., and Wehner, F. C. 1991. Incidence of *Stenocarpella* and
1126 *Fusarium* cob rots in monoculture maize under different tillage systems. J.
1127 Phytopathol. 133:327-333.
1128 25. Flexas, J., Ribas-Carbó, M., Bota, J., Galmés, J., Henkle, M., Martínez-
1129 Cañellas, S., and Medrano, H. 2006. Decreased rubisco activity during water stress is

1130 not induced by decreased relative water content but related to conditions of low
1131 stomatal conductance and chloroplast CO_2 concentration. New Phytol. 172:73-82.
1132 26. Flexas, J., Diaz-Espejo, A., Galmés, J., Kaldenhoff, R., Medrano, H., and
1133 Ribas-Carbo, M. 2007. Rapid variations of mesophyll conductance in response to
1134 changes in CO_2 concentration around leaves. Plant Cell Environ. 30:1284-1298.
1135 27. Godoy, C. V., Amorin, L., and Bergamin Filho, A. 2001. Alterações na
1136 fotossíntese e na transpiração de folhas de milho infetadas por *Phaeosphaeria*
1137 *maydis*. Fitopatol. Bras. 26:209-215.
1138 28. Govindjee. 2004. Chlorophyll *a* fluorescence: a bit of basic and history. Pages 1-
1139 42. in: Chlorophyll a fluorescence: a signature of photosynthesis. G. C.
1140 Papageorgiou, and Govindgee, eds. Kluver Academic Publishers.
1141 29. Kramer, D M., Johnson, G., Kirats, O., and Edwards, G. E. 2004. New
1142 fluorescence parameters for the determination of Q_A redox state and excitation
1143 energy fluxes. Photosynth. Res. 79:209-218.
1144 30. Krause, G. H., and Weis, E. 1991. Chlorophyll fluorescence and photosynthesis:
1145 the basics. Annu. Rev. Plant Physiol. Plant Mol. Biol. 42:313-349.
1146 31. Laluk, K., and Mengiste, T. 2010. Necrotroph attacks on plants: wanton
1147 destruction or covert extortion? The Arabidopsis Book. 12:1-34.
1148 32. Latterell, F. M., and Rossi, A. E. 1983. *Stenocarpella macrospora* (=*Diplodia*
1149 *macrospora*) and *S. maydis* (=*D. maydis*) compared as pathogens of corn. Plant Dis.
1150 67:725-729.
1151 33. Lobell, D. B., Cassman, K. G., and Field, C. B. 2009. Crop yield gaps: their
1152 importance, magnitudes and causes. Annu. Rev. Env. Resour. 34:179-204.
1153 34. Lopes, D. B., and Berger, R. D. 2001. The effects of rust and anthracnose on
1154 the photosynthetic competence of diseased bean leaves. Phytopathology 91:212-220.

1155 35. McGrath, M. T., and Pennypacker, S. P. 1990. Alteration of physiological
1156 processes in wheat flag leaves caused by stem rust and leaf rust. Phytopathology
1157 80:677-686.
1158 36. Martin, P. J. 1986. Gaseous exchanges studies of barley leaves infected with
1159 *Rhynchosporium secalis* (Oudem) J. J. Davis. Physiol. Mol. Plant Pathol. 28:3-14.
1160 37. Maxwell, K., and Johnson, G. N. 2000. Chlorophyll fluorescence - a practical
1161 guide. J. Exp. Bot. 51:659-668.
1162 38. Meyer, S., Saccardy-Adjl, K., Rizza, F., and Genty, B. 2001. Inhibition of
1163 photosynthesis by *Colletotricum lindemuthianum* in bean leaves determined by
1164 chlorophyll fluorescence imaging. Plant Cell Environ. 24:947-955.
1165 39. Muimba, K. A., and Bergstrom, G. C. 2011. Reduced anthracnose stalk rot in
1166 resistant maize is associated with restricted development of *Colletotrichum*
1167 *graminicola* in pith tissues. J. Phytopathol. 159:329-341.
1168 40. Nogués, S., Cotxarrera, L., Alegre, L., and Trillas, M. I. 2002. Limitations to
1169 photosynthesis in tomato leaves induced by *Fusarium* wilt. New Phytol. 154:461-
1170 470.
1171 41. Olatinwo, R., Cardwell, K., Menkin, A., Deadman, M., and Julian, A. 1999.
1172 Inheritance of resistance to *Stenocarpella macrospora* (Earle) ear rot of maize in the
1173 mid-altitude zone of Nigeria. Eur. J. Plant Pathol. 105:535-543.
1174 42. Owera, S. A. P., Farrar, J. F., and Whitbread, R. 1981. Growth and
1175 photosynthesis in barley infected with brown rust. Physiol. Plant Pathol. 18:79-90.
1176 43. Pinkard, E. A., and Mohammed, C. L. 2006. Photosynthesis of *Eucalyptus*
1177 *globulus* with Mycosphaerella leaf disease. New Phytol. 170:119-127.

1178 44. Plazek, A., Rapacz, M., and Hura, K. 2004. Relationship between quantum
1179 efficiency of PSII and cold-induced plant resistance to fungal pathogens. Acta
1180 Physiol. Plant. 26:141-148.
1181 45. Prokopová, J., Mieslerová, B., Hlavácková, V., Hlavinka, J., Lebeda, A.,
1182 Naus, J., and Spundová, M. 2010a. Changes in photosynthesis of Lycopersicon spp.
1183 plants induced by tomato powdery mildew infection in combination with hear shock
1184 pre-treatment. Physiol. Mol. Plant Pathol. 74:205-213.
1185 46. Prokopová, J., Spundová, M., Sedlárová, M., Husicková, A., Novotný, R.,
1186 Doleizal, K., Naus, J., and Lebeda, A. 2010b. Photosynthetic responses of lettuce to
1187 downy mildew infection and cytokinin treatment. Plant Physiol. Biochem. 48:716-
1188 723.
1189 47. Reis, E. M., and Mario, J. L. 2003. Quantification of Diplodia macrospora
1190 and D. maydis inoculum in crop residues, in the air, and its relationship with
1191 infection of corn kernels. Fitopatol. Bras. 28:143-147.
1192 48. Resende, R. S., Rodrigues, F. A., Cavatte, P. C., Martins, S. C. V., Moreira,
1193 W. R., Chaves, A. R. M., and DaMatta, F. M. 2012. Leaf gas exchanges and
1194 oxidative stress in sorghum plants supplied with silicon and infected by
1195 *Colletotrichum sublineolum*. Phytopathology 102:892-898.
1196 49. Rohácek, K. 2002. Chlorophyll fluorescence parameters: the definitions,
1197 photosynthetic meaning, and mutual relationships. Photosynthetica 40:13-29.
1198 50. Rolfe, S. A., and Scholes, J. D. 2010. Chlorophyll fluorescence imaging of
1199 plant-pathogen interaction. Protoplasma 247:163-175.
1200 51. Santos, R. P., Cruz, A. C. F., Iarema, L., Kuki, K. N., and Otoni, W. C. 2008.
1201 Protocolo para extração de pigmentos foliares em porta-enxertos de videira
1202 micropropagados. Ceres 55:356-364.

52. Shaner, G., and Finney, R. E. 1977. The effect of nitrogen fertilization on the expression of slow-mildewing resistance in Knox wheat. Phytopathology 67:1051-1056.

53. Sholes, J. D., and Rolfe, S. A. 2009. Chlorophyll fluorescence imaging as tool for understanding the impact of fungal diseases on plant performance: a phenomics perspective. Funct. Plant Biol. 36:880-892.

54. Shtienberg, D. 1992. Effects of foliar diseases on gas exchanges processes: a comparative study. Phytopathology 82:760-765.

55. Vale, F. X. R., Fernandes Filho, E. I., and Liberato, J. R. 2003. A software plant disease severity assessment. In 8th International Congress of Plant Pathology. Volume 2, 105 pp. Christchurch, New Zealand.

56. van Kan, J. A. L. 2006. Licensed to kill: the lifestyle of a necrotrophic plant pathogen. Trends Plant Sci. 11:248-253.

57. Wellburn, A. R. 1994. The spectral determination of chlorophylls *a* and *b*, as well as total carotenoids, using various solvents with spectrophotometers of different resolution. J. Plant Physiol. 144:307-313.

58. White, D. G. 1999. Compendium of corn diseases. 3rd Ed. St. Paul, MN, USA: The American Phytopythological Society.

LIST OF TABLES AND FIGURES

Variables	C	PI	ET	C × PI	C × ET	PI × ET	C × PI × ET
	F-based P values[a]						
Sev	< 0.001	-	< 0.001	-	< 0.001	-	-
AUDPC	< 0.001	-	-	-	-	-	-
A	0.011	< 0.001	< 0.001	0.472	0.001	< 0.001	0.002
g_s	< 0.001	< 0.001	< 0.001	< 0.001	< 0.001	< 0.001	0.001
E	< 0.001	< 0.001	< 0.001	< 0.001	< 0.001	< 0.001	< 0.001
C_i/C_a	< 0.001	< 0.001	< 0.001	0.066	0.003	< 0.001	0.076
F_0	0.243	< 0.001	< 0.001	0.020	0.270	< 0.001	0.035
F_m	0.413	< 0.001	0.002	0.398	0.458	< 0.001	0.771
F_v/F_m	0.001	< 0.001	< 0.001	< 0.001	0.008	< 0.001	< 0.001
F_v'/F_m'	< 0.001	< 0.001	0.070	0.981	0.135	0.461	0.273
q_P	0.169	< 0.001	< 0.001	0.874	0.809	0.001	0.174
NPQ	0.002	< 0.001	0.779	0.358	0.041	< 0.001	0.304
ETR	0.130	< 0.001	< 0.001	0.445	0.698	0.282	0.181
Chl	0.293	< 0.001	< 0.001	0.272	0.671	< 0.001	0.823
Car	0.028	< 0.001	< 0.001	0.069	0.042	< 0.001	< 0.001
Chl *a*/*b*	0.006	< 0.001	< 0.001	0.523	< 0.001	< 0.001	0.014

[a]Levels of probability: [ns] = not significant, * = 0.05

TABLE 2. Pearson correlation coefficients among the net carbon assimilation rate (A), stomatal conductance to water vapor (g_s), transpiration rate (E), internal to ambient CO_2 concentration ratio (C_i/C_a) and macrospora leaf spot severity (Sev) on the leaves of plants from two maize cultivars.

Variables	A	g_s	E	C_i/C_a	Sev
A		0.781**	0.729**	-0.391	-0.867 **
g_s	0.753**		0.743**	0.255	-0.608**
E	0.762**	0.643**		-0.033	-0.551**
C_i/C_a	-0.239	0.425**	-0.106		0.462*
Sev	-0.870**	-0.617**	-0.571**	0.240	

The values above and below the diagonal are the measurements made on plants from ECVSCS155 and HIB 32R48H cultivars, respectively. Levels of probability * = 0.05 and ** = 0.01.

TABLE 3. Pearson correlation coefficients among the initial fluorescence (F_0), maximum fluorescence (F_m), maximum photochemical efficiency of PSII (F_v/F_m), capture efficiency of excitation energy by the open PSII reaction centers (F_v'/F_m'), coefficient for photochemical quenching (q_P), non-photochemical quenching (NPQ), electron transport rate (ETR), concentrations of total chlorophyll *a* +*b* (Chl) and carotenoids (Car) and chlorophyll *a*/*b* ratio and macrospora leaf spot severity (Sev) on the leaves of plants from two maize cultivars.

Variables	F_0	F_m	F_v/F_m	F_v'/F_m'	q_P	NPQ	ETR	Chl	Chl *a/b*	Car	Sev
F_0		0.757**	0.137	0.055	-0.267	0.455*	-0.165	-0.036	0.024	-0.022	0.110
F_m	0.205		0.747**	0.041	0.085	0.164	0.066	0.493*	-0.276	0.398	-0.460*
F_v/F_m	-0.615**	0.641**		-0.001	0.383	0.407*	0.247	0.778**	-0.430*	0.480*	-0.814**
F_v'/F_m'	-0.049	-0.141	0.043		0.021	-0.591**	0.689**	-0.248	0.251	-0.396	-0.140
q_P	-0.355	0.027	0.301	-0.456*		0.039	0.721**	0.420*	-0.165	0.349	-0.501*
NPQ	-0.273	0.353	0.665**	-0.447*	0.330		-0.484*	0.306	-0.289	0.360	0.006
ETR	-0.308	-0.083	0.209	0.273	0.692**	-0.069		0.119	0.059	-0.024	-0.451*
Chl	0.546**	0.248	0.625**	-0.188	0.294	0.129	0.212		-0.796**	0.855**	-0.718**
Chl *a/b*	0.565**	-0.402*	-0.763**	0.115	-0.148	-0.207	-0.071	-0.827**		-0.876**	0.361
Car	-0.477**	0.386	0.668**	-0.331	0.304	0.271	0.108	0.918**	-0.941**		0.396
Sev	0.401*	-0.615**	-0.814**	0.142	-0.371	-0.089	0.288	-0.591**	0.749**	-0.683**	

The values above and below the diagonal are the measurements made on plants from ECVSCS155 and HIB 32R48H cultivars, respectively. Levels of probability * = 0.05 and ** = 0.01.

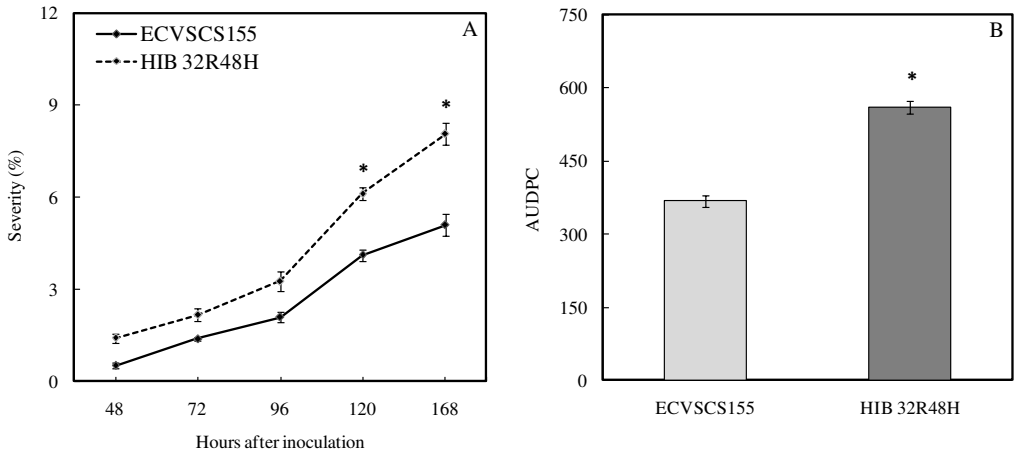

Fig. 1. Macrospora leaf spot progress curves (A) and area under disease progress curve (AUDPC) (B) on leaves of plants from maize cultivars ECVSCS155 and HIB 32R48H. Means from cultivars ECVSCS155 and HIB 32R48H followed by an asterisk (*) for each evaluation time are significantly different ($P \leq 0.05$) by Tukey´s test. Bars represent standard errors of the means. $n = 5$. Three experiments were conducted with consistent results; results from one representative experiment are shown.

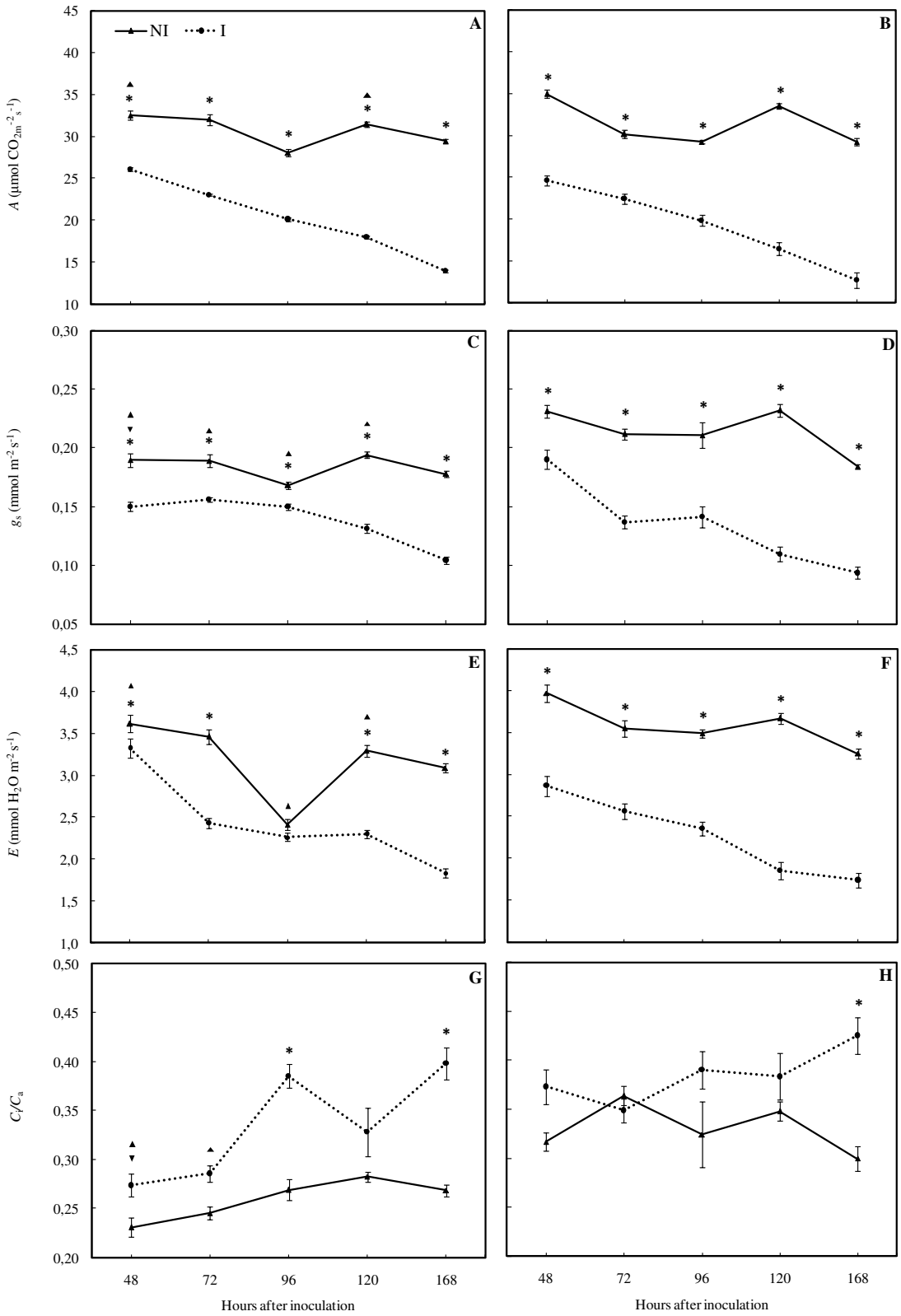

1317

1318

1319

Fig. 2. Leaf gas exchange parameters, including net carbon assimilation rate (A) (A and B), stomatal conductance to water vapor (g_s) (C and D), transpiration rate (E) (E and F) and internal to ambient CO_2 concentration ratio (C_i/C_a) (G and H) determined in leaves of maize plants from cultivars ECVSCS155 (A, C, E, G) and HIB 32R48H (B, D, F, H) non-inoculated (NI) or inoculated (I) with *Stenocarpela macrospora*. Means for the NI and I treatments for each cultivar followed by an asterisk (*) at each evaluation time are significantly different ($P \leq 0.05$) by Tukey´s test. The symbols ▲ and ▼ indicate differences between the cultivars ECVSCS155 and HIB 32R48H, respectively, for NI and I treatments at each evaluation time according to Tukey´s test ($P \leq 0.05$). Bars represent standard errors of the means. $n = 6$. Three experiments were conducted with consistent results; results from one representative experiment are shown.

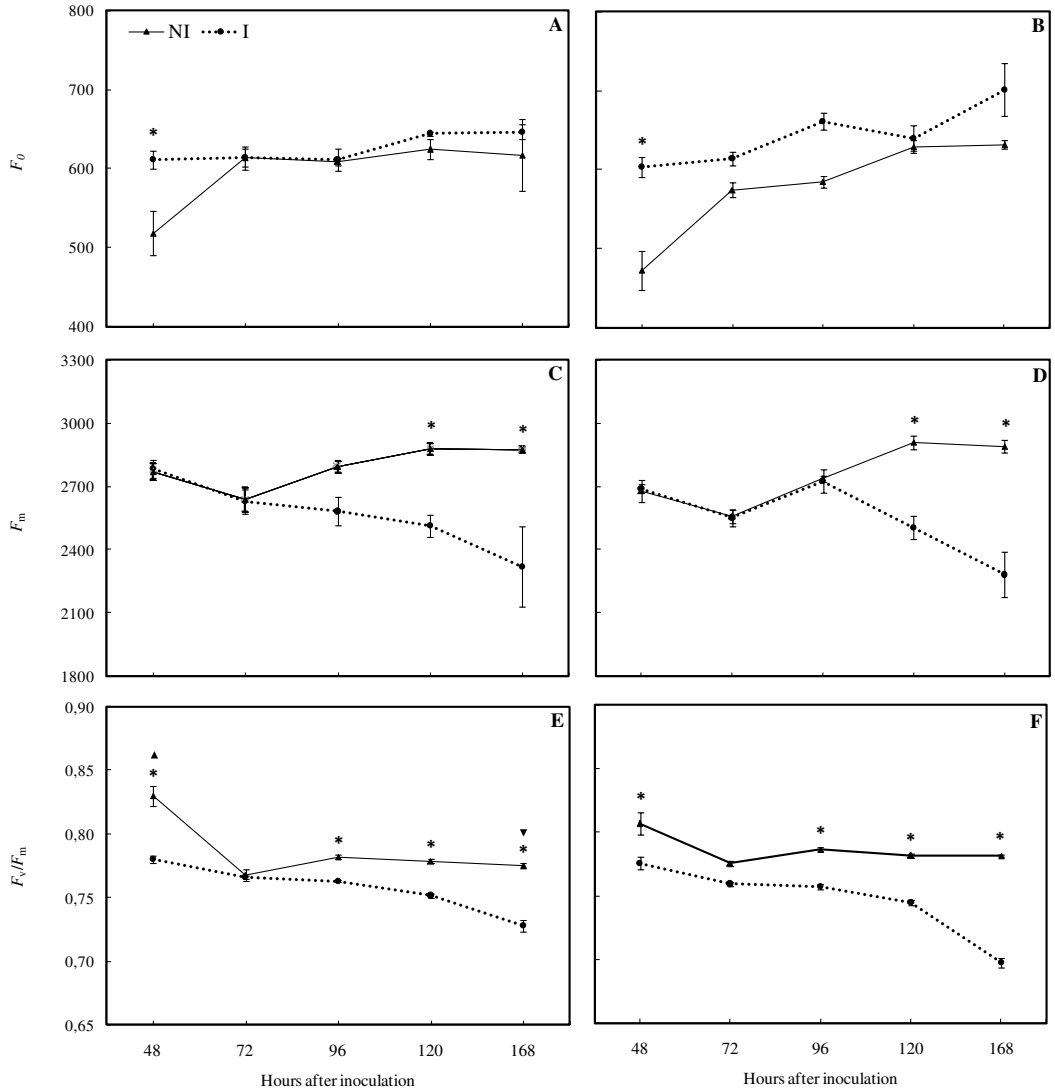

Fig. 3. The initial fluorescence (F_0) (A and B), maximum fluorescence (F_m) (C and D) and maximum PSII quantum efficiency (F_v/F_m) (E and F) determined in leaves of maize plants from cultivars ECVSCS155 (A, C, E) and HIB 32R48H (B, D, F) non-inoculated (NI) or inoculated (I) with *Stenocarpela macrospora*. Means for the NI and I treatments for each cultivar followed by an asterisk (*) at each evaluation time are significantly different ($P \leq 0.05$) by Tukey´s test. The symbols ▲ and ▼ indicate differences between cultivars ECVSCS155 and HIB 32R48H, respectively, for NI and I treatments at each evaluation time according to Tukey´s test ($P \leq 0.05$). Bars represent standard errors of the means. $n = 6$. Three experiments were conducted with consistent results; results from one representative experiment are shown.

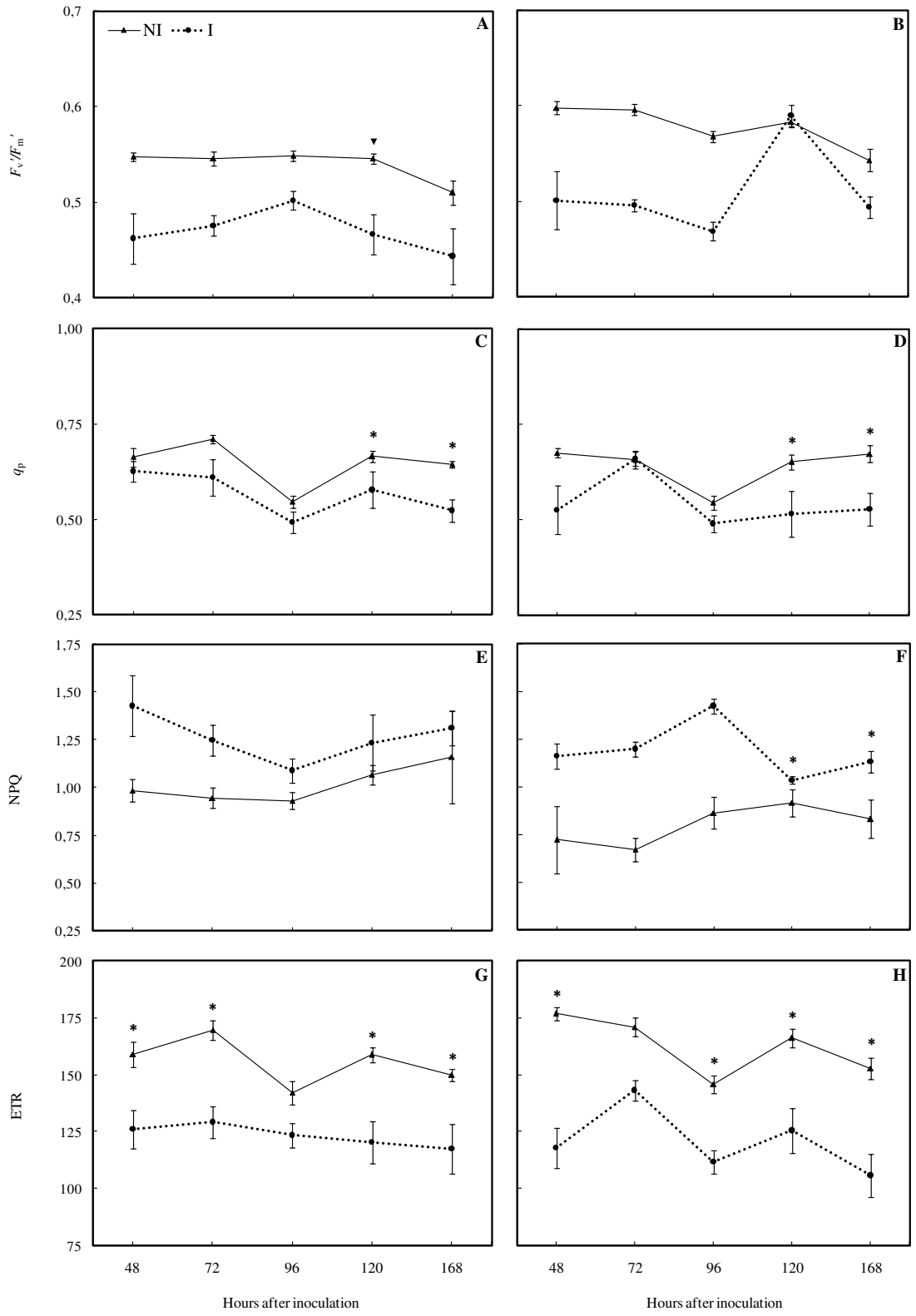

1344

1345

1346

Fig. 4. The capture efficiency of excitation energy by the open PSII reaction centers (F_v'/F_m') (A and B), coefficient for photochemical quenching (q_P) (C and D), non-photochemical quenching (NPQ) (E and F) and electron transport rate (ETR) (G and H) determined in leaves of maize plants from cultivars ECVSCS155 (A, C, E, G) and HIB 32R48H (B, D, F, H) non-inoculated (NI) or inoculated (I) with *Stenocarpela macrospora*. Means for the NI and I treatments for each cultivar followed by an asterisk (*) at each evaluation time are significantly different ($P \leq 0.05$) by Tukey´s test. The symbols ▲ and ▼ indicate differences between cultivars ECVSCS155 and HIB 32R48H, respectively, for NI and I treatments at each evaluation time according to Tukey´s test ($P \leq 0.05$). Bars represent standard errors of the means. $n = 6$. Three experiments were conducted with consistent results; results from one representative experiment are shown.

CHAPTER 3

Physiological and biochemical alterations on maize leaves infected by *Stenocarpella macrospora*

Maria Bianney Bermúdez Cardona*, Wilka Messner da Silva Bispo and Fabrício Ávila Rodrigues

Universidade Federal de Viçosa, Departamento de Fitopatologia, Laboratório da Interação Planta-Patógeno, Viçosa, Minas Gerais State, Zip Code 36.570-900, Brazil

ABSTRACT

Bermúdez-Cardona, M., Messner, W. S. B., and Rodrigues, F. A. 2014. Physiological and biochemical alterations on maize leaves infected by *Stenocarpella macrospora*. Phytopathology 104:xx-xx

This study aimed to analyze the photosynthetic performance and antioxidative systems through the chlorophyll *a* fluorescence imaging, the activities of some antioxidative enzymes and the concentration of ROS in leaves of plants from two maize cultivars (ECVSCS155 and HIB 32R48H) susceptible and highly susceptible, respectively, infected with *Stenocarpella macrospora*. Regardless of maize cultivar, the first changes were observed at 48 hai for all parameters of chlorophyll *a* fluorescence which prominently increased as the MLS progressed. Decreases in maximum fluorescence, maximum PSII quantum efficiency, effective PSII quantum yield and quantum yield of regulated energy dissipation coupled with increases in initial fluorescence and quantum yield of nonregulated energy dissipation were directly related to the progressive loss of photosynthetic activity. In both cultivars the

enzymatic and non-enzymatic components of the antioxidative system were both dramatically altered on infected leaves. The SOD, CAT, POX, APX, GR, GPX and GST activities as well as the concentrations of AsA and GSH+GSSG were quite higher at the early stages of fungal infection, but suffered accentuated decreases as the MLS progressed suggesting the occurrence of an initial mechanism defense from the host's side. As the symptoms of MLS on maize leaves become more drastic, the activities of these enzymes, and the concentration of metabolites buffers decreased. Although, H_2O_2 and MDA concentration increased contributing, therefore, for the intensification of lipid peroxidation upon damage to cell membranes.

INTRODUCTION

Macrospora leaf spot (MLS), caused by *Stenocarpella macrospora* Earle) Sutton (syn. *Diplodia macrospora* Earle) (26,57,96), has resulted in maize yield losses mainly in the tropical and subtropical regions worldwide (3,29,31,69). Under warm and humid conditions, elliptical brown lesions with yellow or orange edges, which may have dark concentric rings, quickly expand on leaf blades (3,29). Pycnidia are produced on the necrotic lesions from which conidia are extruded in long cirri and easily dispersed by insects, rain and wind (3,26,27,28). Maize residue management, use of healthy seed and crop rotation are the most important strategies to control MLS (29) considering the limited efficiency of the fungicides and the unavailability of resistant cultivars (13,72).

Pathogen infection can leads to decrease in photosynthetic efficiency, which is frequently associated with direct damage to the photosynthetic apparatus and consequently with alteration in the balance between light energy absorption and light energy utilization via the Calvin-Benson cycle (60,82). This unbalance can cause inactivation of electrons transport and irreversible photodamage to the reaction centers proteins, with direct effect on the operating efficiency of PSII (Φ_{PSII}) (7,65). The photosynthetic electron transport system is considered one of the major sources for photoreduction of molecular oxygen, with higher potential to generate reactive oxygen species (ROS) (8,21,60,95). Which involves the production of superoxide anion (O_2^-), hydroxyl radical (HO^-) as well as nonradical molecules like hydrogen peroxide (H_2O_2) and singlet oxygen ($^1O_2$) (6,86). One other hand, the rapid host defense reaction against pathogen infection is also related with the oxidative burst induction (20,88,97). It is widely know that the ROS can lead to the oxidative destruction of the cells (8,10,19), which can result from oxidative processes such as

membrane lipid peroxidation, protein oxidation, enzyme inhibition and DNA and RNA damage (45,48,86).

Nevertheless, plants are provided of different protection and repair mechanism to prevent photodamage and to maintain the physiological integrity of photosynthetic apparatus (60). The first protection mechanism is related with regulatory energy dissipation of excess absorbed light (95). Thus, chlorophyll *a* fluorescence imaging is a useful tool to estimate the operating quantum efficiency of photosystem II (PSII), which can be used to reveal heterogeneous patterns of photosynthetic performance occurring within of leaf tissue infected with pathogens (11,18,90). Rapid alteration in the intensity of chlorophyll *a* fluorescence in the chloroplast is correlated with any photooxidative impairment of the photosynthetic apparatus (11). The underlying theoretical base of this technique is the fact that the chlorophyll *a* fluorescence yield of PSII is variable as a result of competition with photochemical and non-photochemical processes and this interaction that allows changes in chlorophyll *a* fluorescence yield to be used to measure photosynthetic function (53,81,82).

According to Rolfe and Scholes (82), infection by pathogens often leads to complex alteration in fluorescence emission; however, a typical host response observed in an host-fungal interaction is an initial reduction in the operating efficiency of PSII of light adapted leaves (Φ_{PSII}), an decrease in the maximum PSII quantum efficiency (F_v/F_m) and increase in the non-photochemical quenching (NPQ), but at advanced stages of fungal infection, the values of these parameters decline because the photosynthetic apparatus is destroyed. These findings were confirmed by Meyer (66), who examined the impact of the necrotrophic phase of *Colletotrichum lindemuthianum* on bean leaves by measurements of chlorophyll *a* fluorescence imaging. According to the author, in the necrotic tissues, the

photosynthetic apparatus was largely destroyed, concomitantly, F_v/F_m decreased and NPQ increased in neighboring green tissue.

The second protection mechanism is the effective re-oxidation of the reduction equivalents, which includes the water-water cycle, the photorespiration, the malate valve and the antioxidative system (36,95). The antioxidative systems is of complex arrays of enzymatic and nonenzymatic systems that detoxify the ROS (10,76). Enzymatic ROS scavenging mechanisms in plants include the enzymes superoxide dismutase (SOD), catalase (CAT), the ascorbate-glutathione (AsA-GSH) and glutathione peroxidase (GPX) cycles (6,19). The SOD act as the first line of defense again ROS, dismutating O_2^- to H_2O_2 in the cytosol, chloroplast and mitochondria (2). The CAT is the primary H_2O_2 scavenger in the peroxisomes and mitochondria (76). Moreover, H_2O_2 generated in the cytosol, chloroplast, mitochondria and peroxisomes is also scavenged by enzymes of AsA-GSH cycle such as ascorbate peroxidase (APX) and glutathione reductase (GR) and by GPX cycle (6,86). Complementarily, nonenzymatic ROS scavenging mechanisms include the major cellular redox buffer ascorbate (AsA) and glutathione (GSH) (9,71). Able (1) reported increases in the concentration of H_2O_2 and O_2^- in barley leaves infected by *Pyrenophora teres*. Accumulation of H_2O_2 and enhanced activities of H_2O_2 scavenging enzymes occurred on leaves of *Lactuca* spp. infected with *Bremia lactucae* (84). Additionally, the ROS can also be considered as secondary messengers involved in the activation of stress-response signal transduction defense pathway (6,37,47,67).

Considering the limited information on the maize-*S. macrospora* interaction at the biochemical and physiological levels, this study aimed to fill out this gap by investigating the spatial-temporal alterations on photosynthetic performance and antioxidative systems on leaves of maize plants during the fungal infection process

through the chlorophyll *a* fluorescence imaging, the activities of some antioxidative enzymes and the concentration of ROS.

MATERIALS AND METHODS

Plant cultivation. Maize seeds from cultivars ECVSCS155 and HIB 32R48H, susceptible and highly susceptible, respectively, to *S. macrospora,* were sown in plastic pots containing 2 kg of Tropstrato® (Vida Verde, Mogi Mirim, São Paulo, Brazil) substrate composed of a 1:1:1 mixture of pine bark, peat and expanded vermiculite. A total of 1.63 g of calcium phosphate monobasic was added to each plastic pot. A total of five seeds were sown per pot, and each pot was thinned to three seedlings five days after seedling emergence. Plants were kept in a greenhouse during the experiments (temperature 28 ± 2°C during the day and 12 ± 4°C at night, relative humidity 70 ± 5%) and were fertilized weekly with 50 mL of a nutrient solution composed of 2.6 mM KCl, 0.6 mM K_2SO_4, 1.2 mM $MgSO_4$, 1.0 mM CH_4N_2O, 1.2 mM NH_4NO_3, 0.0002 mM $(NH_4)_6Mo_7O_{24}$, 0.03 mM H_3BO_4, 0.04 mM $ZnSO_4$, 0.01 mM $CuSO_4$ and 0.03 mM $MnCl_2$. The nutrient solution was prepared using deionized water. Plants were watered as needed.

Inoculum production and inoculation procedure. Plants were inoculated with a monosporic isolate of *S. macrospora* (UFV-DFP *Sm* 01). The isolate of *S. macrospora* was grown in Petri dishes containing oat-agar medium and incubated for 35 days in an incubator (22ºC, photoperiod of 12 h of light and 12 h of darkness). All of the leaves on each plant were inoculated with a conidial suspension of *S. macrospora* (6×10^4 conidia/ml) at 30 days after emergence (growth stage V5) (17) using a VL Airbrush atomizer (Paasche Airbrush Co, Chicago, IL). Gelatin (1% w v^{-1}) was added to the suspension to aid conidial adhesion to the leaf blades. Immediately after inoculation, the plants were transferred to a growth chamber at 25 ± 2ºC, 90 ± 5% relative humidity and a 12 h light: 12 h dark photoperiod for 30 h. After this period, the plants were transferred to a plastic mist growth chamber

(MGC) inside a greenhouse for the duration of the experiments. The MGC was made of wood (2 m wide, 1.5 m high and 5 m long) and covered with 100-µm thick transparent plastic. The temperature inside the MGC ranged from 25 ± 2ºC (day) to 20 ± 2ºC (night). The relative humidity was maintained at 90 ± 5% using a misting system in which nozzles (model NEB-100; KGF Company São Paulo, Brazil) sprayed mist every 30 min above the plant canopies. The relative humidity and temperature were measured with a thermo-hygrograph (TH-508, Impac, São Paulo, Brazil). The maximum natural photon flux density at plant canopy height was approximately 900 µmol m^{-2} s^{-1}.

Assessment of MLS severity. The fourth leaves (counted from the base to the top) of each plant per replication of each treatment were marked and collected to evaluate MLS severity at 48, 72, 96, 120 and 168 hours after inoculation (hai). The collected leaves were scanned at 300 dpi resolution and the obtained images were processed using QUANT software (94) to obtain the severity (chlorosis and necrosis symptoms) values. The area under disease progress curve (AUDPC) for each leaf in each plant was computed using trapezoidal integration of the MLS progress curves over time using the formula proposed by Shaner and Finney (85).

Chlorophyll a fluorescence imaging. Images and parameters of chlorophyll *a* fluorescence were obtained on the 4^{th} leaves, from the base to the apex, at 48, 72, 96, 120 and 168 hai using the MAXI version of the Imaging-PAM fluorometer and the Imaging Win software (Heinz Walz GmbH, Effeltrich, Germany). The Chl fluorescence emission transients were captured by a CCD (charge-coupled device) camera with a resolution of 640 × 480 pixels in a visible sample area of 24 × 32 mm on each leaf. Initially, the leaves were dark-adapted for 30 min, after which they were carefully and individually fixed in a support at a distance of 18.5 cm from the

CCD camera. The leaf tissues were then exposed to a weak, modulated measuring beam (0.5 µmol m^{-2} s^{-1}, 100 µs, 1 Hz) to determine the initial fluorescence (F_0) when all the PS II reaction centers are "open". Next, a saturating white light pulse of 2,400 µmol m^{-2} s^{-1} (10 Hz) was applied for 0.8 s to ensure the maximum fluorescence emission (F_m) when all the PS II reaction centers were "closed". From these initial measurements, the maximum PS II photochemical efficiency of the dark-adapted leaves was estimated through the variable-to-maximum Chl fluorescence ratio, F_v/F_m = [(F_m - F_0)/F_m)]. The leaf tissues were subsequently exposed to actinic photon irradiance (185µmol m^{-2} s^{-1}) for 120 s to obtain the steady-state fluorescence yield (F_s), after which a saturating white light pulse (2,400µmol m^{-2} s^{-1}; 0.8 s) was applied to achieve the light-adapted maximum fluorescence (F_m'). The light-adapted initial fluorescence (F_0') was estimated according to Oxborough and Baker (74). Following the calculations of Kramer et al. (52), the energy absorbed by PS II for the following three yield components for dissipative processes were determined: the effective PS II quantum yield [Y(II) = (F_m' - F_s)/F_m')], the quantum yield of regulated energy dissipation [Y(NPQ) = (F_s/F_m') - (F_s/F_m)] and the quantum yield of nonregulated energy dissipation [Y(NO) = F_s/F_m]. To quantitatively estimate the values of the Chl *a* fluorescence imaging parameters, four leaves per treatment per each evaluation time were selected and five circular leaf areas of 0.78 cm^2 were defined on each leaf.

Biochemical assays. Samples from the fourth leaves from the base of each plant (a total of four leaves per replication of each treatment) were collected at 48, 72, 98, 120 and 168 hai. The leaf samples were kept in liquid nitrogen during sampling and the stores at -80ºC until further analysis.

Enzyme extraction and assays. Leaf samples of inoculated and non-inoculated plants from cultivars ECVSCS155 and HIB 32R48H at 24, 48, 72, 96, 120 and 168

hai were flash frozen in liquid nitrogen and subsequently stored at -80°C until further analysis. For the assays of superoxide dismutases (SOD, EC 1.15.1.1), catalases (CAT, EC 1.11.1.6), non-specific peroxidases (POX, EC 1.11.1.7) and ascorbate peroxidases (APX, EC 1.11.1.11) and a total of 0.3 g of leaf tissues was ground in liquid nitrogen into a fine powder and homogenized in a 2 mL solution containing 0.5 M potassium phosphate buffer (pH 6.8), 0.1 M ethylenediaminetetraacetic acid (EDTA), 0.1% Triton X, 3 mM DL-dithiothreitol (DTT) and 1% (w/v) polyvinylpyrrolidone (PVP). For glutathione reductases (GR, EC 1.8.1.7), glutathione peroxidases (GPX, EC 1.11.1.9) and glutathione-S-transferases (GST, EC 2.5.1.18), the fine powder was homogenized in 2 mL of a solution containing 100 mM potassium phosphate buffer (pH 7.5), 0.1 mM EDTA, 1 mM DL-dithiothreitol (DTT), 1 mM PMSF and 2% (w v^{-1}) PVP. The extracts were centrifuged at 12,000 *g* at 4°C for 15 min for SOD, CAT, POX, APX, GR, GPX and GST. The supernatants were used for the enzymes activities assays. All steps were performed at 4°C.

The total SOD activity was determined by measuring its ability to inhibit photochemical reduction of nitroblue tetrazolium (NBT) as described by Beauchamp and Fridovich (15). The reaction was started after the addition of 20 µL of the crude enzyme extract to 980 µL of a mixture containing 50 mM potassium phosphate buffer (pH 7.8), 13 mM methionine, 75 µM NTB, 0.1 mM EDTA and 2 µM riboflavin. The samples were exposed to 10 min of light and the production of formazan blue, resulting from the photoreduction of NBT, was measured at 560 nm. The absorbance at 560 nm of a reaction mixture with the same composition, but kept in the dark for 10 min, served as a blank. One unit of SOD was defined as the amount of enzyme necessary to inhibit NBT photoreduction by 50%.

The CAT activity was determined by adding 50 µL of the crude enzyme extract to 950 µL of a reaction mixture consisting of potassium phosphate buffer 50 mM (pH 7.0) and 12.5 mM hydrogen peroxide (H_2O_2) (44). The decrease in absorbance at 240 nm was measured for 2 min and the enzyme activity was calculated from the initial rate of the enzyme using the extinction coefficient of 40 mM^{-1} cm^{-1} at 240 nm.

The POX activity was assayed using the colorimetric method by determining the pyrogallol oxidation as proposed by Kar and Mishra (50). The reaction was started after the addition of 20 µL of the crude enzyme extract to 980 µL of a reaction mixture containing 25 mM potassium phosphate (pH 6.8), 20 mM pyrogallol and 20 mM H_2O_2. The activity was determined through the absorbance of colored purpurogallin recorded for 2 min at 420 nm and the enzyme activity was calculated from the initial rate of the enzyme using the extinction coefficient of 2.47 mM^{-1} cm^{-1} (30).

The APX activity assay was conducted as described by Nakano and Asada (70). A total of 20 µL of the crude enzyme extract was added to 980 µL of the mixture containing 50 mM phosphate buffer (pH 7.0), 1 mM H_2O_2 and 0.8 mM sodium ascorbate. The rate of ascorbate oxidation recorded by the decrease in the absorbance at 290 nm was measured for 2 min and the enzyme activity was calculated from the initial rate of the reaction using the extinction coefficient of 2.8 mM^{-1} cm^{-1} for ascorbate.

The GR activity was assayed according to Carlberg and Mannervik (25). The reaction was started after the addition of 50 µL of the crude enzyme extract to a volume of 950 µL of a mixture containing 100 mM potassium phosphate (pH 7.5), 1 mM EDTA, 1 mM oxidized glutathione (GSSG) and 0.1 mM NADPH (prepared in 0.5 mM Tris-HCl buffer, pH 7.5). The decrease in absorbance was determined at 340

nm for 2 min and GR activity was calculated from the initial rate of its activity using an extinction coefficient of 6.22 mM^{-1} cm^{-1} (35).

The GPX activity was estimated according to Lawrence and Burk (58). The reaction mixture consisted of 50 mM potassium phosphate buffer (pH 7), 1 mM EDTA, 1.14 mM NaCl, 0.2 mM NADPH, 1 U/ml GSSG-reductase, 1 mM GSH, 0.25 mM H_20_2 and the enzyme source in a total volume of 1 mL. All components were combined at the beginning of the assay, except for the enzyme source and H_20_2. A total of 50 µL of the crude extract was added to the above mixture and allowed to incubate for 5 min at 25°C and the reaction was initiated by the addition of 100 µL of a H_20_2 solution. The decrease in absorbance was measured at 340 nm for 5 min and the extinction coefficient of 6.22 mM^{-1} cm^{-1} (4) was used to calculate GPX activity.

The GST-like activity was determined using the methodology proposed by Habig et al. (43). A total of 10 µL of the crude enzyme extract was added to 990 µL of the mixture containing 97 mM potassium phosphate buffer (pH 6.5), 0.97 mM EDTA, 2.5 mM reduced glutathione (GSH) and 1.0 mM 1-chloro-2,4-dinitrobenzene (CDNB). The absorbance was measured at 340 nm over 5 min. The extinction coefficient of 9.6 mM^{-1} cm^{-1} was used to determine the enzyme activity.

All enzyme activities were expressed on a protein basis and the soluble protein concentrations of the extracts were measured by the method of Bradford (22) using bovine serum albumin as the standard protein.

Lipid peroxidation assay. The oxidative damage to lipids was estimated as the concentration of the total amount of 2-thiobarbituric acid (TBA) reactive substances and expressed as equivalents of malondialdehyde (MDA) according to Cakmak and Horst (24) with a few modifications. A total of 0.1 g of leaf tissues was ground into a fine powder and homogenized in a 2 mL 0.1% (w/v) trichloroacetic acid (TCA)

solution at 4°C following centrifugation at 10,000 *g* for 15 min. The supernatant was used for the MDA assay. A total volume of 250 µL was added to 750 µL of TBA (0.5% in 20% TCA) and the mixture was incubated for 30 min in a mixer (300 rpm) with control temperature set to 95°C. The reaction was stopped by immersion in an ice bath. The samples were centrifuged at 9.000 *g* for 10 min and the absorbance of the supernatant was recorded at 532 nm. The non-specific absorbance was estimated at 600 nm and subtracted from the specific absorbance values. An extinction coefficient of 155 mM^{-1} cm^{-1} was used to calculate the MDA concentration.

Determination of hydrogen peroxide (H_2O_2) concentration. A total of 0.2 g of leaf tissues was ground in liquid nitrogen into a fine powder and homogenized in 2 mL of a mixture containing 50 mM potassium phosphate buffer (pH 6.5) and 1 mM hydroxylamine. The homogenate was centrifuged at 10,000 *g* for 15 min at 4°C (55) and the supernatant was used as the crude extract. A total of 50 µL of the supernatant was then added to a reaction mixture containing 100 µM ferric ammonium sulfate ($FeNH_4[SO_4]$), 25 mM sulfuric acid, 250 µM xylenol orange and 100 mM sorbitol in a final volume of 2 mL (39). After 30 min of dark incubation at room temperature, the absorbance of the samples was determined at 560 nm. The controls for the reagents and crude extracts were prepared under the same conditions and subtracted from the sample. A standard curve of H_2O_2 (Sigma-Aldrich, São Paulo, Brazil) was used to determine the H_2O_2 concentration.

Determination of ascorbate (AsA) concentration. A total of 0.1 g of leaf tissues was ground in liquid nitrogen into a fine powder and homogenized in 2 mL of a 6% trichloroacetic acid (TCA) (w/v) solution. The homogenate was centrifuged at 15,000 *g* for 5 min at 4°C (49). An aliquot of 25 µL from the supernatant was then added to a 0.02 M sodium phosphate buffer (pH 7.4) solution and the resulting

mixture was incubated at 42°C for 15 min. Subsequently, a reaction mix consisting of 0.02 M sodium phosphate buffer (pH 7.4) solution, 5% TCA (w/v), 8.4% H_3PO_4 (v/v), 0.8% 2,2'-dipyridyl (w/v) and 0.3% $FeCl_3$ (w/v) was added to the mixture and brought to a final volume of 1 mL. After agitation, the solution was again incubated at 42°C for 40 min and the reaction was stopped in ice bath. The absorbance was recorded at 525 nm and the concentration of AsA was determined according to a calibration curve of AsA (Sigma-Aldrich, São Paulo, Brazil).

Determination of total glutathione concentration (GSH+GSSG). A total of 0.2 g of leaf tissues was ground in liquid nitrogen and the obtained powder was homogenized in 2 ml of a mixture consisting of 0.1 M HCl and 1 mM EDTA. The homogenate was centrifuged at 12,000 *g* for 10 min at 4°C (Anderson, 1985). In order to determine the total glutathione (GSH+GSSG) concentration, 50 µL of the supernatant was added to a reaction mixture consisting of 125 mM sodium phosphate buffer (pH 7.5), 6.3 mM EDTA, 0.3 mM NADPH and 6 mM 5,5'-dithio-bis-2-nitrobenzoic acid (DTNB) in a total volume of 1 mL. After incubation for 5 min at 30°C, 10 µL of glutathione reductase enzyme (50 U ml^{-1}) was added to the mix and the absorbance was determined at 412 nm during 2 min. The concentration of GSH+GSSG was determined by using a calibration curve of glutathione (Sigma-Aldrich, São Paulo, Brazil) according to Griffith (42).

Determination of electrolyte leakage (EL). The EL was determined according to the methodology of Lima et al. (59) with a few modifications. A total of 20 leaf discs (o mm in diameter) were collected from the fourth leaves from the base of each plant per replication and treatment at 48, 72, 96, 120 and 168 hai. The leaf discs were thoroughly washed in deionized water immediately after being sampled. Then, the leaf discs were left to float on 60 mL of deionized water in sealed glass for 4 h at

25ºC. After this period, the first value of conductivity (reading one) was obtained using a conductivity meter (Tecnopon *m*CA-150; MS Tecnopon Instrumentação Cientifica, São Paulo, Brazil). Next, the vials were transferred to an oven for 2 h at 90ºC to obtain a new value for conductivity (reading two). The EL, given as a percentage, was obtained by dividing the value of reading one by the value of reading two.

Experimental design and data analysis. A 2 × 2 factorial experiment, consisting of two maize cultivars (ECVSCS155 and HIB 32R48H) and non-inoculated or inoculated plants was arranged in a completely randomized design with six replications. The experiment was repeated three times. Each experimental unit corresponded to a plastic pot containing three plants. A total of 120 plants were used in each experiment (24 plants per treatment at each evaluation time). All variables were subjected to an analysis of variance (ANOVA) and the treatments means were compared by Tukey's test ($P \leq 0.05$) using the SAS software (SAS Institute Inc., Cary, NC). For MLS severity, the ANOVA was considered to be a 2 × 5 factorial experiment, consisting of two maize cultivars and five evaluation times. For the photosynthetic measurements, the activities of the seven antioxidative enzymes, the concentrations of MDA, H_2O_2, reduced AsA and total glutathione (GSH+GSSG) and the EL values, ANOVA was considered to be a 2 × 2 × 5 factorial experiment, consisting of two maize cultivars, non-inoculated and inoculated plants and five evaluation times.

RESULTS

MLS severity and AUDPC. The factors cultivars and evaluation times as well as their interaction were significant ($P \leq 0.05$) for MLS severity (Table 1). Cultivar was the only significant factor ($P \leq 0.05$) for AUDPC (Table 1). MLS severity was significantly lower on the leaves of plants from cultivar ECVSCS155 relative to the leaves of plants from cultivar HIB 32R48H (Fig. 1A). From 48 to 168 hai, MLS severity increased from 0.4 to 4.2% on the leaves of plants from cultivar ECVSCS155 and from 1.4 to 7.5% on the leaves of plants from cultivar HIB 32R48H. For plants of cultivar ECVSCS155, AUDPC was significantly reduced by 54.4% compared to plants from cultivar HIB 32R48H (Fig. 1B).

Imaging of chlorophyll a fluorescence. Semi-quantitative and quantitative examination of the Chl *a* fluorescence images were used to study the photosynthetic performance of maize leaves of non-inoculated and inoculated plants. Using the approach of a semi-quantitative examination, visual changes on the images of the Chl *a* fluorescence on the leaves of inoculated plants was detected. The first changes were observed at 48 hai for all parameters of Chl *a* fluorescence which prominently increased as the MLS progressed (Fig. 2 and 3). Nevertheless, changes in F_0 was less perceptible at 48 hai (Fig. 2 and 3 a_0-a_5), whereas for F_m, F_v/F_m, Y(II), Y(NPQ) and Y(NO), the first changes became evident at 48 hai and the greater changes occurred at 120 and 168 hai (Fig. 2 and 3 b_0-b_5, c_0-c_5, d_0-d_5, e_0-e_5 and f_0-f_5). Indeed, decreases in F_m, F_v/F_m, Y(II) and Y(NPQ) coupled with increases in Y(NO) were directly related to the progressive loss of photosynthetic activity as indicated by the black areas in the images.

Additionally, assessment of the photosynthesis was performed by means the quantitative examination of Chl *a* fluorescence images. At least one of the evaluated

factors (cultivars, plant inoculation and evaluation times) as well as some of their interactions were significant ($P \leq 0.05$) for F_0, F_m, F_v/F_m, Y(II), Y(NPQ) and Y(NO). Plant inoculation was the most important factor due to its higher F values explaining, therefore, the variation in all variables evaluated. The interactions cultivars × plant inoculation × evaluation times was significant only for F_0, Y(II) and Y(NO) (Table 1).

For both cultivars, F_0 and Y(NO) significantly increased for the inoculated plants relative to their non-inoculated counterparts (Fig. 4A and B; 5E and F). Increases in the values for the above parameters were greater at 168 hai for plants of cultivar HIB 32R48H than for plants of cultivar ECVSCS155 with increases of 29 and 23% for F_0 (Fig. 4A and B) and 84 and 51% for Y(NO) (Fig. 5E and F) in the inoculated plants relative to the non-inoculated ones, respectively. The F_m, F_v/F_m, Y(II) and Y(NPQ) significantly decreased for the inoculated plants in comparison to their non-inoculated counterparts (Fig. 4C, D, E and F; 5A, B, C and D). Reductions in the values of the above mentioned parameters were greater at 168 hai for plants of cultivar HIB 32R48H than for plants of cultivar ECVSCS155 with decreases of 69 and 62% for F_m (Fig. 4C and D) 45 and 41% for F_v/F_m (Fig. 4E and F), 57 and 45% for Y(II) (Fig. 5A and B) and 51 and 32% for Y(NPQ) (Fig. 5C and D). For the non-inoculated plants, significant differences between cultivars occurred at 48, 72, 96, 120 and 168 hai for F_m (Fig. 4C and D) and at 72 and 168 hai for Y(II) (Fig. 5A and B). For the inoculated plants, significant differences between cultivars occurred at 72 hai for Y(II) (Fig. 5A and B) and at 96 and 168 hai for Y(NO) (Fig. 5E and F).

Antioxidative systems. At least one the factors (cultivars, plant inoculation and evaluation times) as well as some of their interactions were significant ($P \leq 0.05$) for SOD, CAT, POX, APX, GR, GPX, GST, MDA, H_2O_2, AsA, (GSH+GSSG) and EL

(Table 1). The interaction cultivar × plant inoculation × evaluation times was not significant only for the SOD, CAT, MDA and GSH (Table 1). The SOD activity was higher for the inoculated plants of cultivars ECVSCS155 and HIB 32R48H compared with the non-inoculated plants at 48, 72, and 96 hai (Fig. 6A and B). The inoculated plants of cultivars ECVSCS155 and HIB 32R48H showed increases of 149 and 123% at 48 hai, 171 and 151% at 72 hai and 94 and 40% at 96 hai, respectively, for SOD activity compared with the non-inoculated plants. Differences between the inoculated and non-inoculated plans for CAT activity occurred at 48, 72, 96 and 120 hai for cultivar ECVSCS155 and only at 72 and 96 hai for cultivar HIB 32R48H, with the highest values occurring for the inoculated plants (Fig. 6C and D). Increases in CAT activity were greater at 72 and 96 hai for plants of cultivar ECVSCS155 than for plants of cultivar HIB 32R48H with increases of 145 and 111% at 72 hai and 157 and 54% at 96 hai, respectively, on inoculated plants in comparison to the non-inoculated ones.

The inoculated plants of cultivars ECVSCS155 and HIB 32R48H showed a significant increase in POX activity compared with the non-inoculated plants at 96 and 120 hai (Fig. 6E and F). Increases of 72 and 69% at 96 hai and 131 and 72% at 120 hai were obtained for the inoculated plants of cultivars ECVSCS155 and HIB 32R48H, respectively, compared with the non-inoculated plants.

The APX activity was higher for the inoculated plants of both cultivars compared to the non-inoculated plants at 72 and 96 hai (Fig. 6G and H). The inoculated plants of cultivars ECVSCS155 and HIB 32R48H showed increases of 44 and 43% and 41 and 38% at 96 hai, respectively, for APX activity compared with the non-inoculated plants.

There was a significant increase in GR activity for the inoculated plants of cultivars ECVSCS155 and HIB 32R48H at 72 and 96 hai compared with the non-inoculated plants (Fig. 6I and J). For the inoculated plants of cultivars ECVSCS155 and HIB 32R48H, there were increases of 80 and 69% at 72 hai and 76 and 66% at 96 hai, respectively, for the GR activity compared with the non-inoculated.

The inoculated plants of both cultivars showed a significant increase in GPX activity compared with the non-inoculated plants at 48, 72, 96 and 120 hai for cultivar ECVSCS155 and only at 72, 96 and 120 hai for cultivar HIB 32R48H with the highest values occurring for the inoculated plans (Fig. 6K and L). The GPX activity increased by 93 and 81% at 72 hai, 86 and 66% at 96 hai and 29 and 26% at 120 hai for the inoculated plants of cultivars ECVSCS155 and HIB 32R48H, respectively, compared with the non-inoculated plants.

Differences between the inoculated and non-inoculated plants for GST activity were found at 48, 72, 96 and 120 hai for cultivar ECVSCS155 and only at 48, 72 and 96 hai for cultivar HIB 32R48H, with the highest values occurring for the inoculated plants (Fig. 6M and N). However, increases in the GST activity were greater at 72 hai for plants of cultivar HIB 32R48H than for plants of cultivar ECVSCS155 with increases of 104 and 80%, respectively, on inoculated plants in comparison to the non-inoculated ones.

Regarding the AsA and GSH+GSSG concentrations, there was significant difference between the inoculated and non-inoculated plants at 48 and 72 hai for AsA and 48, 72 and 96 hai for GSH, with the higher values occurring for the inoculated plants of the cultivar ECVSCS155 (Fig. 7A-D).

For the MDA and H_2O_2 concentrations, there was a significant difference between the inoculated and non-inoculated plants for cultivars ECVSCS155 and HIB 32R48H

at 48, 72, 96, 120 and 168 hai, with the highest values occurring for the inoculated plants of the cultivar HIB 32R48H (Fig. 8A-D). The inoculated plants of both cultivars showed a significant increase in the EL values compared with the non-inoculated plants at 48, 72, 96, 120 and 168 hai, with the highest values occurring for the inoculated plants (Fig. 9A and B). Increases in the EL values were greater at 120 and 168 hai for plants of cultivar HIB 32R48H than for plants of cultivar ECVSCS155 with increases of 190 and 140% at 120 hai and 225 and 165% at 168 hai, respectively, on inoculated plants in comparison to the non-inoculated ones.

DISCUSSION

The results from the present study provide, to the best of the authors' knowledgment, novel information about the physiological features that were associated with alterations on the photosynthetic performance and antioxidative systems arising from the colonization of maize leaves by the necrotrophic fungus *S. macrospora*. Different studies using the chlorophyll *a* fluorescence imaging monitored the spatial patterns of the operating efficiency of PSII revealing, therefore, different patterns of damage to the photosynthetic machinery on leaves infected with pathogens of different life styles (11,18,90). In the present study, there was a progressive increase in F_0 values for the infected leaves in comparison to the leaves of non-inoculated plants regardless of cultivars. This finding indicates that there was some photoinhibitory process that led to oxidative damage in the reaction center of PSII or that the transfer of excitation energy from the antenna system to the reaction center was dramatically impaired. According to Plazek et al. (76), the increase in the F_0 values on barley leaves infected by *Bipolaris sorokiniana* suggested the occurrence of damage to the ***photosynthetic antenna*** system. Concomitant decreases in F_m and F_v/F_m as the MLS progressed were also observed leading to the conclusion of an proportional decrease in the rate constant for photochemistry and a direct photodamage to PSII reaction centers (7,75). Kuckenberg et al. (54) reported that F_0 increased and F_v/F_m decreased on wheat leaves infected by *Puccinia recondite* and *Blumeria graminis* f.sp. *tritici*. Also, for the maize-*Colletotrichum graminicola* (16), tomato-*Botrytis cinerea* (18) and wheat-*Mycosphaerella graminicola* (90) interactions, the reduction in F_v/F_m values were associated with the degradation of the photosynthetic apparatus caused by these pathogens.

Regardless of maize cultivar, there was a progressive decrease in Y(II) and Y(NPQ) coupled with increase in Y(NO) in the infected leaves in contrast to the leaves of non-inoculated plants suggesting that the ability for photochemical energy conversion was strongly compromised due to fungal infection. According to Melis (65) the photodamage may be consequence of the impairment of the primary charge separation between P680 and pheophytin and subsequent alteration in electron-transfer reactions due to the increase in the fraction of reduced Q_A. Concomitantly, decrease in Y(NPQ) coupled with increase in Y(NO) as MLS progressed suggest that the mechanisms of energy dissipation via the regulated photoprotective NPQ-mechanism were inefficient. Therefore, the chances to occur photodamage in the PSII as indicated by lower values of F_m, F_v/F_m and Y(II) on the infected leaves increased. Early increases in Y(NO) that was correlated with the impairment of the PSII were reported to occur on wheat leaves infected with *Puccinia triticina* (23).

Stronger photoinhibition on the infected leaves of plants from the two cultivars was noticed as the MLS progressed leading to the hypothesis that both the energy assimilation and the energy dissipation capacities of the photosynthetic apparatus were negatively impaired. This damage in the photosynthetic apparatus may have favored oxygen molecular reduction and induced subsequent generation of ROS in the infected leaves. Several studies reported changes in the antioxidative system on infected leaves of many plant species as a strategy to afford the oxidative stress provoked by pathogens infection (38,45,47,80).

The enzymatic and non-enzymatic components of the antioxidative system were both dramatically altered on infected leaves. Indeed, the SOD, CAT, POX, APX, GR, GPX and GST activities as well as the concentrations of AsA and GSH+GSSG were quite higher at the early stages of fungal infection, but suffered accentuated

decreases as the MLS progressed suggesting the occurrence of an initial mechanism defense from the host's side. As the symptoms of MLS on maize leaves become more drastic, the activities of these enzymes, and the concentration of metabolites buffers decreased. Although, H_2O_2 and MDA concentration increased contributing, therefore, for the intensification of lipid peroxidation upon damage to cell membranes.

Regardless of maize cultivar, the SOD, CAT and APX activities showed an initial increase in the infected leaves than on the leaves of non-inoculated plants, confirming that they were the first line of defense mounted by the host to cope with *S. macrospora* infection. It is known that the SOD is the multimeric metalloprotein catalyzing the dismutation of the O_2^- to molecular oxygen and H_2O_2 (9,40). The SOD activity increased at early stages of *S. macrospora* infection, but decreased thereafter, which contributed to an accumulation the O_2^- in the chloroplasts that resulted in photooxidative damage. The SOD and POX activities did not change on lettuce leaves infected with *Bremia lactucae* (84).

The CAT, POX and APX are main H_2O_2-scavenging enzymes in plant leaves (36,64). The CAT is responsible for H_2O_2 removal generated during mitochondrial electron transport, β-oxidation of fatty acids and in the photorespiratory oxidation (21,73). The CAT activity increased in the infected maize leaves of both cultivars, but decreased as the MLS progressed in a scenario where the H_2O_2 concentration was kept at high levels. This finding confirms the key role played by CAT in the H_2O_2 scavenger in the peroxisomes and mitochondria in maize plants (77,78,83). The CAT and POX activities increased while the H_2O_2 concentration increased on the necrotic tissue from roots and shoots of pea plants infected with *Fusarium oxysporum* f.sp. *pisi* and *F. solani* (61).

In plants, POX is a heme-containing glycoprotein encoded by a large multigene family and plays a significant role in tissue lignification that helps to slow pathogens colonization (79). POX was important for maize resistance at the early stages of *S. macrospora* infection regardless of the basal resistance of the cultivars used. According to Hong-xia et al. (46), POX activity was higher on plants of a resistant wheat cultivar to *Rhizoctonia cerealis* in contrast to the susceptible one.

The AsA-GSH cycle involve successive oxidation and reduction of AsA, GSH and NADPH catalyzed by the enzymes APX, monodehydroascorbate reductase, dehydroascorbate reductase and GR (6). The APX is a central component of AsA-GSH cycle and plays a key role in the H_2O_2 removal in mitochondria, chloroplasts and peroxisomes (86) using two molecules of AsA as a specific electron donor to reduce H_2O_2 to water (36). In the present study, APX activity increased in response to *S. macrospora* infection, but decreased at advanced stages of fungal infection. El-Zahaby et al. (34) reported that the APX activity markedly increased on barley leaves of a susceptible cultivar infected with *Erysiphe graminis* while remained unchanged on the leaves of a resistant cultivar.

The GR belongs to a group of flavoenzymes and acts as an antioxidant due to its participation in enzymatic as well as nonenzymatic oxidation-reduction cycles (19,86). GR is responsible to catalyze the reduction of oxidized glutathione (GSSG) to GSH and, thus, maintains high cellular GSSG/GSH ratio (Asada, 2006). The GR activity increased in the leaves of maize plants in response to *S. macrospora* infection, but declined at advanced stages of fungal infection. By contrast, GR activity remained unchanged during the infection process of *Erysiphe graminis* f.sp. *hordei* on barley leaves (34).

GPX is a family of isoenzymes that uses GSH to reduce H_2O_2 to water forming GSSG besides participating in lignin biosynthesis (9,63,68). GPX activity was high on infected leaves than on the leaves of non-inoculated plants. SOD, CAT, GPX, APX and GR activities were higher at early stages of *Botrytis cinerea* infection on tomato leaves, but decreases as the disease symptoms become more severe (56). The APX, GR and GPX activities also increased in the roots of plants from a susceptible cultivar of chickpea infected with *Fusarium oxysporum* (38).

GST catalyzes the conjugation of GSH to a variety of hydrophobic, electrophilic and citotoxic substrates and participates in the detoxification of fatty acids hydroperoxides produced during lipid peroxidation (63,91). In this present study, the GST activity was kept higher at early stages of *S. macrospora* infection and decreased at MLS symptoms increased in comparison to what was observed for the leaves of non-inoculated plants.

AsA is involved in the removal of H_2O_2 via AsA-GSH cycle because of its ability to donate electrons in a number of enzymatic and nonenzymatic reactions (8,86). Additionally, AsA provides membrane protection by directly reacting with O_2^- and H_2O_2 (14). In maize leaves, there is differential compartmentation of antioxidants, which need the transport of reduced forms of AsA and GSH from the mesophyll to the bundle sheath cells (71). Additionally, proteins in the bundle sheath are much more susceptible to oxidative damage than those of found in the mesophyll suggesting that stress conditions may lead to a deficit in the antioxidant ability of bundle sheath cells (33,51).

In the present study, the AsA concentration increased in the leaves in response to *S. macrospora* infection, but was lower that for the non-inoculated plants. This finding is in agreement with Dias et al. (32) who reported that AsA concentration

1978 was high at early stages of *Moniliophthora perniciosa* infection on the cacao leaves
1979 of a susceptible cultivar while was kept stable during the fungal infection process on
1980 the s of a resistant cultivar. AsA concentration decrease in the barley leaves of a
1981 susceptible cultivar infected with *Erysiphe graminis* f.sp. *hordei* but remained stable
1982 on the leaves of a resistant cultivar explaining, therefore, the strong APX activity on
1983 the infected leaves (34).

1984 GSH acts as disulphide reductant to protect thiol groups on enzymes, regenerate
1985 AsA and react directly with $^1O_2$ and HO^- (8). Plants increase the activity of GSH
1986 biosynthetic enzymes and GSH concentration in response to pathogens infection
1987 (71). The GSH+GSSG concentration increased in the early stages of *S. macrospora*,
1988 but decreased with the intensification of the MLS symptoms. On barley leaves
1989 infected with *Erysiphe graminis* f.sp. *hordei*, GSH concentration increased at 3 and 4
1990 dai followed by a sharp decrease as disease progressed (34).

1991 The concomitant decrease in GR activity and GSH+GSSG concentration at
1992 advanced stage of *S. macrospora* infection on leaves of plants from both cultivars
1993 highlights the importance of GR to maintain the high cellular GSSG/GSH ratio.
1994 Additionally, for the inoculated plants of both cultivars, there was a consistent
1995 decrease in the GPX and GST activities coupled with decrease in GSH+GSSG
1996 concentration during fungal infection confirming, therefore, the key role of GHS as a
1997 specific electron donor by maintain the GPX and GST activities at desirable levels
1998 The APX and GR activities as well as the concentrations of AsA and GSH were
1999 dramatically decreased in tomato leaves infected with *Botrytis cinerea* (56). It was
2000 postulated that *B. cinerea* was able to trigger changes in the antioxidative system
2001 leading to a collapse of the protective mechanism at advanced stages of fungal
2002 infection.

The H_2O_2, unlike other oxygen radicals, can readily cross biological membranes and consequently cause oxidative damage far from the site of its production (84,86). At high concentration, H_2O_2 can oxidize the cysteine or methionine residues and inactivate enzymes by oxidizing their thiol groups such as the enzymes of the Calvin cycle (36,86). In the present study, the H_2O_2 concentration increased in the infected leaves, especially at advanced stages of fungal infection while the activities of all enzymes dramatically decreased. Several studies have suggested that the redox status of a certain host may play a major role in the facilitation of hemibiotrophic and necrotrophic fungal infections for the bean-*Botrytis cinerea* (92,93), barley-*Rhynchosporium secalis* (1), japanese pear-*Alternaria alternata* (89) and wheat-*Septoria tritici* (87) interactions.

Lipid peroxidation is a biochemical marker for the free radical in response to abiotic and biotic types of stress (21) According to Mandal et al. (62), the peroxidation of unsaturated lipids of biological membranes is the most prominent signal of oxidative stress in plants. Several studies have shown that the lipid peroxidation, measured as the concentration of MDA, is induced upon pathogens infection (41). In the present study, the increase in H_2O_2 concentration that contributed to the higher concentration of MDA and the higher EL values occurred on the leaves infected with *S. macrospora*. Mandal et al. (62) reported a high MDA concentration on the tomato roots infected with *Fusarium oxysporum* f.sp. *lycopersici*.

The results of the present study indicated that the photosynthetic apparatus as well as the antioxydative system in the leaves of maize plants were dramatically altered during the infection process of *S. macrospora* causing an impairment on the

protective mechanism of the maize plants that could be used to counteract the fungal infection.

LITERATURE CITED

1. Able, A. J. 2003. Role of reactive oxygen species in the response of barley to necrotrophic pathogens. Protoplasma 221:137-143.

2. Alscher, R. G., Erturk, N., and Heath, L. S. 2002. Role of superoxide dismutase (SODs) in controlling oxidative stress in plants. J. Exp. Bot. 53:1331-1341.

3. Anderson, B., and White, D. G. 1987. Fungi associated with corn stalks in Illinois in 1982 and 1983. Plant Dis. 71:135-137.

4. Anderson, J. V., and Davis, D. G. 2004. Abiotic stress alters transcript profiles and activity of glutathione-S-transferase, glutathione peroxidase, and glutathione reductase in *Euphorbia esula.* Physiol. Plant. 120:421-433.

5. Anderson, M. E. 1985. Determination of glutathione and glutathione disulfide in biological samples. Methods Enzymol. 113:548-555.

6. Apel, K., and Hirt, H. 2004. Reactive oxygen species: metabolism, oxidative stress, and signal transduction. Annu. Rev. Plant Biol. 55:373-399.

7. Aro, E. M., Virgin, I., and Andersson, B. 1993. Photoinhibition of photosystem II. Inactivation, protein damage and turnover. Biochim. Biophys. Acta 1143:113-134.

8. Arora, A., Sairam, R. K, and Srivastava, G. C. 2002. Oxidative stress and antioxidative system in plants. Curr. Sci. India 82:1227-1238.

9. Asada, K. 1999. The water-water cycle in chloroplasts: scavenging of active oxygens and dissipation of excess photons. Annu. Rev. Plant Physiol. Plant Mol. Biol. 50:601-639.

10. Asada, K. 2006. Production and scavenging of reactive oxygen species in chloroplasts and their functions. Plant Physiol. 141:391-396.

11. Baker, N. R., Oxborough, K., Lawson, T., and Morison, J. I. L. 2001. High resolution imaging of photosynthetic activities of tissues, cells and chloroplast in leaves. J. Exp. Bot. 52:615-621.

12. Baker, N. R. 2008. Chlorophyll fluorescence: a probe of photosynthesis In Vivo. Annu. Rev. Plant Biol. 59:89-113.

13. Bampi, D., Casa, R. T., Bogo, A., Sangoi, L., Sachs, C., Bolzan, J. M., and Piletti, G. 2012. Fungicide performance on the control of macrospora leaf spot in corn. Summa Phytopathol. 38:319-322.

14. Bartoli, C. G., Pastori, G. M., and Foyer, C. H. 2000. Ascorbate biosynthesis in mitochondria is linked to the electron transport chain between complexes III and IV[1]. Plant Physiol. 123:335-343.

15. Beauchamp, C., and Fridovich, I. 1971. Superoxide dismutase: improved assays and an assay applicable to acrylamide gels. Anal. Biochem. 44:276-287.

16. Behr, M., Humbeck, K., Hause, G., Deising, H. B., and Wirsel, S. G. R. 2010. The hemibiotroph *Colletotrichum graminicola* locally induces photosynthetically active green islands but globally accelerates senescence on aging maize leaves. Mol. Plant Microbe Interact. 23:879-892.

17. Bensch, M. J., Van Staden, J., and Rijkenberg, F. H. J. 1992. Time and site inoculation of maize for optimum infection of ears by *Stenocarpella maydis*. J. Phytopathol. 136:265-269.

18. Berger, S., Papadopoulos, M., Schreiber, U., Kaiser, W., and Roitsch, T. 2004. Complex regulation of genes expression, photosynthesis and sugar levels by pathogen infection in tomato. Physiol. Plantarum 122:419-428.

19. Blokhina, O., Virolainen, E., and Fagerstedt, K. V. 2003. Antioxidants, oxidative damaged and oxygen deprivation stress: a review. Ann. Bot. 91:179-194.

20. Bolwell, G. P., and Wojtaszek, P. 1997. Mechanisms for the generation of reactive oxygen species in plant defence-a broad perspective. Physiol. Mol. Plant Pathol. 51:347-366.

21. Bowler, C., Van Montagu, M., and Inzé, D. 1992. Superoxide dismutase and stress tolerance. Annu. Rev. Plant Physiol. Plant Mol. Biol. 43:83-116.

22. Bradford, M. N. 1976. A rapid and sensitive method for the quantitation of microgram quantities of protein utilizing the principle of protein-dye binding. Anal. Biochem. 72:248-254.

23. Burling, K., Hunsche, M., and Noga, G. 2010. Quantum yield of non-regulated energy dissipation in PSII (Y(NO)) for early detection of leaf rust (*Puccinia triticina*) infection in susceptible and resistant wheat (*Triticum aestivum* L.) cultivars. Precis. Agric. 11:703-716.

24. Cakmak, L., and Horst, W. J. 1991. Effect of aluminum on lipid peroxidation, superoxide dismutase, catalase, and peroxide activity in root tip of soybean (*Glycine max*). Plant Physiol. 83:463-468.

25. Carlberg, C., and Mannervik, B. 1985. Glutathione reductase. Methods Enzymol. 113:488-495.

26. Casa, R. T., Zambolim, L., and Reis, E. M. 1998. Transmissão e controle de *Diplodia* em sementes de milho. Fitopatol. Bras. 23:436-441.

27. Casa, R. T., Reis, E. M., and Zambolim, L. 2003. Decomposição dos restos culturais do milho e sobrevivência saprofítica de *Stenocarpella macrospora* e *Stenocarpella maydis*. Fitopatol. Bras. 28:355-361.

28. Casa, R. T., Reis, E. M., and Zambolim, L. 2004. Dispersão vertical e horizontal de conídios de *Stenocarpella macrospora* e *Stenocarpella maydis*. Fitopatol. Bras. 29:141-147.

29. Casa, R. T., Reis, E. M., and Zambolim, L. 2006. Doenças do milho causadas por fungos do gênero *Stenocarpella*. Fitopatol. Bras. 31:427-439.

30. Chance, B., and Maehley, A. C. 1955. Assay of catalases and peroxidases. Methods Enzymol. 2:764-775.

31. Dai, K., Nagai, M., Sasaki, H., Nakamura, H., Tachechi, K., and Warabi, M. 1987. Detection of *Diplodia maydis* (Berkeley) Saccardo from imported corn seed. Res. Bull. Plant Protect. Serv. 23:1-6.

32. Dias, C. V., Mendes, J. S., dos Santos, A. C., Pirovani, C. P., da Silva Gesteira, A., Micheli, F., Gramacho, K. P., Hammerston, J., Mazzafera, P., and de Mattos Cascardo, J. C. 2011. Hydrogen peroxide formation in cacao tissues infected by the hemibiotrophic fungus *Moniliophthora perniciosa*. Plant Physiol. Bioch. 49:917-922.

33. Doulis, A. G., Debian, N., Kingston-Smith, A. H., and Foyer, C. H. 1997. Differential localization of antioxidants in maize leaves. Plant Physiol. 114:1031-1037.

34. El-Zahaby, H. M., Gullner, G., and Király, Z. 1995. Effects of powdery mildew infections of barley on the ascorbate-glutathione cycle and other antioxidants in different host-pathogen interactions. Phytopathology 85:1225-1230.

35. Foyer, C. H., and Halliwell, B. 1976. The presence of glutathione and glutathione reductase in chloroplasts: a proposed role in ascorbic acid metabolism. Planta 133:21-25.

2127 36. Foyer, C. H., and Noctor, G. 2000. Oxygen processing in photosynthesis:
2128 regulation and signaling. New Phytol. 146:359-388.
2129 37. Foyer, C. H., and Noctor, G. 2003. Redox sensing and signaling associated
2130 with reactive oxygen in chloroplasts, peroxisomes and mitochondria. Physiol.
2131 Plantarum 119:355-364.
2132 38. García-Limones, C., Hervás, A., Navas-Cortés, J. A., Jiménez-Díaz, R. M.,
2133 and Tena, M. 2002. Induction of an antioxidant enzyme system and other oxidative
2134 stress markers associated with compatible and incompatible interactions between
2135 chickpea (*Cicer arietinum* L.) and *Fusarium oxysporum* f.sp. *ciceris*. Physiol. Mol.
2136 Plant Pathol. 61:325-337.
2137 39. Gay, C., Gebicki, J. M. 2000. A critical evaluation of the effect of sorbitol on
2138 the ferric-xylenol orange hydroperoxide assay. Anal. Biochem. 284:217-220.
2139 40. Giannopolitis, C. N., and Ries, S. K. 1977. Superoxide Dismutase. Plant
2140 Physiol. 59:309-314.
2141 41. Göbel, C., Feussner, I., and Rosahl, S. 2003. Lipid peroxidation during the
2142 hypersensitive response in potato in the absence of 9-lipoxygenases. J. Biol. Chem.
2143 278:52834-52840.
2144 42. Griffith, O. W. 1980. Determination of glutathione and glutathione disulfide
2145 using glutathione reductase and 2-vinylpyridine. Anal. Biochem. 106:207-212.
2146 43. Habig, W. H., Pabst, M. J., and Jakoby, W. B. 1974. Glutathione-S-
2147 transferases. The first enzymatic step in mercapturic acid formation. J. Biol. Chem.
2148 249:7130-7139.
2149 44. Havir, E. A., and McHale, N. A. 1987. Biochemical and developmental
2150 characterization of multiple forms of catalase in tobacco leaves. Plant Physiol.
2151 84:450-455.

2152 45. Heller, J., Tudzynski, P. 2011. Reactive oxygen species in phytopathogenic
2153 fungi: signaling, development, and disease. Annu. Rev. Phytopathol. 49:369-390.
2154 46. Hong-xia, L., Zhi-yong, X., and Zeng-yan, Z. 2011. Changes in activities of
2155 antioxidant-related enzymes in leaves of resistant and susceptible wheat inoculated
2156 with *Rhizoctonia cerealis*. Agr. Sci. China 10:526-533.
2157 47. Hückelhoven, R., and Kogel, K. H. 2003. Reactive oxygen intermediates in
2158 plant-microbe interactions: who is who powdery mildew resistance? Planta 216:891-
2159 902.
2160 48. Imlay, J. A. 2003. Pathways of oxidative damage. Annu. Rev. Microbiol.
2161 57:395-418.
2162 49. Kampfenkel, K., Van Montagu, M., and Inzé, D. 1995. Extraction and
2163 determination of ascorbate and dehydroascorbate from plant tissue. Anal. Biochem.
2164 225:165-167.
2165 50. Kar, M., and Mishra, D. 1976. Catalase, peroxidase, and polyphenoloxidase
2166 activities during rice leaf senescence. Plant Physiol. 57:315-319.
2167 51. Kingston-Smith, A. H., and Foyer, C. H. 2000. Bundle sheath proteins are
2168 more sensitive to oxidative damage than those of the mesophyll in maize leaves
2169 exposed to paraquat or low temperatures. J. Exp. Bot. 51:123-130.
2170 52. Kramer, D. M., Giles, J., Olavi, K., and Gerald, E. E. 2004. New fluorescence
2171 parameters for the determination of Q_A redox state and excitation energy fluxes.
2172 Photosynth. Res. 79:209-218.
2173 53. Krause, G. H., and Weis, E. 1991. Chlorophyll fluorescence and
2174 photosynthesis: the basics. Annu. Rev. Plant Physiol. Plant Mol. Biol. 42:313-349.

54. Kuckenberg, J., Tartachnyk, I., and Noga, G. 2008. Temporal and spatial changes of chlorophyll fluorescence as a basis for early and precise detection of leaf rust and powdery mildew infections in wheat leaves. Precis. Agric. 10:34-44.

55. Kuo, M. C., and Kao, C. H. 2003. Aluminium effects on lipid peroxidation and antioxidative enzyme activity in rice leaves. Biol. Planta. 46:149-152.

56. Kuzniak, E., and Sklodowska, M. 2005. Fungal pathogen-induced changes in the antioxidative systems of leaf peroxisomes from infected tomato plants. Planta 222:192-200.

57. Latterell, F. M., and Rossi, A. E. 1983. *Stenocarpella macrospora* (=*Diplodia macrospora*) and *S. maydis* (=*D. maydis*) compared as pathogens of corn. Plant Dis. 67:725-729.

58. Lawrence, R. A., Burk, R. F. 1976. Glutathione peroxidase activity in selenium-deficient rat liver. Biochem. Bioph. Res. Co. 71:952-958.

59. Lima, A. L. S., DaMatta, F. M., Pinheiro, H. A., Totola, M. R., and Loureiro, M. E. 2002. Photochemical response and oxidative stress in two clones of *Coffea canephora* under water deficit conditions. Environ. Experim. Bot. 47:239-247.

60. Logan, B. A., Koryeyev, D., Hardison, J., and Holaday, S. 2006. The role of antioxidant enzymes in photoprotection. Photosynth. Res. 88:119-132.

61. Luhová, L., Lebeda, A., Kutrová, E., Hedererová. D., and Pec, P. 2006. Peroxidase, catalase, amine oxidase and acid phosphatase activities in *Pisum sativum* during infection with *Fusarium oxysporum* and *F.* solani. Biol. Plantarum 50:675-682.

62. Mandal, S., Mitra, A., and Mallick, N. 2008. Biochemical characterization of oxidative burst during interaction between *Solanum lycopersicum* and *Fusarium oxysporum* f. sp. *lycopersici*. Physiol. Mol. Plant Phatol. 72:56-61.

2200 63. Marrs, K. L. 1996. The functions and regulation of glutathione S-transferases
2201 in plants. Annu. Rev. Plant Physiol. Plant Mol. Biol. 47:127-158.
2202 64. Mhamdi, A., Queval, G., Chaouch, S., Vanderauwera, S., Van Breusegem, F.,
2203 and Noctor, G. 2010. Catalase function in plants: a focus on *Arabidopsis* mutants as
2204 stress-mimic models. J. Exp. Bot. 61:4197-4220.
2205 65. Melis, A. 1999. Photosystem-II damage and repair cycle in chloroplasts: what
2206 modulates the rate of photodamage *in vivo*?. Trends Plant Sci. 4:130-135.
2207 66. Meyer, S., Saccardy-Adjl, K., Rizza, F., and Genty, B. 2001. Inhibition of
2208 photosynthesis by *Colletotricum lindemuthianum* in bean leaves determined by
2209 chlorophyll fluorescence imaging. Plant Cell Environ. 24:947-955.
2210 67. Mittler, R. 2002. Oxidative stress, antioxidants and stress tolerance. Trends
2211 Plant Sci. 7:405-410.
2212 68. Moller, I. M. 2001. Plant mitochondria and oxidative stress: electron
2213 transport, NADPH turnover, and metabolism of reactive oxygen species. Annu. Rev.
2214 Plant Physiol. Plant Mol. Biol. 52:561-591.
2215 69. Muimba, K. A., and Bergstrom, G. C. 2011. Reduced anthracnose stalk rot in
2216 resistant maize is associated with restricted development of *Colletotrichum*
2217 *graminicola* in pith tissues. J. Phytopathol. 159:329-341.
2218 70. Nakano, Y., and Asada, K. 1981. Hydrogen peroxide is scavenged by
2219 ascorbate-specific peroxidase in spinach chloroplasts. Plant Cell Physiol. 22:876-
2220 880.
2221 71. Noctor, G., Gomez, L., Vanacker, H., and Foyer, C. H. 2002. Interactions
2222 between biosynthesis, compartmentation and transport in the control of glutathione
2223 homeostasis and signalling. J. Exp. Bot. 53:1283-1304.

2224 72. Olatinwo, R., Cardwell, K., Menkin, A., Deadman, M., and Julian, A. 1999.
2225 Inheritance of resistance to Stenocarpella macrospora (Earle) ear rot of maize in the
2226 mid-altitude zone of Nigeria. Eur. J. Plant Pathol. 105:535-543.
2227 73. Orendi, G., Zimmermann, P., Baar, C., and Zentgraf, U. 2001. Loss of stress-
2228 induced expression of catalase3 during leaf senescence in *Arabidopsis thaliana* is
2229 restricted to oxidative stress. Plant Sci. 161:301-314.
2230 74. Oxborough, K., and Baker, N. R. 1997. Resolving chlorophyll *a* fluorescence
2231 images of photosynthetic efficiency into photochemical and non-photochemical
2232 components-calculation of q_P and F_v'/F_m' without measuring F_0'. Photosynth. Res.
2233 54:135-142.
2234 75. Oxborough, K. 2004. Imaging of cholorophyll *a* fluorescence: theoretical and
2235 practical aspects of an emerging technique for the monitoring of photosynthetic
2236 performance. J. Exp. Bot. 55:1195-1205.
2237 76. Plazek, A., Rapacz, M., and Hura, K. 2004. Relationship between quantum
2238 efficiency of PSII and cold-induced plant resistance to fungal pathogens. Acta
2239 Physiol. Plant. 26:141-148.
2240 77. Prassad, T. K., Anderson, M. D., Martin, B. A., and Stewart, C. R. 1994.
2241 Evidence for chilling-induced oxidative stress in maize seedlings and regulatory role
2242 for hydrogen peroxide. The Plant Cell. 6:65-74.
2243 78. Prasad, T. K., Anderson, M. D., and Stewart, C. R. 1995. Localization and
2244 characterization of peroxidases in the mitochondria of chilling-acclimated maize
2245 seedlings. Plant Physiol. 108:1597-1605.
2246 79. Quan, L. J., Zhang, B., Shi, W. W., and Li, H. Y. 2008. Hydrogen peroxide in
2247 plants: a versatile molecule of the reactive oxygen species network. J. Integr. Plant
2248 Biol. 50:2-18.

2249 80. Radwan, D. E. M., Fayez, K. A., Mahmoud, S. Y., and Lu, G. 2010.
2250 Modification of antioxidant activity and protein composition of bean leaf due to
2251 *Bean yellow mosaic virus* infection and salicylic acid treatments. Acta Physiol. Plant.
2252 32:891-904.
2253 81. Rohácek, K. 2002. Chlorophyll fluorescence parameters: the definitions,
2254 photosynthetic meaning, and mutual relationships. Photosynthetica 40:13-29.
2255 82. Rolfe, S. A., and Scholes, J. D. 2010. Chlorophyll fluorescence imaging of
2256 plant-pathogen interaction. Protoplasma 247:163-175.
2257 83. Scandalios, J. G., Tong, W. F., and Roupakias, D. G. 1980. Cat3, a third gene
2258 locus coding for a tissue-specific catalase in maize: genetics, intracellular location,
2259 and some biochemical properties. Molec. Gen. Genet. 179:33-41.
2260 84. Sedlárová, M., Luhová, L., Patrivalsky, M., and Lebeda, A. 2007.
2261 Localisation and metabolism of reactive oxygen species during *Bremia lactucae*
2262 pathogenesis in *Lactuca sativa* and wild *Lactuca* spp. Plant Physiol. Bioch. 45:607-
2263 616.
2264 85. Shaner, G., and Finney, R. E. 1977. The effect of nitrogen fertilization on the
2265 expression of slow-mildewing resistance in Knox wheat. Phytopathology 67:1051-
2266 1056.
2267 86. Sharma, P., Jha, A. B., Dubey, R. S., and Pessarakli, M. 2012. Reactive
2268 oxygen species, oxidative damage, and antioxidative defense mechanism in plants
2269 under stressful conditions. J. Bot. 2012:1-26.
2270 87. Shetty, N. P., Mehrabi, R., Lutken, H., Haldrup, A., Kema, G. H. J., Collinge,
2271 D. B., and Jorgensen, H. J. L. 2007. Role of hydrogen peroxide during the interaction
2272 between the hemibiotrophic fungal pathogen *Septoria tritici* and wheat. New Phytol.
2273 174:637-647.

88. Shetty, N. P., Jorgensen, H. J. L., Jensen, J. D., Collinge, D. B., and Shetty, H. S. 2008. Roles of reactive oxygen species in interactions between plants and pathogens. Eur. J. Plant Pathol. 121:267-280.

89. Shimizu, N., Hosogi, N., Jiang, G. H. S., Inoue, K., and Park, P. 2006. Reactive oxygen species (ROS) generation and ROS-induced lipid peroxidation are associated with plasma membrane modifications in host cells in response to AK-toxin I from *Alternaria alternata* japanese pear pathotype. J. Gen. Plant Pathol. 72:6-15.

90. Sholes, J. D., and Rolfe, S. A. 2009. Chlorophyll fluorescence imaging as tool for understanding the impact of fungal diseases on plant performance: a phenomics perspective. Funct. Plant Biol. 36:880-892.

91. Takesawa, T., Ito, M., Kanzaki, H., Kameya, N., and Nakamura, I. 2002. Over-expression of ζ glutathione S-transferase in transgenic rice enhances germination and growth at low temperature. Mol. Breeding 9:93-101.

92. Tiedemann, A. V. 1997. Evidence for a primary role of active oxygen species in induction of host cell death during infection of bean leaves with *Botrytis cinerea.* Physiol. Mol. Plant Pathol. 50:151-166.

93. Unger, Ch., Kleta, S., Jandi, G., and Tiedemann, A. V. 2005. Suppression of the defence-related oxidative burst in bean leaf tissue and suspension cells by the necrotrophic pathogen *Botrytis cinerea*. J. Phytopathol. 153:15-26.

94. Vale, F. X. R., Fernandes Filho, E. I., and Liberato, J. R. 2003. A software plant disease severity assessment. In 8th International Congress of Plant Pathology. Volume 2, 105 pp. Christchurch, New Zealand.

95. Wilhelm, C., and Selmar, D. 2011. Energy dissipation is an essential mechanism to sustain the viability of plants: the physiological limits of improved photosynthesis. J. Plant Physiol. 168:79-87.

96. White, D. G. 1999. Compendium of corn diseases. 3rd Ed. St. Paul, MN, USA: The American Phytopathological Society.

97. Wojtaszek, P. 1997. Oxidative burst: an early plant response to pathogen infection. Biochem. J. 322:681-692.

LIST OF TABLES AND FIGURES

Variables	C	PI	ET	C × PI	C × ET	PI × ET	C × PI × ET
	F-based P values[a]						
Sev (%)	< 0.001	-	< 0.001	-	< 0.001	-	-
AUDPC	< 0.001	-	-	-	-	-	-
SOD	0.942	< 0.001	< 0.001	0.824	0.595	< 0.001	0.714
CAT	0.597	< 0.001	< 0.001	0.448	0.621	< 0.001	0.988
POX	0.036	< 0.001	< 0.001	0.001	< 0.001	< 0.001	< 0.001
APX	0.165	< 0.001	< 0.001	0.061	0.003	< 0.001	0.038
GR	0.004	< 0.001	< 0.001	0.001	0.002	< 0.001	< 0.001
GPX	0.016	< 0.001	< 0.001	0.630	< 0.001	< 0.001	< 0.001
GST	< 0.001	< 0.001	< 0.001	< 0.001	< 0.001	< 0.001	< 0.001
MDA	0.538	< 0.001	< 0.001	0.003	0.147	< 0.001	0.058
H_2O_2	< 0.001	< 0.001	< 0.001	< 0.001	< 0.001	< 0.001	0.001
AsA	0.734	< 0.001	< 0.001	0.399	< 0.001	< 0.001	< 0.001
GSH	0.235	< 0.001	< 0.001	< 0.001	< 0.001	< 0.001	0.068
EL(%)	< 0.001	< 0.001	< 0.001	< 0.001	< 0.001	< 0.001	< 0.001
F_0	< 0.001	< 0.001	< 0.001	< 0.001	< 0.001	< 0.001	< 0.001
F_m	0.147	< 0.001	0.017	0.007	0.231	< 0.001	0.481
F_v/F_m	0.955	< 0.001	< 0.001	0.007	0.173	< 0.001	0.118
Y(II)	< 0.001	< 0.001	< 0.001	0.348	0.001	< 0.001	0.780
Y(NPQ)	< 0.001	< 0.001	0.054	0.015	0.005	< 0.001	< 0.001
Y(NO)	0.056	< 0.001	< 0.001	< 0.001	< 0.001	< 0.001	< 0.001

[a]Levels of probability: [ns] = not significant, * = 0.05

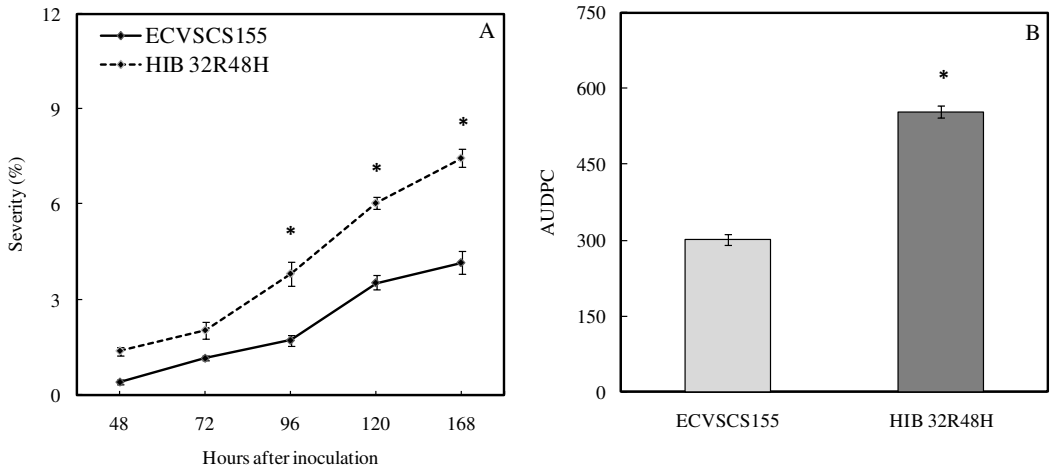

Fig. 1. Macrospora leaf spot progress curves (A) and area under disease progress curve (AUDPC) (B) on leaves of plants from maize cultivars ECVSCS155 and HIB 32R48H. Means from cultivars ECVSCS155 and HIB 32R48H followed by an asterisk (*) for each evaluation time are significantly different ($P \leq 0.05$) by Tukey´s test. Bars represent standard errors of the means. $n = 5$. Three experiments were conducted with consistent results; results from one representative experiment are shown.

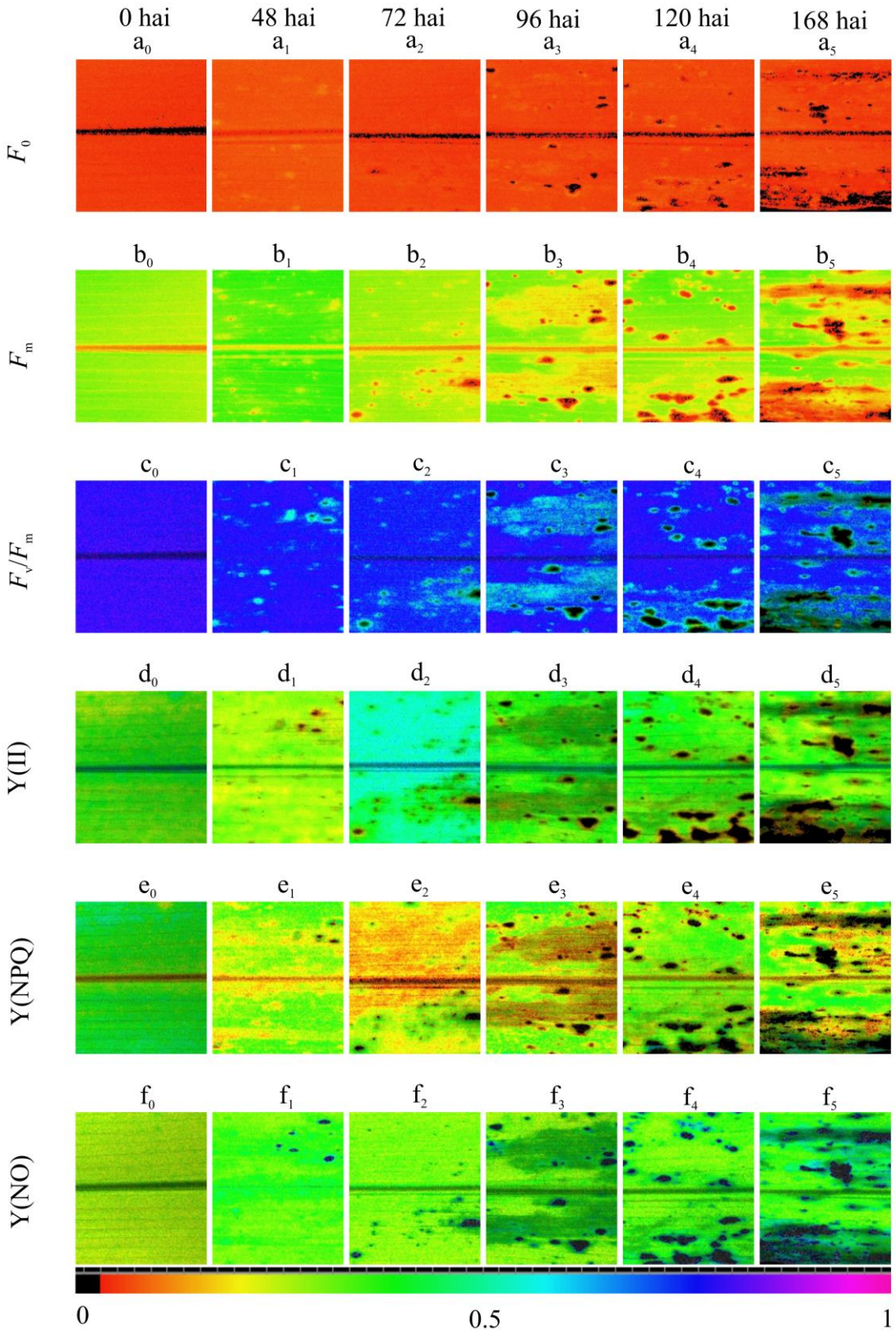

2348

2349

2350

Fig. 2. Parameters of chlorophyll *a* fluorescence, initial fluorescence (F_0) (a_0-a_5), maximum fluorescence (F_m) (b_0-b_5), maximum PSII quantum efficiency (F_v/F_m) (c_0-c_5), effective PS II quantum yield Y(II) (d_0-d_5), quantum yield of regulated energy dissipation Y(NPQ) (e_0-e_5) and quantum yield of nonregulated energy dissipation Y(NO) (f_0-f_5), determined on leaves of maize plants from cultivar HIB 32R48H. 0 hai (plants non-inoculated) and 48, 72, 96, 120 and 168 hai for plants inoculated. Three experiments were conducted with consistent results; results from one representative experiment are shown.

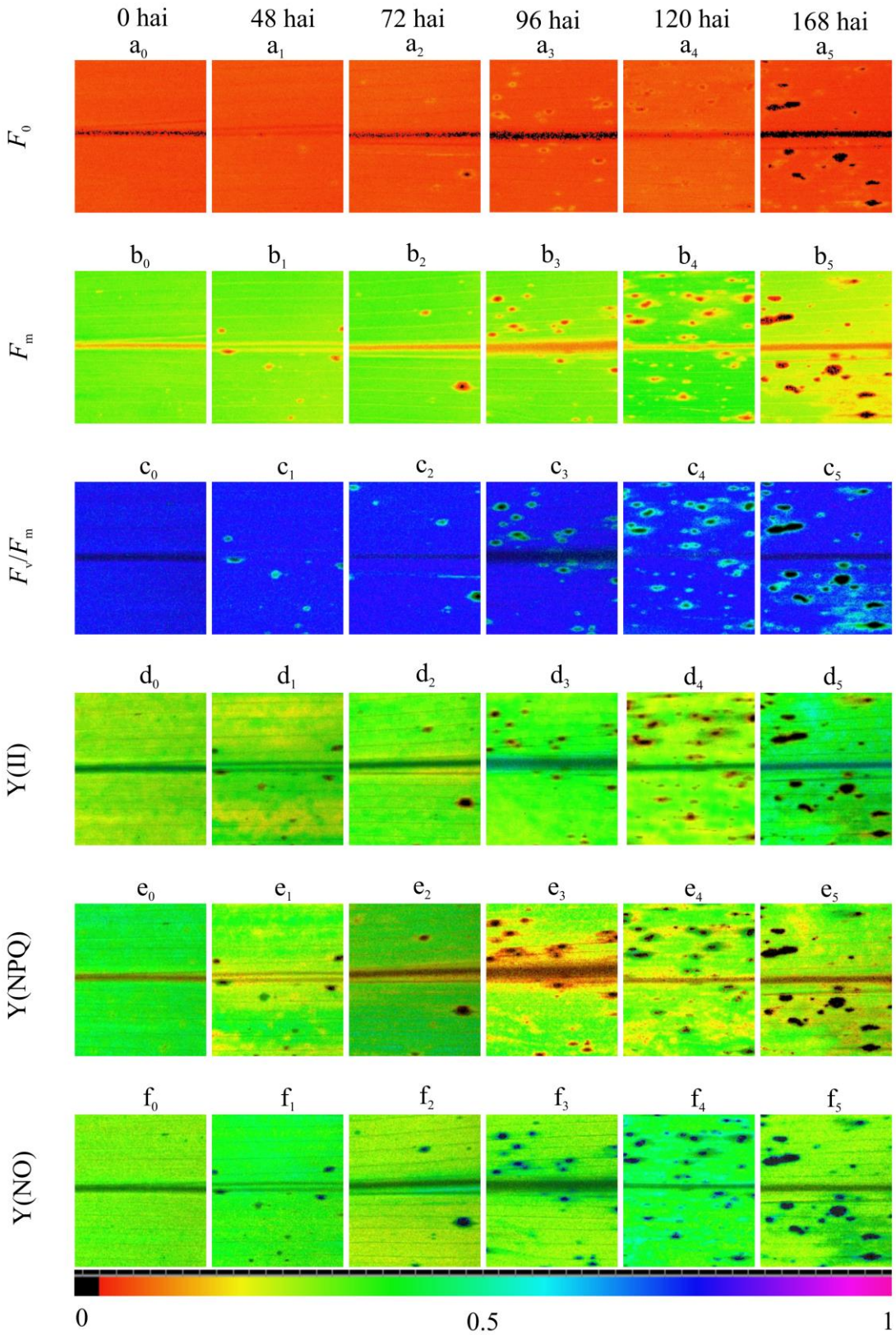
0 hai
48 hai
72 hai
96 hai
120 hai
168 hai
a0
a1
a2
a3
a4
a5
F0
b0
b1
b2
b3
b4
b5
Fm
c0
c1
c2
c3
c4
c5
Fv/Fm
d0
d1
d2
d3
d4
d5
Y(II)
e0
e1
e2
e3
e4
e5
Y(NPQ)
f0
f1
f2
f3
f4
f5
Y(NO)
0
0.5
1

2376

2377

Fig. 3. Parameters of chlorophyll *a* fluorescence, initial fluorescence (F_0) (a_0-a_5), maximum fluorescence (F_m) (b_0-b_5), maximum PSII quantum efficiency (F_v/F_m) (c_0-c_5), effective PS II quantum yield Y(II) (d_0-d_5), quantum yield of regulated energy dissipation Y(NPQ) (e_0-e_5) and quantum yield of nonregulated energy dissipation Y(NO) (f_0-f_5), determined on leaves of maize plants from cultivar ECVSCS155. 0 hai (plants non-inoculated) and 48, 72, 96, 120 and 168 hai for plants inoculated. Three experiments were conducted with consistent results; results from one representative experiment are shown.

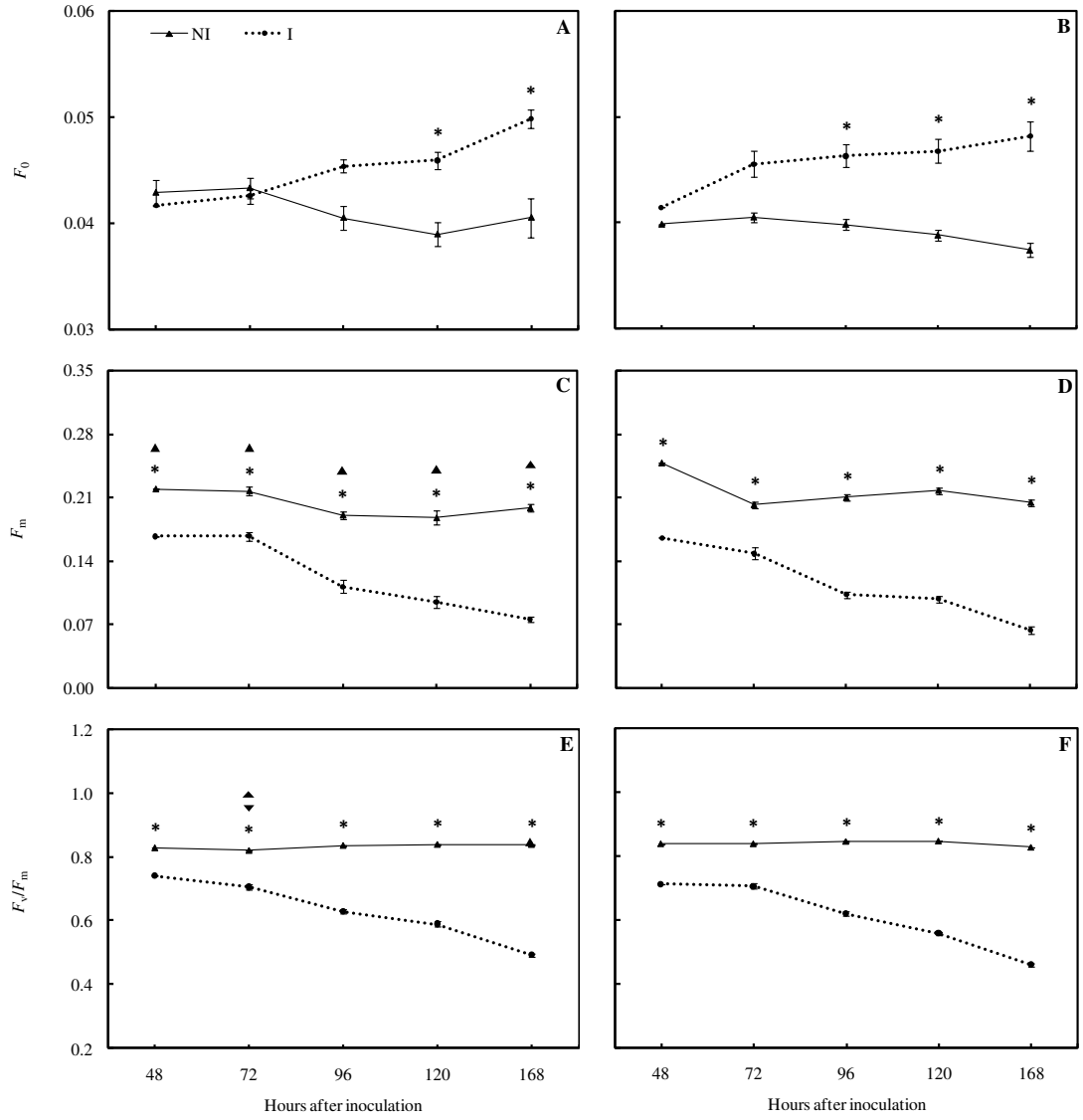
NI
I
A
B
C
D
E
F
F_0
F_m
F_v/F_m
Hours after inoculation
Hours after inoculation

Fig. 4. The initial fluorescence (F_0) (A and B), maximum fluorescence (F_m) (C and D) and maximum PSII quantum efficiency (F_v/F_m) (E and F) determined on leaves of maize plants from cultivars ECVSCS155 (A, C and E) and HIB 32R48H (B, D and F) non-inoculated (NI) or inoculated (I) with *Stenocarpela macrospora*. Means for the NI and I treatments for each cultivar followed by an asterisk (*) at each evaluation time are significantly different ($P \leq 0.05$) by Tukey´s test. The symbols ▲ and ▼ indicate differences between cultivars ECVSCS155 and HIB 32R48H, respectively, for NI and I treatments at each evaluation time according to Tukey´s test ($P \leq 0.05$). Bars represent the standard errors of the means. $n = 20$. Three experiments were conducted with consistent results; results from one representative experiment are shown.

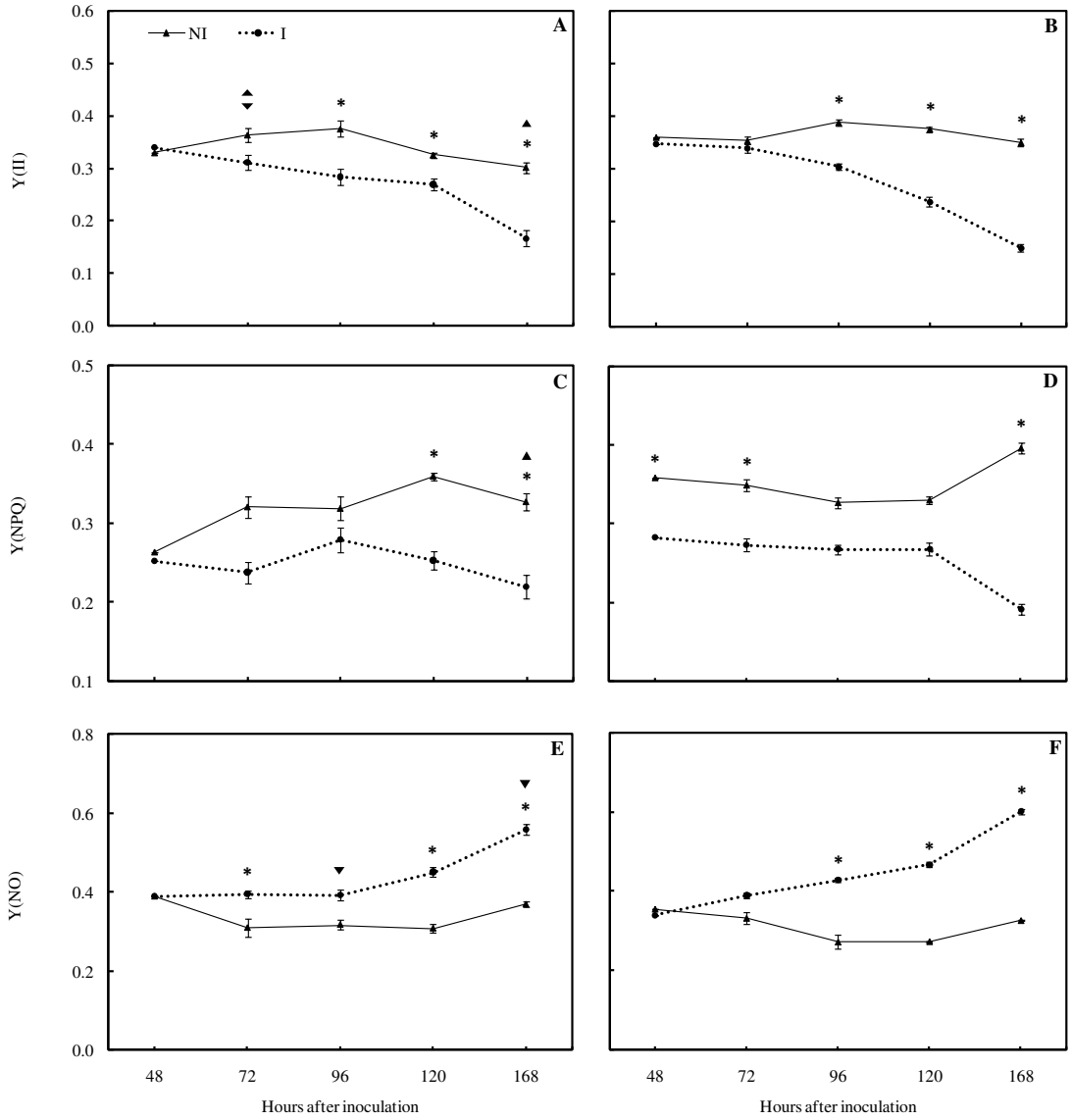

2421

2422

2423

2424

2425

2426

2427

2428

2429

2430

Fig. 5. The effective PS II quantum yield Y(II) (A and B), quantum yield of regulated energy dissipation Y(NPQ) (C and D) and quantum yield of nonregulated energy dissipation Y(NO) (E and F) determined on leaves of maize plants from cultivars ECVSCS155 (A, C and E) and HIB 32R48H (B, D and F) non-inoculated (NI) or inoculated (I) with *Stenocarpela macrospora*. Means for the NI and I treatments for each cultivar followed by an asterisk (*) at each evaluation time are significantly different ($P \leq 0.05$) by Tukey´s test. The symbols ▲ and ▼ indicate differences between cultivars ECVSCS155 and HIB 32R48H, respectively, for NI and I treatments at each evaluation time according to Tukey´s test ($P \leq 0.05$). Bars represent the standard error of the means. $n = 20$. Three experiments were conducted with consistent results; results from one representative experiment are shown.

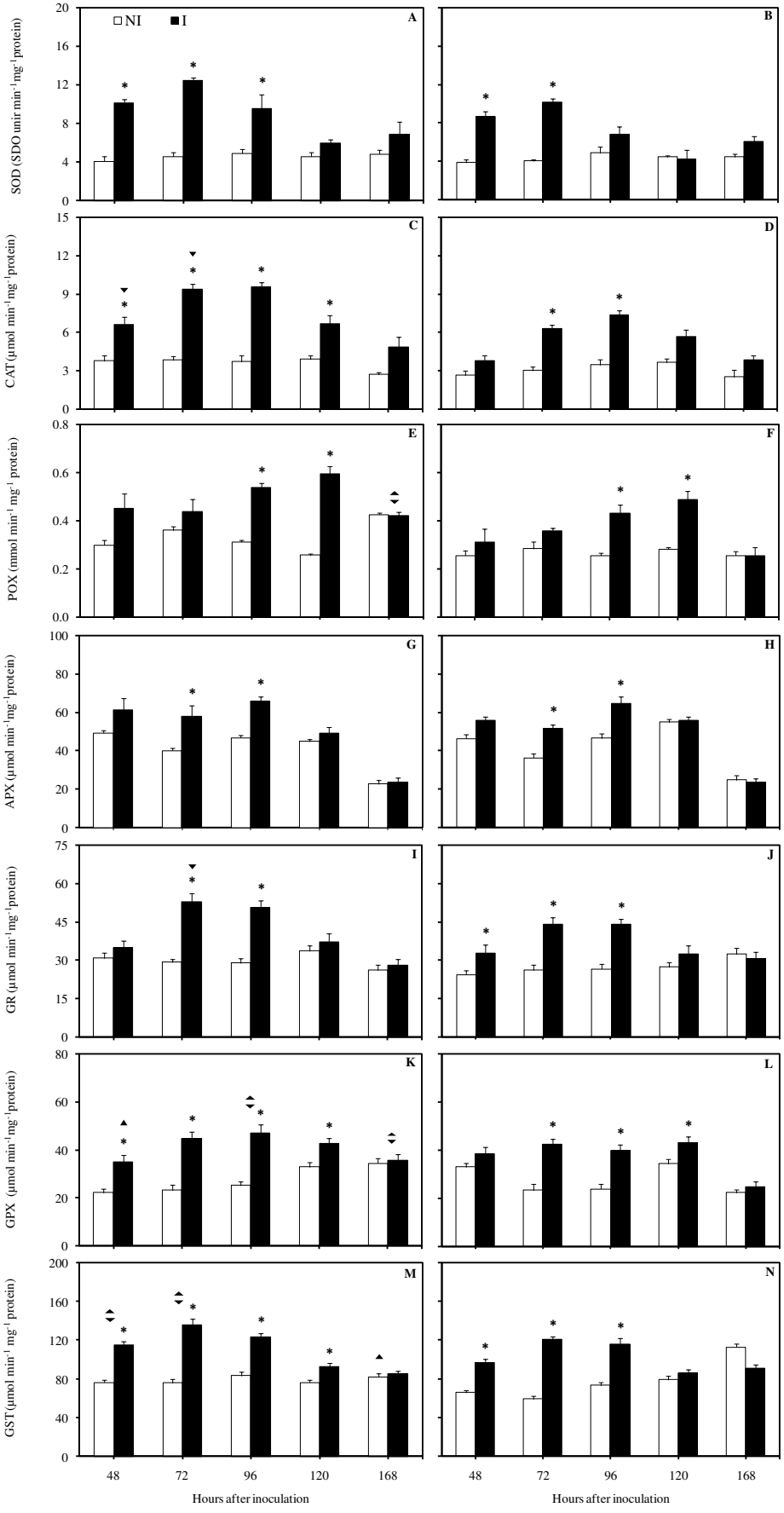
□NI ■I
A
B
C
D
E
F
G
H
I
J
K
L
M
N
SOD (SDO unir min-1mg-1protein)
CAT (µmol min-1mg-1protein)
POX (mmol min-1 mg-1 protein)
APX (µmol min-1mg-1protein)
GR (µmol min-1mg-1protein)
GPX (µmol min-1mg-1protein)
GST (µmol min-1 mg-1 protein)
48
72
96
120
168
Hours after inoculation
Hours after inoculation

2443

Fig. 6. Activities of superoxide dismutase (SOD) (A and B), catalase (CAT) (C and D) and peroxidase (POX) (E and F), ascorbate peroxidase (APX) (G and H), glutathione reductase (GR) (I and J), glutathiones peroxidase (GPX) (K and L) and glutathione-S-transferase (GST) (M and N) determined on leaves of maize plants from cultivars ECVSCS155 (A, C, E, G, I, K and M) and HIB 32R48H (B, D, F, H, J, L and N) non-inoculated (NI) or inoculated (I) with *Stenocarpela macrospora*. Means for the NI and I treatments for each cultivar followed by an asterisk (*) at each evaluation time are significantly different ($P \leq 0.05$) by Tukey´s test. The symbols ▲ and ▼ indicate differences between cultivars ECVSCS155 and HIB 32R48H, respectively, for NI and I treatments at each evaluation time according to Tukey´s test ($P \leq 0.05$). Bars represent the standard error of the means. $n = 5$. Three experiments were conducted with consistent results; results from one representative experiment are shown.

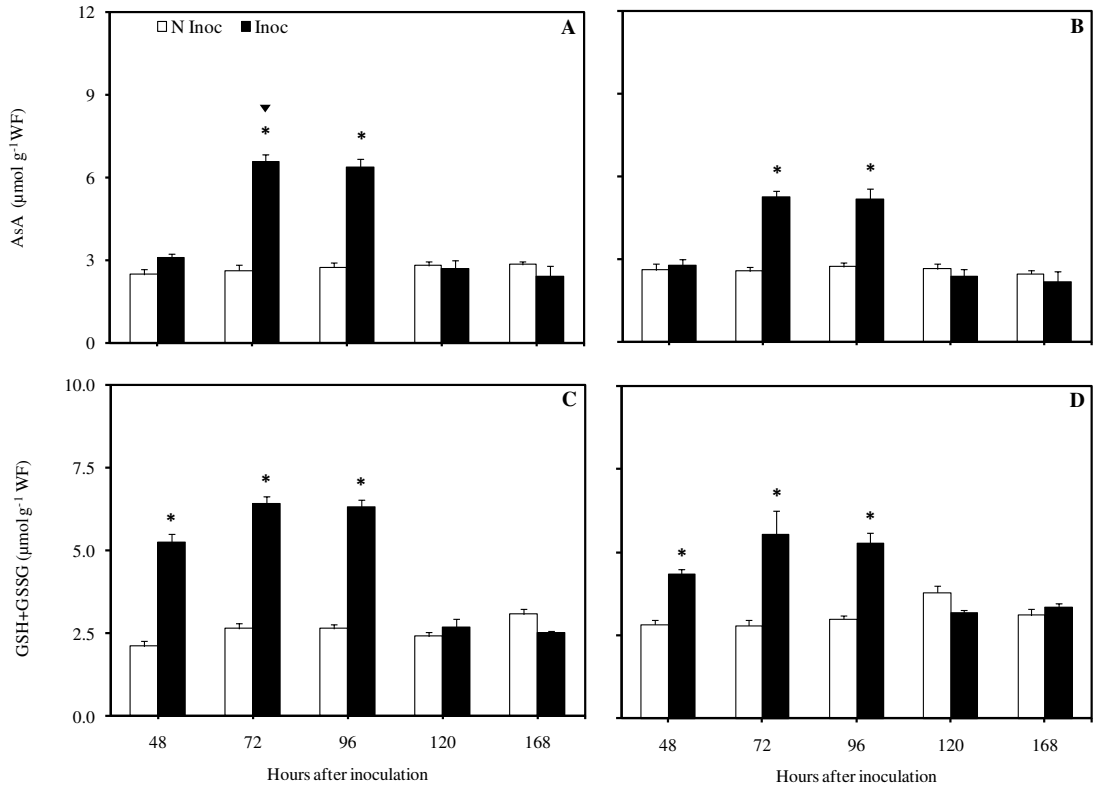

2469

2470 **Fig. 7.** Concentrations of reduced ascorbate (AsA) (A and B) and total glutathione
2471 (GSH+GSSG) (C and D) determined on leaves of maize plants from cultivars
2472 ECVSCS155 (A and C) and HIB 32R48H (B and D) non-inoculated (NI) or
2473 inoculated (I) with *Stenocarpela macrospora*. Means for the NI and I treatments for
2474 each cultivar followed by an asterisk (*) at each evaluation time are significantly
2475 different ($P \leq 0.05$) by Tukey´s test. The symbols ▲ and ▼ indicate differences
2476 between cultivars ECVSCS155 and HIB 32R48H, respectively, for NI and I
2477 treatments at each evaluation time according to Tukey´s test ($P \leq 0.05$). Bars
2478 represent the standard error of the means. $n = 5$. Three experiments were conducted
2479 with consistent results; results from one representative experiment are shown.

2480

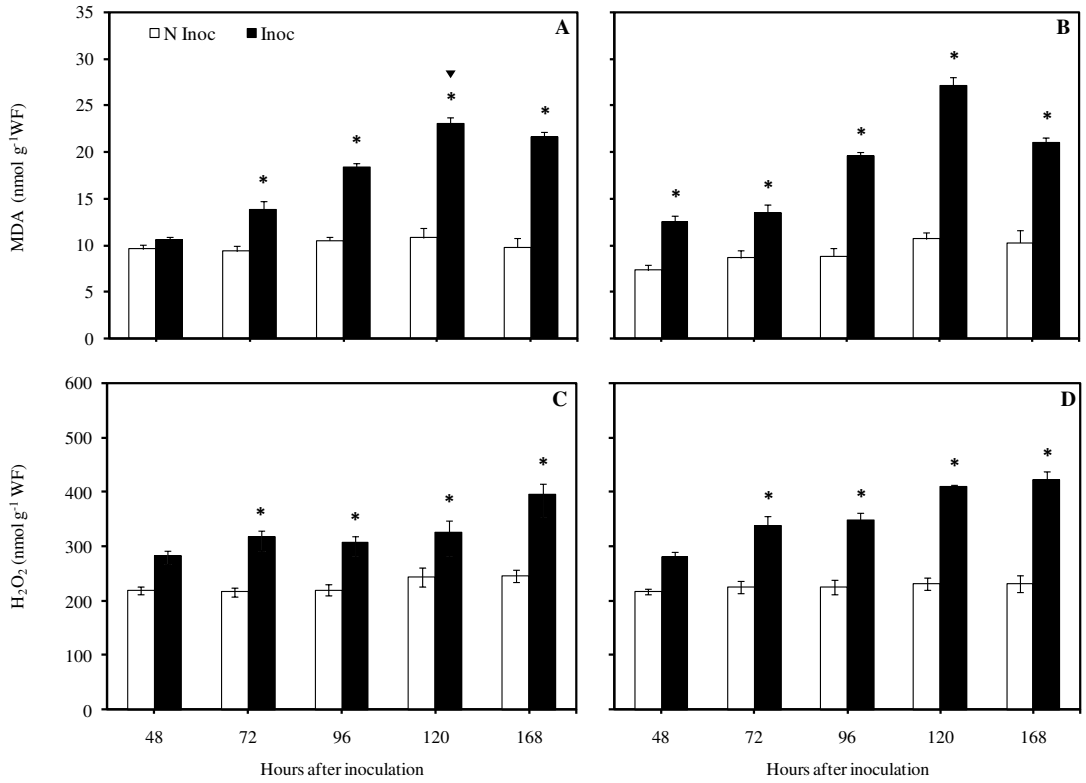

Fig. 8. Concentrations of malondialdehyde (MDA) (A and B) and hydrogen peroxide (H_2O_2) (C and D) determined on leaves of maize plants from cultivars ECVSCS155 (A and C) and HIB 32R48H (B and D) non-inoculated (NI) or inoculated (I) with *Stenocarpela macrospora*. Means for the NI and I treatments for each cultivar followed by an asterisk (*) at each evaluation time are significantly different ($P \leq 0.05$) by Tukey´s test. The symbols ▲ and ▼ indicate differences between cultivars ECVSCS155 and HIB 32R48H, respectively, for NI and I treatments at each evaluation time according to Tukey´s test ($P \leq 0.05$). Bars represent the standard error of the means. $n = 5$. Three experiments were conducted with consistent results; results from one representative experiment are shown.

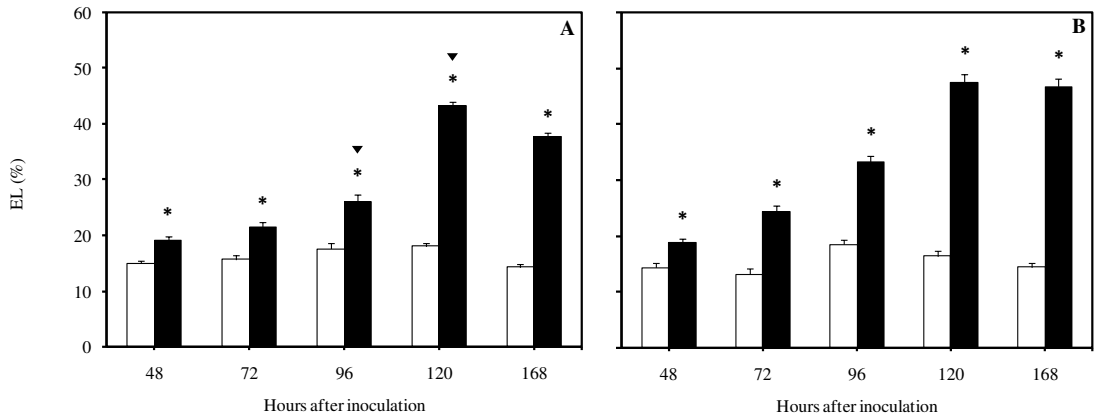

Fig. 9. Electrolyte leakage (EL) determined on leaves of maize plants from cultivars ECVSCS155 (A) and HIB 32R48H (B) non-inoculated (NI) or inoculated (I) with *Stenocarpela macrospora*. Means for the NI and I treatments for each cultivar followed by an asterisk (*) at each evaluation time are significantly different ($P \leq 0.05$) by Tukey´s test. The symbols ▲ and ▼ indicate differences between cultivars ECVSCS155 and HIB 32R48H, respectively, for NI and I treatments at each evaluation time according to Tukey´s test ($P \leq 0.05$). Bars represent the standard error of the means. $n = 5$. Three experiments were conducted with consistent results; results from one representative experiment are shown.

GENERAL CONCLUSIONS

1. Histopathological observations showed that *S. macrspora* massively colonized the leaf tissue of maize plants of the susceptible cultivar HIB 32R48H, starting from the epidermal cells and continued to the phloem vessels, the xylem vessels and the bundle sheath cells, the parenchyma cells, the phloem vessels amd the fungal hyphae colonize the entire vessels element.
2. SEM observations showed bipolar-germinated conidium with germ tubes emerging from each cell. Germ tubes grow through the stomata without any evidence of penetration. Erosion of the host cuticle around the conidia and germ tubes on the adaxial leaf surface and evidence for the direct penetration. As well as pycnidia formation into the necrotic regions of the leaf blades.
3. The progressive decline in A, g_s and E as the MLS progressed demonstrate, for the first time, that photosynthesis in the leaves of maize plants is dramatically impacted during the infection process of *S. macrospora*, and impacts are primarily associated with limitations of a diffusive and biochemical nature.
4. The observed decreases in F_m, F_v/F_m, F_v'/F_m, ETR and q_P suggesting that the ability of the *S. macrospora* infected leaves to capture and to transfer collected energy was dramatically compromised.
5. The concentration of pigments was negatively impacted in the leaves of inoculated plants from both cultivars as the MLS progressed. The reduction in chlorophyll concentration could be associated with the action of lytic enzymes and non-selective toxins released in the infected tissues by *S. macrospora*.
6. Decreases in F_m, F_v/F_m, Y(II) and Y(NPQ) coupled with increases in F_0 and Y(NO) were directly related to the progressive loss of photosynthetic activity.

7. The accentuated decreases of the SOD, CAT, POX, APX, GR, GPX and GST activities as well as the concentrations of AsA and GSH+GSSG as the MLS progressed indicated that the antioxydative system in the leaves of maize plants were dramatically altered during the infection process of *S. macrospora* causing an impairment on the protective mechanism of the maize plants that could be used to counteract the fungal infection.
8. Considering the importance of MLS to maize production worldwide and the lack of information in the literature regarding maize-*S. macrospora* interaction, the results from the present study brings novel information for a better understanding of the fungal pathogenesis as well as some alterations at biochemical and physiological level that may help for evolving more effective disease control strategies.